Année 2012

THESE

Présentée pour obtenir le titre de

DOCTEUR DE L'UNIVERSITE DE HAUTE ALSACE

Discipline : Mécanique

Par

Sheraz AHMAD

_____

Etude du frottement inter-fibre pour le coton

Study of the inter-fiber friction for cotton fibers

_____

Soutenue le – Octobre 2012 devant le jury composé de :

Pr. Eric DEVAUX	Rapporteur
Dr. René ROSSI	Rapporteur
Pr. Marc RENNER	Examinateur
Dr. Jean-Francis BLOCH	Examinateur
Pr. Jean-Yves DREAN	Examinateur
Pr. Artan SINOIMERI	Directeur de thèse
Dr. Jean-Paul GOURLOT	Codirecteur de thèse
Dr. Gérald BARBIER	Codirecteur de thèse

Table of Contents

Chapter 1-Introduction

Fibre characteristics play a very important role during all processing stages. The fibre parameters such as the fibre length, fineness, maturity, fibre tensile properties, colour, trash content etc. are used to characterize the fibres. These parameters affect the yarn quality to varying degrees. The characterization of surface properties is only used in specific studies, although it is accepted tacitly that the forces of inter-fibre friction and cohesion also exert an influence in the transformation of fibre to yarn and the quality of the latter.

Friction defines the resistant force between two bodies in contact and under pressure when they are in relative movement with a certain speed. The relative slippage between the fibres during the drawing is greatly influenced by the surface properties of the fibres. The surface properties also affect the sliver internal structure and the relative fibre movement during the drawing process. However, the surface properties, especially in terms of friction, have a significant influence. The characterization of natural fibres in terms of friction is very delicate and difficult. This is due to the fact that irregular and variable cross section shape and the outer surface from one fibre to another exist. The correlation between all the fibre characteristics, including the yarn parameter and friction characteristics is even more difficult in terms of statistical interpretation.

The importance of fibre to fibre friction has resulted in extensive research about the nature of friction, its effect on textile processing and its role in determining the resulting product properties. For years, researchers have been working on developing new devices, formulate new models and equations to calculate precisely the inter-fibre friction.

This thesis entitled "Study of the inter-fiber friction for cotton fibers" aims at analysing the effects of inter-fibre friction on the quality of the yarn. The aim is to enhance our understanding of the behaviour of fibre spinning and to improve the relationship between fibre characteristics and those of the yarn. The present research work is divided in two parts. The 1st part concerns the modification of Static Friction Tester (SFT) and its verification and the 2nd part is to find correlations between fibre properties, yarn properties and inter-fibre friction.

This thesis consists of six chapters. In the first chapter, a brief description of the present research work is given. Also the importance of surface

properties especially inter-fibre friction is also discussed briefly. In the second chapter, the literature is reviewed related to the fibre properties, factors affecting inter-fibre friction and a brief description of the different measuring devices.

Chapter 3 is devoted to the design and modification of Static Friction Tester, a device for measuring inter-fibre friction. Several preliminary trials were conducted to point out any problems in the earlier version. A brief description of Static friction tester and its method of working are as follows: The SFT consists of two identical clamps. One of them is fixed, whereas the second is moving through a linear guide. The load type cell force sensor is attached with the fixed clamp. A piece of sliver is put down in the channel of the two clamps which are initially in zero gauge position. The sliver is compressed with the upper clamp sides where two identical weights are loaded. The moving one is tracked with a constant speed, whereas the fixed one is attached, by the intermediate of a force sensor, to the frame. The distance between the two carriages is measured by displacement sensor. The SFT is modified due to the following short comings: the earlier SFT was connected to dynamometer to apply pulling force to the moving carriage. A string was used to connect moving carriage with the dynamometer. This string might be a cause of errors during the testing. The force sensor used was not highly accurate and sensitive it only gave the accurate values to first decimal point. The SFT should be levelled properly to get more accurate result but it was not possible easily with the earlier version.

The improved and modified Static Friction Tester consists of two parts: the control unit and the measuring unit. The control unit was a fully secured electricity supplying system which was incorporated with the modified static friction tester to make it safe and secures to operate. Data acquisition cards were also used in the control unit to get analogue signals from the instrument and deliver it in the form of data to the connected PC for further statistical analysis. These were also used to operate the measuring unit to make the testing operation automatic. The measuring unit was equipped with a more precise force sensor which is load cell type sensor. The load cell gave accurate value up to three decimal points. A linear actuator was integrated with SFT to operate the instrument. The

precise displacement sensor gave the value of displacement. The force sensor was connected with fixed carriage using the mechanical linkage liaison (spherical). This was also used to connect slider of the linear actuator with the moving carriage to apply the pulling force. The improved SFT was mounted on an aluminium plate that was equipped with four adjustable feet so that SFT could be levelled easily. The use of linear actuator eradicated the error that might be generated by the use of string in the earlier version of SFT. The Labview software was used to write a small programme that was used to control the SFT and acquisition of analogue signal in the form of data. The modified Static Friction Tester solved all the problems faced in the earlier version and was verified.

Chapter 4 describes a series of tests performed on a panel of 30 cottons of different origins. The panel of 30 cottons was selected randomly from the available cottons in the stock. A sample of 800 grams was collected from each cotton. The selected samples were opened thoroughly by the use of opening and blending machine. The random sampling was carried out after opening. The samples were tested for fibre properties, like length, strength, micronaire, cotton stickiness etc. The panel of cottons was then processed on the lab scale spinning machines to convert it into yarn. The sampling was carried out at different stages of spinning process to carry out AFIS and inter-fibre friction testing. The yarn of 25 tex was spun by using three different twist multipliers. The resultant yarn was tested for Unevenness and tensile properties. The samples collected at drawing process were tested for inter-fibre friction on Static Friction Tester. The testing was carried out four different weights applied perpendicularly on the carriages and 6 repetitions were performed for each case. The spinning process and inter-fibre friction testing was carried out randomly (randomization was done on the order of testing the cottons).

In the Chapter 5, the statistical analysis carried out on fibre properties, yarn properties and frictional properties are discussed. In this chapter, we will describe different models linking the parameters estimated by the SFT device. The different statistical techniques were applied on the fibre, yarn and friction results. Based on the statistical analysis, correlations were

discussed between inter-fibre friction, fibre properties and yarn properties (especially the tensile properties of fibre and yarn).

The final chapter, Chapter 6 includes the conclusions of our study and provides an overview of prospects for future research in this area. The thesis ends with a list of works and references that we used in our study. A set of annexes includes the features and specifications of parts and sensors used in our experimental work and other individual values and the measurements results.

Chapter 2-Bibliography

2.1 Introduction

In this chapter we will discuss fibre, cotton fibre, friction, inter-fibre friction, the properties affecting friction and different methods to measure inter-fibre friction. The research work is carried out to determine the effect of fibre properties on the fibre to fibre friction.

2.2 Fibre

Textile fibre is a generic term for the various types of matter that form the basic elements of textile fabrics and other textile structure. More specifically, a textile fibre is "a unit of matter that is characterized by having a length at least 100 times its diameter width and which can be spun into yarn or made into fabric" Hatch [46]. There are two main types of fibres namely natural fibres and synthetic fibres. The natural fibres are further classified in to different class. The classification of fibres is shown in the Figure 2-1.

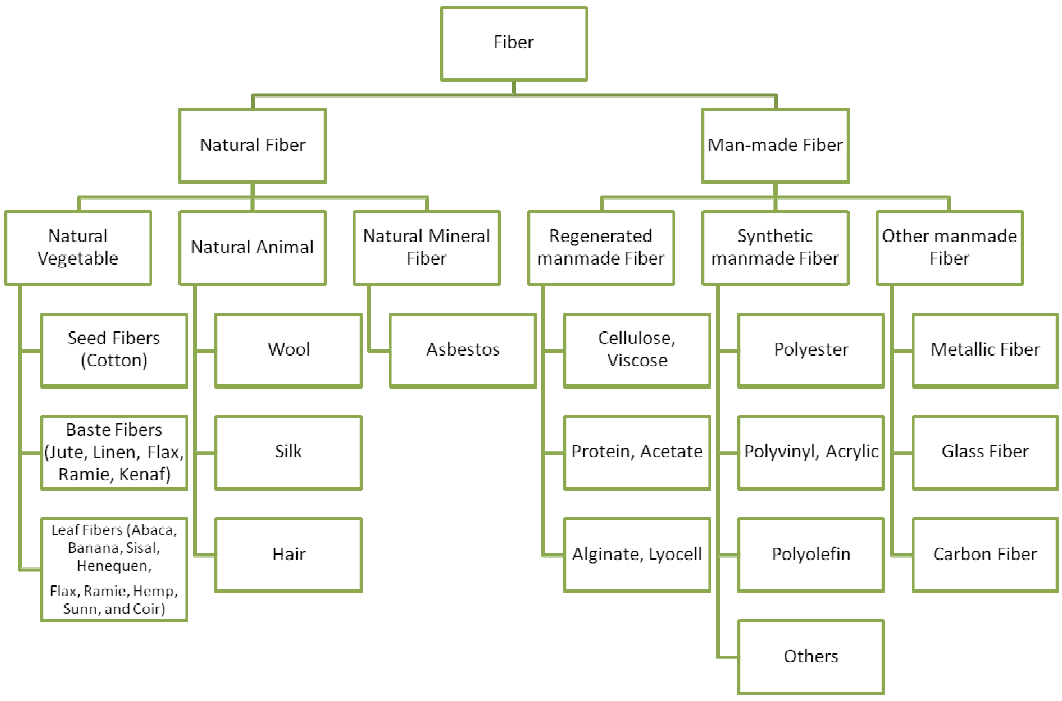

Figure 2-1 Fibre Classification.

On the basis of length, fibres are called stable fibres or filament. Textile filament is "a variety of fibre having extreme length, not readily measured." Staple fibres are natural or cut from filament having a known

length. Fibres differ from each other in chemical nature, cross-sectional shape, surface contour, length and width.

2.2 Cotton Fibres

I concentrate on cotton as it is the main material studied during this research. Cotton today is the most used textile fiber in the world. Its current market share is 35-36 percent for all fibers used for apparel and home furnishings. Cotton is a soft staple fibre that grown in a form, known as a boll around the seeds of the cotton plant, a shrub native to tropical and subtropical regions. The cotton fibres grow inside the capsules which are the fruit of the plant Hsieh [55]. Cotton fiber has the form of a perfectly circular section when it is in the cotton boll; however, when the boll opens, fibers dry out and they then form a ribbon-like fiber (see Figure 2-3). The thickness of the tube wall depends on the speed and duration of fiber growth and the varietal character. The boll of cotton fibre and the microscopic view of cotton fibres can be seen in Figure 2-2 and 2-3 respectively.

Figure 2-2 Cotton boll Figure

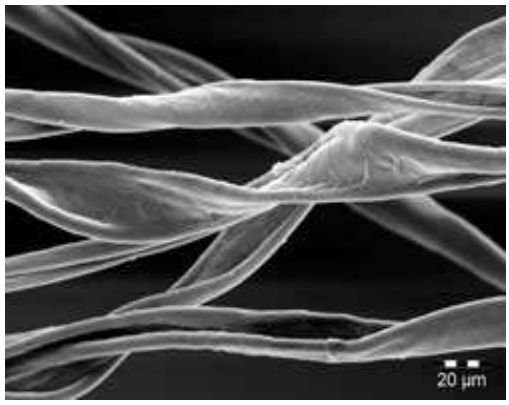

2-3 Microscopic view of Cotton Fibres

Cotton fibers are mainly made up of cellulose. The cotton fibers are attached to the seeds inside the boll of the plant. There are usually six or seven seeds in a boll and up to 20,000 fibers attached to each seed. The length of these fibers (also called staples) is the main determining factor in the quality of the cotton. In general, the longer the staple grows the higher the quality of the cotton. Staple lengths are divided into short, medium, and long (and extra-long, in some cases).

2.3 Friction

Friction is defined as the resistant force between two bodies in contact and under pressure when they are in relative movement with a certain speed. There are two types of friction: Static Friction and Dynamic Friction. The static friction is the friction when motion start from rest while the dynamic friction corresponds to the friction in the course of the motion. Static friction is generally higher than the dynamic friction. The coefficient of friction is defined as the ratio of frictional force and normal load. The measurement of friction can be carried out on the same principle. According to Amontons (1663-1705), when two bodies slide past each other at a certain speed v, the tangential frictional force F is proportional to the coefficient of friction μ and the normal force N as shown in equation 2-1.

$$F = \mu \cdot N \qquad (2\text{-}1)$$

The coefficient of friction depends on the materials used; for example, ice on steel has a low coefficient of friction, while rubber on pavement has a high coefficient of friction. Coefficients of friction range from near zero to greater than one – under good conditions.

2.4 Fibre Friction

The frictional behaviour of fibres greatly influences their processing, their performance and the performance of the final product. According to Sinoimeri [104], the importance of friction has led to extensive research about the nature of friction, its impact on textile processing and its role in determining yarn and fabric properties. The fibres are subjected to different forces during spinning process. The most important of them, which play very important role, are cohesion and frictional forces. Cohesion represents the force which is opposed to the fiber relative movement while there is no inter fiber normal forces. Friction and cohesion forces are very important in determining the behaviour of fibre during processing and it also helps in controlling the fibre flow. Inter-fibre friction is an important facet in relation to yarn and fabric properties. However, Coulomb (1736-1806) and Amontons's law is eventually not true for inter-fibre friction measurement in many cases and certain points should be considered. These points are as follows:

- The nature and extent of the contact surfaces,
- Intrinsic characteristics of the fibers,
- Treatment applied on the fibres,
- Orientation of the fibres.

In 1950, the theory of shear-adhesion presented by Bowden and Tabor [16] made a revolution in the study of friction and cohesion. According to this theory, the frictional force (*F*) is connected to the normal force (*N*) using the following equation 2-2.

$$F = \alpha \cdot N^{n} \qquad (2\text{-}2)$$

The surface structure and properties of fibre has an effect on fibre friction.

2.5 Factors Affecting Fibre Friction

Fibre friction is related to the surface properties and the bulk properties of the fibres. Gupta and El Mogahzy [31] divided the factors into two main groups: (i) factors affecting morphology of contact and (ii) factors affecting mechanical properties of junctions. The first group includes the nature of the surface, such as cross-sectional shape, presence of convolutions, crimp and scales, and contact mode during testing (point contact, line contact and area contact). The second group includes the chemical and physical structure of the fibre such as functional groups molecular orientation and crystallinity.

2.5.1 Effects of Fibre Parameters

In this group the fibre properties such as length, fibre cross section, will be discussed.

2.5.1.1 Length and Fineness

The surface density depends upon the area of surface contact; it is obvious that both the length and fineness will affect the cohesion and friction. According to the measurements made by Burlet [21] indicate that the tenacity (cN/tex) of a sliver, which can be considered as a cohesion force, increases as the average length increases. The same results are true for wool fibre fineness as found by Hannah [45]. Barella and Sust [7,8] established a relationship to determine minimum twist of cohesion T_c by using their particular measuring method. The minimum twist of

cohesion T_c has been defined as the limit of twist at which the sliver does not break by sliding under a given load. The range of the load is 0.2-3 cN/tex. The minimum twist of cohesion T_c is given by the following equation 2-3.

$$TC = \frac{K \cdot M^{a}}{L^{b} \cdot \sqrt{n}} \qquad (2\text{-}3)$$

Where

M: Micronaire (fineness),

L: Average fibre length,

n: number of fibres in the cross-section,

a, b and K are frictional coefficients of the material,

According to the equation, the minimum twist of cohesion is directly dependent on the Micronaire index and the hank of the sliver, and inversely dependent on the length.

Barella [9, 10] also find second degree curvilinear relationship between the coefficient of cohesion and the fibre length for wool fibre. The results show that the fibre length is much more important for cotton than for wool, because of important differences between these two fibres: wool, almost cylindrical having a surface with scales, cotton ribbon-like flattened, with relatively smooth surface. Graham and Bragg [41] found by using the Rothschild Cohesion Meter that the drawing force is correlated with SL 2,5% but was not affected by the tenacity of the fibre or micronaire. The force of cohesion showed a positive correlation with the mean length (ML), upper half mean length (UHML) of the yellowness index and fibre tenacity and a negative correlation with the degree of reflection (Rd). Doraiswamy [27] measured the cohesive strength for polyester and viscose by using the Rothschild Cohesion Meter. He found that the cohesive force increases as the length and fibre tenacity increases. Audivert and Castellar [3] have shown that friction and cohesion increases with an increase in the fibre length. Vernekar [113] measured friction force and he observed that the friction force for the longest fibres is greater than for the shorter fibres but it is statistically insignificant. El Mogahzy [28, 29] showed that the maximum friction force is independent of the length of the fibre, but the cohesive force increases linearly with fibre length.

2.5.1.2 Fibre Maturity

Castellar and Audivert [3] were able to establish a relationship by performing measurements on different American cottons. By applying multiple regression and correlations statistical analysis, they found that drawing force is dependent on the length and micronaire. The micronaire was much more important than length.

According to the equation of Barella and Sust [8], it is clear that minimum the value of twist of cohesion, minimum is the micronaire value. They also found that micronaire value seems to have a greater influence than the fibre length on the twist of cohesion.

Pierce and Lord [86] found a relationship between the ratio of cotton maturity *M*, the fibre fineness t and the specific surface area of the fibre *S* as given in equation 2-4.

$$S = \frac{3{,}79}{\sqrt{M \times t}} \qquad (2\text{-}4)$$

Lord [68] found that the coefficient of friction for cotton tends to decrease with increasing in fibre maturity due to the modification of the fibre cross section. Hannah [45] showed that there is a positive relationship between maturity and the minimum cohesion twist. Barella [10] confirmed these results and showed that this relationship is curvilinear.

2.5.1.3 Fibre Cross-section Shape

Doraiswamy [27] indicated that the round fibres have a more cohesive force than the tri-lobal fibres. The hollow fibres have little cohesive strength compared to solid round fibres. In general the samples composed of fibres of circular cross section have a higher cohesion than the same sample of tri-lobal fibres. The difference in cohesive strength is about 26%. This difference can be explained by the fact that the circular fibre has a larger contact area with the adjacent fibres as compared to tri-lobal fibre. El Mogahzy [31] tested the polypropylene and acrylic fibres. The results indicate that the coefficient of friction for the fibre having circular cross section is generally higher than the fibre having non-circular cross-section. The fibres of non-circular cross section are more rigid and resistant to compression.

2.5.1.4 Fibre Surface

The friction and cohesion of the fibres in the sliver or web depend strongly not only on the fibres surface contact but also its characteristics. Plonsker and Backer [87, 88] attribute the frictional interaction between fibres to not only the nature of the contact surfaces but also the number of contact points. They also showed that rougher the fibres require a higher drawing force.

Scadino and Lyons [96, 97, and 98] showed that for drawing slivers, cohesion is greater if they are composed of finer fibres as compared to those composed of coarse fibres, such as in wool spinning and cotton spinning type. Main objective of the study was to determine the influence of geometric roughness and fibre surface friction depending on their structural form (sliver, roving, and yarn). The change in fibre roughness was obtained by adding TiO_2 on the surface of PET fibres. Two slivers having identical characteristics were produced with "finer" fibres and "coarse" fibres. The inter-fibre friction was measured by using the method of Scheier and Lyons [99] and it was found that cohesion for sliver with finer fibres is more significant than the one with coarse fibres. Martindale [73] measured the drawing force of two cottons. He revealed that the drawing force for card sliver for cotton varieties Tanguis and Sakel is three to five times higher than the force required to draw drawing slivers and 25% higher than the force required to draw combed slivers. But if the drawing force of the Sakel is more than 1.3 times the one of Tanguis, then the two cottons have identical drawing forces.

It has been observed that card slivers give more inter-fibre cohesion compared to other slivers. This is explained by the fact that the fibres are less aligned at the later stage of processing.

Doraiswamy [27] measured the cohesive strength for polyester and viscose with "Rothschild Cohesion Meter". He found that the fibres with more lustre have more cohesion force than the brittle one. The fibres having a surface gloss are "finer". Thus geometrically finer fibres lead to greater cohesion of the fibres. Bartlett, Smith and Thompson [12, 13] measured the friction of the yarn with their device called as "slow speed tester". The lustrous yarn has a high "stick-slip" and as a result higher

average friction than the brittle yarns. The frictional properties of spun filament are mainly determined by the finish applied.

2.5.1.5 Crimp and elasticity

The crimp, rigidity and elasticity depend upon the characteristics of the material. In textiles, it can be observed that when the fibre crimp decreases, the apparent rigidity and elasticity increases strongly. On the other hand, by straightening, there is strong possibility that the number of point contact between the fibres increases. This increase may result in the increase of the inter-fibre cohesion. Coarser the fibres, more rigid they are and more difficult is the removal of their crimp. As a result, for identical sliver, there will be better cohesion with finer fibres than with the coarse fibres. Backer and Plonsker [87, 88] worked with the polyester fibres of identical characteristics, but with different amount of crimp. They found that the more crimped fibre showed a higher drawing force because it has more opportunity to entangle with neighbouring fibres.

Olsen [84] established, by performing measurements on the same type of fibre (Dacron in this case), a relationship between the crimp and the force required to draw the sliver. Olsen [84] established a relationship between the crimp and draw force *F* for polyester fibres (Dacron) as shown in the equation 2-5.

$$F = 10^{(0{,}061 cpi + 1{,}54)} \qquad (2\text{-}5)$$

Where

cpi: crimps per inch.

Burte [22] and Wagget [118] observed the increase in the maximum force or elongation according to the amplitude and density of the crimps. Burlet [21] experimentally confirmed our initial comments about the roughness, so the cohesion of the sliver increases when the elastic modulus decreases. He also found that the cohesion increases proportionally with the degree of crimp in the wool fibre. The amount of crimp increases with the fibre fineness. Doraiswamy [27] measured the cohesive strength for polyester and viscose with "Rothschild Cohesion Meter". He found that high crimp gave greater cohesive strength than the sample with low crimp. An increase of two crimps/cm raises the cohesive strength about 39%. Ghosh [40] by using the "Rotor Ring" instrument has shown that the

opening energy for fibre-fibre and fibre-metal in the case of polyester and polyamide increases with the percentage of crimp. Ahmad [1] used four types of cotton card slivers to evaluate the inter-friction forces developed in the sliver after passing through successive drafting and drawing processes. The sliver structure in terms of hooks and crimps affect strongly the inter-fibre movement and drawing force. It was also observed that the independent evaluation of hooks and crimp can explain the evolution of the force developed within the sliver at different processing stages.

2.5.1.6 Other Fibre Properties

Guo [44] showed that the irregularity of the yarn increases when the friction force increases. A high frictional force limits the slip between the fibres thereby providing a uniform linear distribution. The correlations found in this study (between -0.56 and -0.74 between friction force and yarn tenacity) lead the authors to conclude that a lower force of friction gives the higher yarn end resistance. According to them, another reason for the decrease in strength, as the inter-fibre friction increases that may damage the fibre and that may result in loss of yarn tenacity. On the other hand, the irregularity has a negative correlation with the cohesive strength of the fibres. This force has a positive contribution to the formation of uniform yarn.

2.5.2 Effects of Fibre treatments and conditions of implementation

The treatment to the fibre surface changes the apparent roughness and consequently the inter-fibre friction coefficient. To spun wool fibres, a surface treatment is applied on the fibres.

2.5.2.1 Lubrication

Krugger [60] and Henshaw [48] studied the influence of the type and amount of lubrication on the quality of spinning. Olsen [84], Averous and Karrer [5], Vernekar [113] and Anderson [2] also studied the effects of the lubrication on the drawing force. But it is difficult to derive a general relationship to predict the effect of lubrication, as it varies with the type of lubrication. They also found an increase in drawing force with an increase in the amount of lubrication. The force increase significantly with an increase of about 5% of oil, but between 2.5% and 5% of oil the increase

in force is not significant. Viswanathan [114, 115] studied the friction of lubricated cotton fibres. The lubrification was carried out by immersing fringe of cotton fibres in a 10% solution of Sorbital in water for two minutes. The wetting agent Lissapol was added to the solution. The fringes were then placed between two sheets of blotting paper for 5 minutes. The results show a significant amount of increase in friction coefficient for both cottons. Further experiments of immersing the cottons and other chemical fibres (Tufcel, Polycot, and Viscose Rayon) in water reported significant increase in the friction coefficient. It was also observed that the increase in friction was greater when the wetting time was longer. Considering that the wax content of cotton fibres is not significantly affected during the mechanical treatment.

Doraiswamy [27] measured the cohesive strength for polyester and viscose with Rothschild Cohesion Meter. He found that the cohesive force increases as the rate of lubrication increase during spinning process but after a certain level, the cohesive force decreases rapidly. Gamble [38] showed that the inter-fibre friction increases as the wax content decreases. In addition he noted that the natural wax content has a weak relationship with the fibre cohesion. Cui [25] studied the effect of wax on the properties of thirty six cottons. Fibre properties were measured by HVI and AFIS and yarns properties were measured by the Uster Tensorapid and Uster Evenness Tester. HVI data show significant correlation between the wax content and fineness. They measured the cohesion force for a sliver of 1.5 ktex. After the wax extraction, the cohesive force is increased by a factor 3, but statistically, the wax content shows an insignificant correlation with the cohesive force. Moreover, the average fibre length decreases with wax content but not significantly. However there is an important correlation between the rate of wax and micronaire (negative) and the specific surface area (positive) and a weak positive correlation with the yarn tenacity. Berberi [15] tested four different lubricants on cotton. He found that the cohesive force increases at the beginning (0.1%) then decreases (0.5%). Vernekar [113] also observed the same type of results. El Mogahzy [31] indicated that the value of the frictional force for wet testing is higher than that for the dry testing. This effect may be due to the absorption of water by the yarn and as this increase

the contact surface area. Another possibility the shearing of the water surface that can contribute to increased friction.

2.5.2.2 Special Treatments

Lawson *et al.* [63], by applying corona treatment (plasma), noted a significant change in the inter-fibre cohesion due to this treatment. They conducted this experiment on the tensile strength of a cotton-viscose sliver before and after treatment. Another case of special treatment is wet spinning. Kamarov *et al.* [58] studied the quality of the yarn and the breakage rate in ring spinning machine under wet and dry conditions. They found a relationship between the degree of wetting (stiffness modulus) and the drawing force F. These authors concluded that when the average value of F decreases, the stiffness modulus decreases in parallel. They also concluded that when the variations in F are small, the CV% of yarn breaking strength of is also low.

2.5.2.3 Dyeing

Wegener and Bechlenberg [119] showed that dyeing treatment has a significant effect on the sliver cohesion. It may be noted that the lubrication significantly alters the effect of the dye. Monfort [78] observed that the dyeing depend upon lubrication of the fibre. The cohesion force varies significantly for dyed fibres that are lubrified or not.

2.5.2.4 Conditioning

It is interesting to note that in industrial practice, problems related to cohesion are corrected by changing the relative humidity of ambient air and the nature of the lubrication. Tarrin and Gouault [108] was able to correlate the increase in moisture with the slip threshold of the sliver by measuring the tensile force on it. Baril, De Luca and Mayer [11] showed that there are optimum atmospheric conditions reducing fibre cohesion which gave drawing force with a small CV%. In general, the cohesion of the fibres increases as the temperature and relative humidity RH decreases. However beyond 95% relative humidity, temperature has no significant influence on cohesion as practically possible temperature variations remain small. Cavaney and Foster [23] showed that for cotton Giza the drawing force decreases by 8% when the relative humidity percentage increases by 10%. Berberi [15] observed that the change in temperature affects the cohesion force for cotton slivers. Cohesion

decreases with increase in the moisture content and this effect depends on the temperature.

2.5.2.5 Storage

Simpson and De Luca [101, 102] studied the effect of storage on the drawing force with the "West Point Cohesion Tester". They found that the storage did not cause any significant difference between the values of drawing force for each distance between the cylinders. Thus the large enough quantity of slivers may be stored in cans without any apparent drawing force and sliver tenacity. Anderson [2] showed an increase in the percentage of the drawing force after storage for 30 minutes. The increase occurs in two steps, the first step being complete after about 100 hours. The second step is much slower and continues after 3000 hours (125 days). The second gradual rise in tensile strength may be due to oxidation of the oil on the fibers.

2.5.2.6 Mixing and Blending

Viswanathan [115] studied the friction between the cotton fringe (Kranak and Kalyan) and fringes of synthetic fibers with the modified apparatus of Lord. He found that if the two sections of fibers are different, the friction is more important. Jackowski [56] mixed cotton with flax in the ratio of 10% and 50% and measured the drawing force with a device similar to "American Viscose Instrument". The results showed that the irregularity of linear density of the sliver increases and consequently the drawing force decreases.

2.5.2.7 Bleaching and mercerizing

The bleaching and bleach-mercerization process may result as an increase in the friction coefficient. In fact, mercerizing after bleaching increases friction considerably Bardy [6].

2.5.3 Fibre Orientation in sliver and Web

The orientation of sliver plays a role in the fibre friction.

2.5.3.1 Degree of Fibre Parallelization of the fibres

Martindale [73] and Wegener *et al*. [120] have verified that the average drawing force is a function of "opening" (the compactness) of the sliver, as well as the degree of parallelism of the fibers in the sliver. Graham [44] observed that the degree of parallelism of fibers as they pass through

drawing and drafting. Martindale [73] studied the drawing force for cotton fibres. The forces required to draw slivers of cotton Sakel and Tanguis showed that if the sliver is entering the drafting zone with trailing hooks (fibers entering the drafting zone in the form:) the drawing force is larger (15-20%) than if the leading hooks fed to delivery rollers (the fibers entering the drafting zone in the form:). The difference is obviously due to the fact that when non hooked ends are captured first by the front rollers, hooks are straightened, but when the hooked ends are captured first they are not straightened. In addition, he found that the average drawing force depends on the opening of the sliver and the degree of fiber alignment. For example, the force required to draw the third passage drawing sliver is about a quarter of that required for drawing an identical card sliver.

Barella and Sust [8] found that the minimum twist of cohesion (TMC) decreases as the degree of parallelism increases. Because straighter and more parallel fibers have the greater cohesion between them and lower will be the twist applied. They conclude that this measure of TMC evaluates the degree of parallelism of the fibers during the spinning process and to compare different materials in a similar stage of spinning. Lysenko and Kreitsberg [71] used radioactive isotopes to label fibers during drafting. They found that the fiber alignment improves as the sliver pass through successive drawing stages. Postle and Ingham [89] measured the force required to extract a long wool fiber from a sliver of wool that is under increasing loads. Similarly, they evaluated the porosity of the sliver according to the applied pressure P, by measuring the extraction force of a fiber in relation to the compressed height of the ribbon, the height being determined by using a scanning microscope. Porosity ε is defined as the volume of air of the total volume of the sliver. This is explained by the relation in equation 2-6.

$$1-\varepsilon=\frac{T}{S\times\rho} \qquad (2\text{-}6)$$

Where

T: Sliver hank (linear density)

ρ: The density of the fiber

S: "inflated" section of the sliver

Simpson and De Luca [102] noted that the increased sliver hank on the draw frames results in poor hooks removal. Audivert, Villaronga and Coscolla [4] studied the effect of leading and trailing hooks during the drawing process. The tests were conducted for two types of cotton. It shows that the influence seems weak in the case of locks. They found that after successive drawing passage the effect of hooks is reduced as the hooks are removed by previous drawing passages. The results are significant: the leading hooks gave a drawing force lower than the trailing hooks.

2.5.3.2 Material Orientation

Plonsker and Backer [87, 88] studied the influence of superposing or juxtaposing the slivers of different roughness on the drawing force. According to these researchers, the drawing force (mgf/tex) would be independent of the sliver hank in the case of juxtaposed and would be proportional in the case of superposed although they do not apply pressure in the normal drafting zone. This could be due to the fact that in the case of overlap, there is an increase in the number of contact points between the fibre layers as compared to the fibres juxtaposed. Wegener and Bechlenberg [119] have demonstrated the relationship between changes in sliver cohesion for the combed wool and variations in fibre length, conducting periodic accumulations of long or short fibres. The results verified that a contribution of long fibers leads to an increase in the sliver cohesion.

2.5.3.3 Twisting

The cohesion measurement for the web show that twist play an important part at this stage and works as multiplier for the cohesion force due to the effect of centripetal pressure it produces. By analyzing the figure 2-4, the force applied on the web can be divided into two components: GT (tangential force) and FC (centripetal force) which corresponds respectively to sliding forces in the axis of the fibers and those which tend to compress the fibers in the sliver.

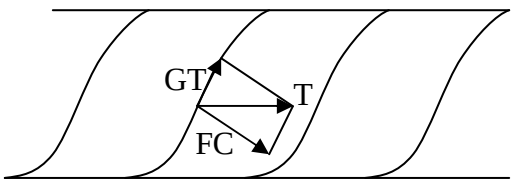

Figure 2-4. Vectors of forces on the Web

In the case of high twist, the fibres may block and create "hard pass" if the drafting zone setting is not proper and will produce irregularities in the sliver or irregular sliver. There is also problem due to accidental torsion caused by the coiler system for the cans Plonsker and Backer [87, 88].

2.5.3.4 Cohesion and Characteristics of Yarns

At the ring frame delivery, cohesion given by the twist should be maximum; this will give a regular yarn. The regularity of the yarn depends upon the regularity of the roving and sliver cohesion. Graham and Bragg [41] showed that spinning quality can be maintained by periodic measurement of the drawing force and its variability.

2.5.4 Machine Settings

In this section we will discuss the effect of machine setting on the fibre friction and cohesion.

2.5.4.1 Drawing and Drawing speed

Anderson, Cox and Hardy [2] showed the influence of the drawing a fiber from a sliver of wool. Similarly, Cavaney and Foster [23] examined the effect of the drawing speed for cotton slivers and Fibro slivers for a range of higher speeds. For cotton slivers, the force increases by 20% when the speed of the front roller increases from 0.02 to 1.5 cm/sec and then remains almost constant up to 7 cm/sec. But for a Fibro sliver the drawing force is independent of the speed. At very low speeds, the vibrations due to "stick-slip" were observed with the Fibro and some other artificial fibers. These results indicated a difference of more than 10% between the static and kinetic friction. But with cotton and silk vibrations do not occur. Anderson *et al*. [2] measured the extraction force for a fiber pulled from an uncompressed sliver. Audivert *et al*. [4] studied the influence of the draw ratio to the drawing force for different speeds of drawing roller unit. They confirmed that at constant drawing roller speed, the sliver drawing force decreases as the total draw ratio increases but for low and constant draw ratios, the drawing force increases significantly with the output

speed. Olsen [84] established a relationship between the drawing force F and the draw ratio E shown in equation 2-7.

$$\text{for } E > 1.5 \quad E \times F = k \qquad (2\text{-}7)$$

Where k is a constant value if all other parameters influencing the sliver cohesion are maintained constant. Martindale [73] had showed that for different cottons having low draw ratio (E <2), the stretching force is proportional to the number of fibers gripped by the delivery rollers and does not depend on the drawing speed, provided that the variation in the number of fibers is not due to a change in sliver count fed. Cavaney and Foster [23] examined the drawing force as a function of speed. They found an increase in strength, but this increase is not significant. Anderson, Cox and Hardy [2] measured the tensile strength of a wool sliver and also force to stretch a fiber. For both the measurements, they found an increase of approximately 50% for a speed increase from 0.13 to 3.2 cm/sec.

Plonsker and Backer [87] reported that the drawing force starts at zero for a draft of one and then increases to a maximum to decrease thereafter. Jackowski [56] measured the drawing force for cotton sliver. He found that the drawing force increases with increasing speed and also confirmed the results of Plonsker and Backer [88] due to the decreasing number of drawing fibers. Moreover, he showed that the values of the drawing force for the sliver obtained by his dynamic method are 3.5 to 5 times larger than those obtained by his static method.

2.5.4.2 Number of Drawing Passages

Vroomen [117] established a relationship between relative machine efficiency under ideal conditions by using the coefficient "K of Huberty", actual coefficient of variation CV% (measured by Uster evenness) and theoretical CV%, the latter being assessed by the following relationship:

$$Theoretical CV\% = \frac{100}{\sqrt{ns}} \qquad (2\text{-}8)$$

Where *ns* is the average number of fibers in the sliver cross-section.

$$K = Actual CV\% \times \sqrt{ns} \qquad (2\text{-}9)$$

The repeated passages of drawing such as "Dubbing-drawing" by keeping the delivered sliver constant give a curve that shows the value of K decreases with increasing number of passages.

2.5.4.3 Influence of Drafting Zone Setting

The wider spacing between drafting rollers could facilitate the individualization of fibers and consequently a better fibre orientation, which would correspond to an improved inter-fiber cohesion or better sliver tensile strength. Martindale [73] measured the drawing force of cotton. He showed that cohesion decreases while increasing the distance between the draw rolls, for cotton slivers. With decreasing the spacing between the rollers, the force increases gradually until the spacing of the rollers is so small that the longer fiber is then held by the two ends. Simpson and De Luca [102] defined the drawing tenacity as the drawing force per unit of average linear density of the sliver given in g/tex. By Using the West Point Cohesion Tester and testing three cottons, they modeled the drawing tenacity depending on the draw rollers spacing:

$$T = a \cdot e^{b(1/ERE)} \qquad (2\text{-}10)$$

Where

T: Drawing tenacity (g/tex) x 100

a and b: constants.

Plonsker and Backer [87] showed that increasing the length of the drawing area reduces the number of sliver contact points. This causes a reduction in the pulling force due to the lowering of the relative movement. Cavany and Foster [23], Simpson and De Luca [101] showed the same results.

2.5.4.4 Elements in the drafting zone

In wool spinning, a system of lateral movement wipers was introduced to give a false twist to the sliver. This give the false twisted sliver more inter-fiber cohesion by centripetal effect of alternating S and Z twist: it is quite logical to find an even stronger cohesion as the amount of false twist is increased. These studies can be compared to that of Barella [8] with his minimal twist of cohesion (TMC) on the one hand, and Anderson, Cox and Hardy [2] on the "porosity" (apparent volume) on the other: the twist decreases the porosity of the sliver and increases the cohesion. Another

element that can be introduced in the stretching zone is constituted by perpendicular strips to the axis of the sliver with needles generally similar to a "comb". All the strips form a "field hands" which allows for better control and better alignment of the fibers, and a reduction in square brackets. One can notice that the stretching force necessary to extract the fibers from the scope of needles is not representative of the cohesion of the sliver. Averous [5], Wegener *et al*. [119] and Krugger [60] measured the stretching force by the dynamometer on sliver before and after passage through a drawing machine equipped with needle ("Intersecting"). They assessed the sliver cohesion after passing through this type of machine.

2.6 Measurement of Fibre Friction

The friction measuring methods can be divided into two classes according to Howell [50, 51, and 53]. In the first method, we measure the friction at a point of contact: between two identical fibres or two different fibres or between the fibre and non-fibrous material such as plastic, metal or ceramic. In the second method, the friction is measured globally among a large number of fibres and other material. The measurement is averaged by the number of contacts. For theoretical investigations, the first type of methods is more suitable, because of the better control of measurement conditions. Therefore they should give more accurate results and easier to interpret. The methods of the second type give generally average values.
Nowrouzieh [80] divided the fiction measurement methods in the following six groups based on their respective measurement technique:

- The first group is based on the measurement of friction by assuming the contact as punctual and in this case the movement is often of a "stick-slip".
- The second is based on direct measurement of the force required to overcome the force of friction between the fibres or filaments having a number of contact points. The method of the inclined plane is a typical example.
- The third group, based on a method of twisting that was proposed by Lindberg [64, 65]. It is also an example of a method for measuring the average friction over a given fibre length.

- The fourth group deals with the measurement of inter-fibre friction by estimating the force required to remove a fibre from the fibre bundle or by measuring the force required to break a sliver or any other kind of fibre assembly.
- A fifth group is based on measuring the drawing forces.
- A final group of methods which is very important for measuring the friction is based on measuring the force in each strand on each side that touched the corner of a cylinder. These methods are particularly well adapted for measuring the coefficient of kinetic friction.

The importance of fibre to fibre friction has resulted in extensive research about the nature of friction, its effect on textile processing and its role in determining the resulting product properties. In this chapter, we will examine the techniques and devices for measuring friction and cohesion proposed by various researchers. Then we review the bibliography facts about cohesion and inter-fiber friction.

We have divided the different fibre friction measurement devices in two simple groups:

- Measurement of friction between identical materials
- Measurement of fibre between different materials

Based on this classification we will discuss different inter-fibre measuring devices.

2.6.1 Measurement of friction between identical materials

In this group, the friction measurement between identical materials will be discussed as the function of the material type, for example fibre to fibre, filament to filament etc.

An instrument is developed by Lindberg and Gralen [65, 66] based on twisting method. In this method two filaments A and B were twisted *n* times and an angle β was formed between two filaments as the result of the twist. At the start, a known force P_1 applied on both the filaments and the filaments are kept at a certain distance. (Figure 2-5)

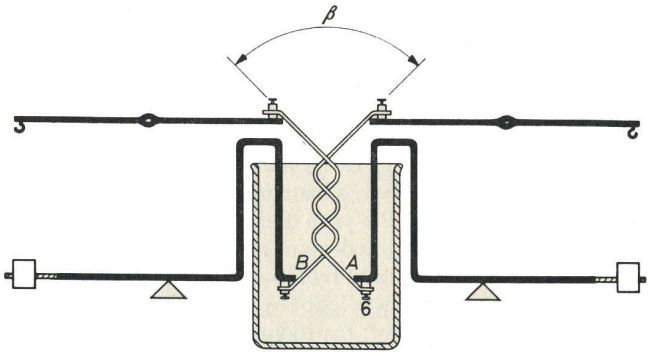

Figure 2-5. Lindberg and Gralen Friction Measuring Device

By releasing a filament end and fixing the other end, a force P_2 was obtained as the slippage of filaments occurred, this slippage gave the value of the static friction force. According to Lindberg and Gralen, the coefficient of static friction was given by the following equation:

$$\mu = \frac{Ln\frac{P_2}{P_1}}{\pi n\beta} \quad \text{Or} \quad P_2 = P_1 \cdot e^{\mu \pi n \beta} \qquad (2\text{-}11)$$

Lindberg [66, 67] proposed a modified friction measurement equipment based on twist method. In this method, two fibers were twisted and each of their ends were wound on cylinder as shown in Figure 2-6. One end of fibre B was fixed while the other end was loaded with a mass *P1*. The fibre A was loaded with the mass *P2* at one end while the other end was connected to the load sensor with the help of spring. As the pulling force is applied on A, the equilibrium will be disturbed as the pulling force is increased as compared to the friction.

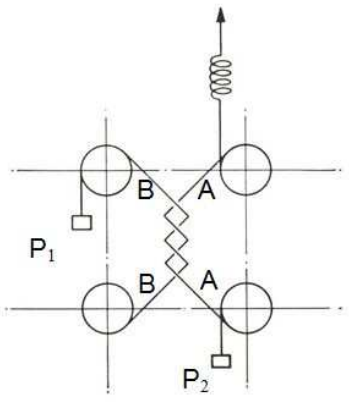

Figure 2-6. Lindberg Friction Measuring Device

The coefficient of friction μ can be calculated by using the following equation:

$$\mu = \frac{(P2 - P1) \times l}{2(P2 + P1) \times \pi^2 n^2 r} \qquad (2\text{-}12)$$

Where:

P2 and *P1*: loads applied to the ends of the fiber A and B respectively,

n: the twist,

l: the length of the twist

r: the radius of the fiber.

Hood [49] developed an instrument based on the principle proposed by Lindberg and Gralen [64].Fibers *a* and *b* are each suspended by one end to the alternating arms *c* and *d*. Weights *Wa* and *Wb* are applied to the other ends of the fibres as shown in the figure 2-7.

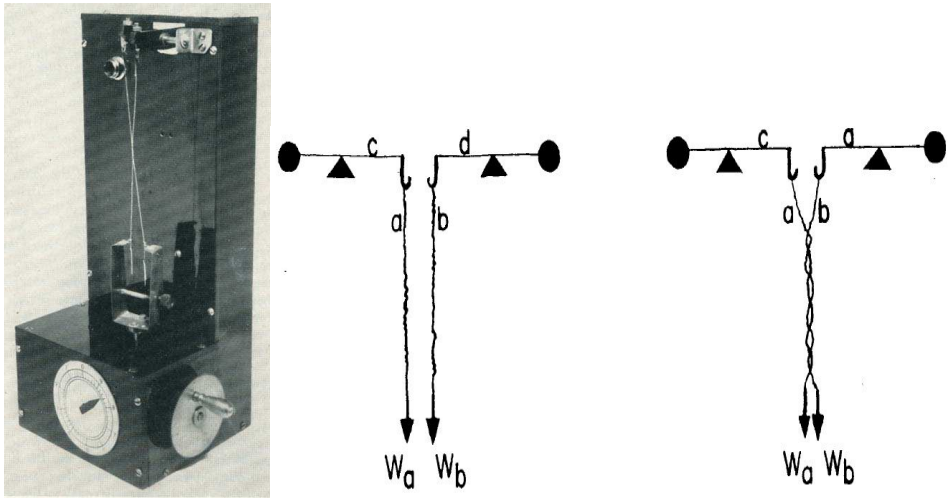

Figure 2-7. Hood Friction Measuring Device

Simultaneously the fibers are twisted and the number of turns required to stop the slide is taken as the arbitrary unit of friction measurement.

A device of fibre friction measurement was developed by Van der Vegt and Schuringa [112]. In this case, the force is kept constant and the twist is varied and a very simple device was developed. Two fibers were suspended on two pulleys, B and C, under equal loads *W1*, (Figure 2-8). Axis A rotates until a sufficiently amount of twist was inserted. Then the load E was increased to *W2*. The load should be to a certain value that will not disturb the twist equilibrium.

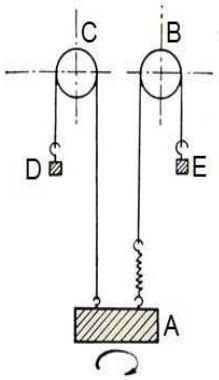

Figure 2-8. Van der Vegt and Schuringa Friction Measuring Device

The fibers were then untwisted until slippage occurs. At that point, the number of turns *n* is estimated and the corresponding twist angle was also measured. The author applied the following equation to calculate the fibre friction.

$$\mu = \frac{Ln\dfrac{W2}{W1}}{\pi n\beta} \qquad (2\text{-}13)$$

To calculate the coefficient of kinetic friction, the torsion was reduced a second time and the second slippage occurred at an angle β and at a different number of turns and twist.

El Mogahzy [31] derived an equation which characterizes the friction by the twist method:

$$\mu = a\left[P_1\beta^2/4r\right]^{n-1} \quad \text{or} \quad P_2 = P_1 \cdot e^{\left[\pi n\beta\alpha\left(P_1\beta^2/4r\right)^{n-1}\right]} \qquad (2\text{-}14)$$

This equation was based on the simple principle of friction and derived from the basic friction equation.

The instrument of Martindale (Figure 2-9) contained three pairs of drawing rollers, the front pair was fixed in a cradle suspended from a leaf spring and a fixed frame. The forces exerted during drawing cause the displacement of the first pair of cylinder. The drawing force in this case will be evaluated by the holding spring arrow that kept the roller pair in equilibrium. To avoid the problems of vibration, the measurement system is mechanically decoupled from the rest of the device. But there remains the problem of torque due to the driving torque of the drawing roller unit.

Indeed, the drive motor of the drawing roller unit transmits a constant motor torque to the system.

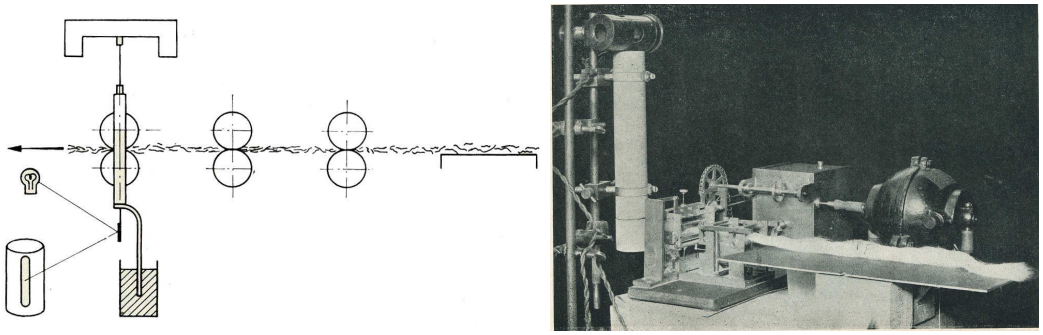

Figure 2-9. Martindale Friction Measuring Device

The drawing force applied to the pair of rollers gave the value of fibre friction. On the basis of this principle, an equipment was developed by Brook and Hannah [17] which measured at speeds similar to drawing speeds.

Based on the work of Martindale, many devices and methods have been developed. Cavaney and Foster [23] modified Martindale' device. They replaced the optical system by a mechanical system. Grimshaw [43] and Bevoort and Lake [62] have changed the measuring device of the drawing force. They also eliminated the measurement defects due to vibration.

A fibre friction measuring technique was developed by Henning [47]. In this instrument a vertical fiber was stretched by a known weight at one end. The other end was fixed to the horizontal axis of a balance. The axis was held in a position by a weight at one end and the other end was attached to a sliding spring. A second fiber, under a known tension, was positioned horizontally. The friction between these two perpendicular fibers produces a sliding effect on the axis of the balance. The measurement of the oscillations, the equipment constant and the fiber bending and tension observations were sufficient for coefficient of friction calculation.

Postle, Ingham and Cox [89] described another method in which a long fiber was removed from a bundle of fibres (Figure 2-10). A long fibre D was held inside a piece of fibre bundle that was kept in a rectangular support B compressed under a weight C. The other end of the fiber D was attached to the axis F which was fixed to a spiral spring G.

The force required to extract the fiber was given by the spring force G. This force was then recorded.

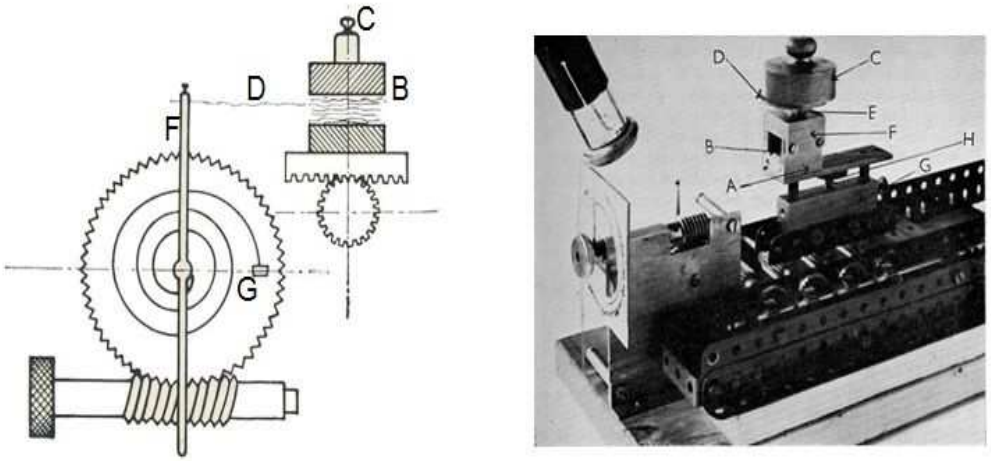

Figure 2-10. Postle, Ingham and Cox Friction Measuring Device

The formula for the relationship between the coefficient of friction and the force required to remove the fiber is as follows:

$$F = \frac{P}{1-\varepsilon} \times 2d\mu\left(1 + \frac{5V^2}{4}\right) + \beta \qquad (2\text{-}15)$$

Where

F: Pulling force applied on the fibre,

P: External pressure on Sliver,

e: Porosity of sliver

μ: Frictional coefficient

d: Average diameter of fibres

V: Coefficient of variation for fibre diameter

β: constant.

Anderson, Cox and Hardy [2] described a static method of measuring the drawing force that can be used to calculate the frictional force (Figure 2-11).

A piece of sliver, longer than the longest fibers, was mounted between two clamps A and B. The upper clamp A was attached to a cantilever spring C which was the force measuring element as the clamp B moved to break the sliver.

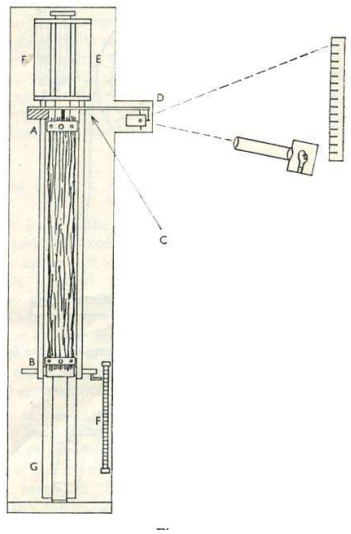

Figure 2-11. Anderson, Cox and Hardy Friction Measuring Device

Howell [52, 54] used a very simple technique to measure fibre friction. A filament C is fixed at point A under the load W.

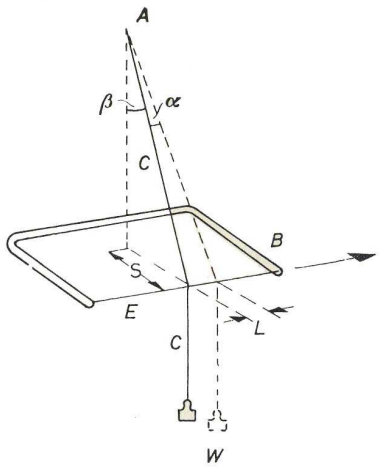

Figure 2-12. Howell Friction Measuring Device

A second filament was mounted horizontally on a frame B. The horizontal filament E was brought into contact with the filament C until it makes a vertical angle β. When this position was reached, the frame B was shifted in the direction of the arrow. Because of the frictional force, the filament E caused the filament C to achieve an equilibrium position. The filament C and then slips back a distance L. The author concluded that:

$$\mu = \frac{L}{S} \qquad (2\text{-}16)$$

On a similar principle Pascoe and Tabor [85] proposed the device as shown in the (Figure 2-13) that was used to measure the friction in the vacuum.

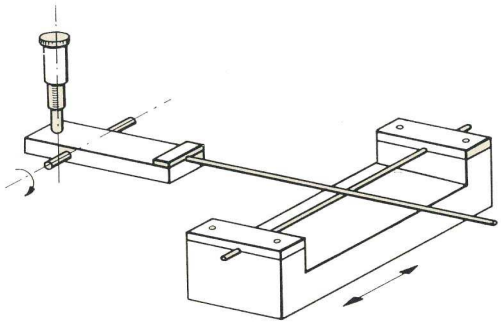

Figure 2-13. Pascoe and Tabor Friction Measuring Device

A device very similar to that of Mercer and Makinson (Figure 2-34) was adapted by Olofsson and Gralen [81, 82] although the mechanical system was slightly different. The filament A was fixed at one end of a balance B which was suspended on horizontal pins attached to a piano wire C. The load was obtained by fixing a known weight E on the side having the filament. The second filament F was mounted on another support that can move up and down using a support which is attached to a rotating disc. The rotating disc, A and F being in contact, the friction was measured by the torsion of the piano wire C (Figure 2-14).

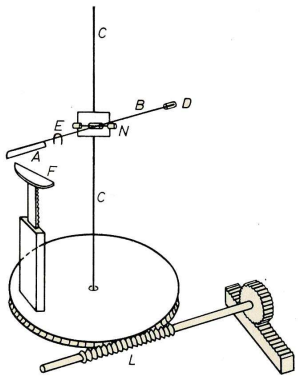

Figure 2-14. Olofsson and Gralen Friction Measuring Device

A more sensitive apparatus was described by Taylor [110] by using the same measuring principle as proposed by Postle and Ingham (Figure 2-10). In this instrument, the force required to remove a fibre from a bundle of known density was measured. The fibre bundle or a piece of sliver was held in a carriage. The carriage was pulled at a varying speed and the extracting force of the fiber was measured using a load cell. Lord [69] presented a very simple method of measuring the inter-fiber friction. Instead of measuring the force required to pull a fiber from a bundle of fibres he assembled a thin, fairly uniform parallel layer of fibers

(Figure 2-15). These fringes were about 2.54 (mm) wide and fiber density about 5 (mg/cm^2). The fringes AB and CD of are superimposed on a tray K capable of moving and loaded by a weight P. The end of the fringe CD is connected to the plate K while that of AB is linked to a measuring spring. By moving the tray K, the friction coefficient was estimated by the deflection of the spring S.

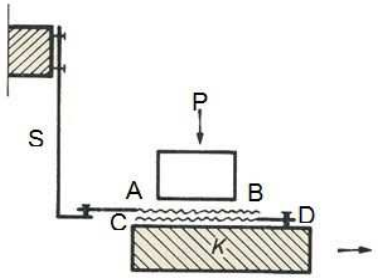

Figure 2-15. Lord Friction Measuring Device

Bartlett, Smith and Thompson [12] developed two systems to measure fibre friction. One system was the modified version of Anderson, Cox and Hardy' apparatus (Figure 2-11). This system was modified to use web instead of sliver to get drawing force and ultimately fibre cohesion and friction (Figure 2-16). Bartlett, Smith and Thompson [13] developed another testing device with only two sets of rollers driven directly by small synchronous motors (Figure 2-16) that was used to measure drawing force of roving. The measurement was performed by load cells mounted on the front rollers.

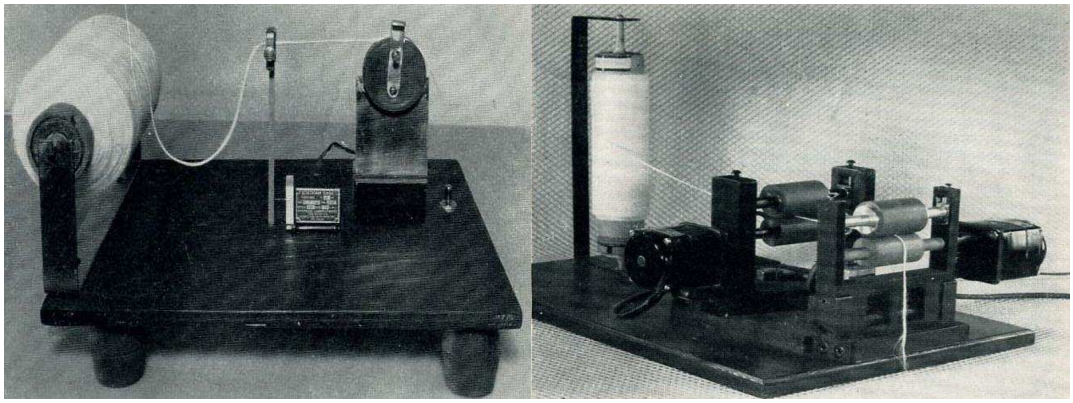

Figure 2-16. Bartlett, Smith and Thompson Friction Measuring Device

Davis [26] described an instrument based on the inclined plane method. In this device a single yarn was set as the level and movement of different materials has been studied with the help of a small needle. By using the same principle of the inclined plane, Howell [53] and Howell and Mazur [50] developed an apparatus for fiber to fiber friction

measurement. A fiber was placed on top of the fixed fiber and was slightly twisted. The inclination of the fixed fiber was increased until sliding of the yarn began to give the value of fibre friction (Figure 2-17).

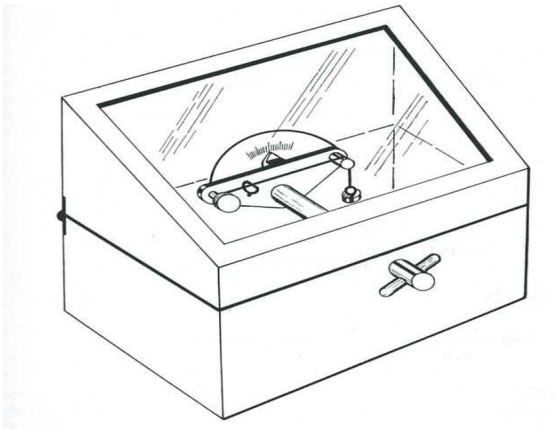

Figure 2-17. Howell and Mazur Friction Measuring Device

El Mogahzy [28] modified the device of Lord (Figure 2-15). El Mogahzy's device was containing a bottom clamp (C2) and top clamp (C1) with the fibre beard (B2) and (B1) on each clamps. The top clamp (C1) is attached to the load cell of the Instron tensile tester. Lateral pressure is applied by using a pneumatic system (Figure 2-18).

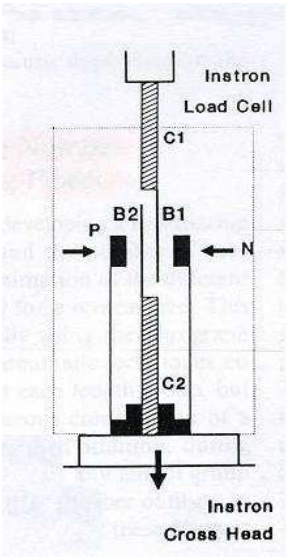

Figure 2-18. El Mogahzy Friction Measuring Device

Both the pressure bar (P) and the bottom clamp (C2) are mounted on the Instron cross head and move down with it. With this device we could measure the fibre-to-fibre frictional force and the fibre-to-metal frictional force.

The device of Armentieres (Figure2-19) was used by Burte [22] mainly to study the slivers of wool, while the cohesion meter "CRITER" was used by

Tarrin and Gouault [108]. This device was modified to study the short fibres. Mechanical decoupling was required to avoid the mechanical vibration and resonance. The spacing is adjustable between 3 to 10 cm as this device was developed to examine the medium and short staple fibers. The problem of noise was faced while measuring the signal frequency especially for speeds above 30m/min. This problem was solved by measuring the torque transmission to drawing roller unit, either by a power meter, a solution adopted by Olsen [84] or by measuring system torque by using load cells as the Kamarov [58] applied this principle in his apparatus.

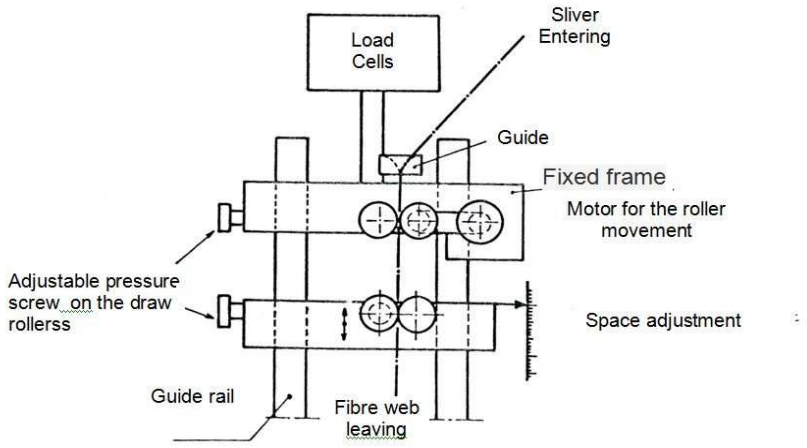

Figure 2-19. Armentieres Friction Measuring Device

Averous [5] adopted the principle of measuring the torque transmission to drawing roller unit by measuring the stretched side tension of the transmission belt that was connecting the drive pulley to drawing rollers that control its rotation. Its working principle was based on the fact that the sliver tension was proportional to the driving torque of the drawing rollers (Figure 2-20).

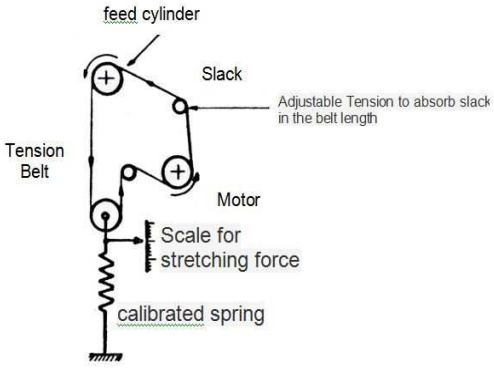

Figure 2-20. Averous Friction Measuring Device

Bartlett, Smith and Thompson [12, 13] developed three different devices to measure yarn friction based by using different measuring techniques. One simple device was developed to measure yarn to yarn friction at the point H (Figure 2-21). The measurement was performed by the use of a piezoelectric sensor.

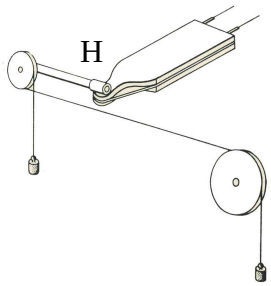

Figure 2-21. Bartlett, Smith and Thompson Friction Measuring Device

Taylor [110, 111] and Vittie [116] have done extensive amount of research to study the behavior of fibres during drawing process. Taylor studied fibre movement in the drafting zone by the use of radioactive fibers and with the help of two sensors located at the front roller and back roller. Vittie [116] developed a new method to visually observe the different fibers as they pass drafting zone (Figure 2-22). Cotton fibers were dyed red and their movement was observed as the fibres pass through the drafting zone.

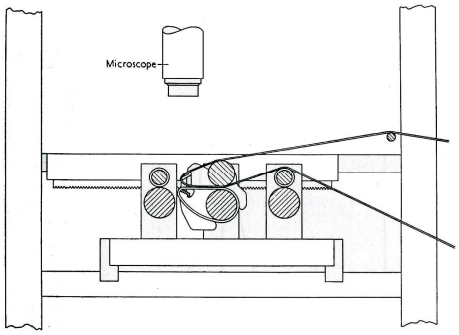

Figure 2-22. Vitti Friction Measuring Device

Scheier and Lyons [99] modified the Olfson's instrument. He used an electric sensor to measure frictional force instead of a piano cord.

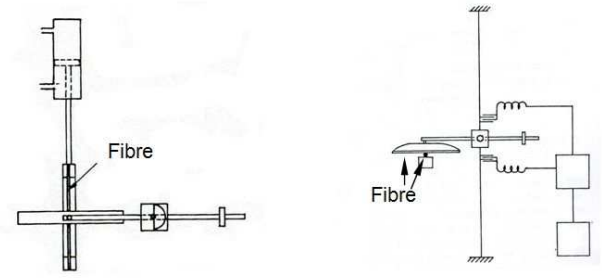

Figure 2-23. Scheier and Lyons Friction Measuring Device

Wood [121, 122] described an instrument for the measurement of fiber kinetic friction A single fibre was pulled from a package. A filament was attached with an adhesive to a horizontal bar suspended on wire torsion (Figure 2-24). The compressed bundle of fibres was held in a movable carriage, which can be moved at different speeds.

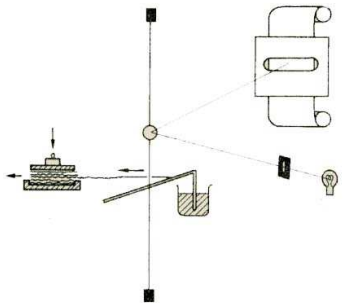

Figure 2-24. Wood Friction Measuring Device

A mirror was fixed to the torsion wire and its arrow. The frictional forces between the filament and the fibre bundle were recorded.

Graham [41] and Brook [18] used a cohesion measuring device "Spin Draft Tester". This device was used to measure drawing force between the drafting rollers (Figure 2-25).

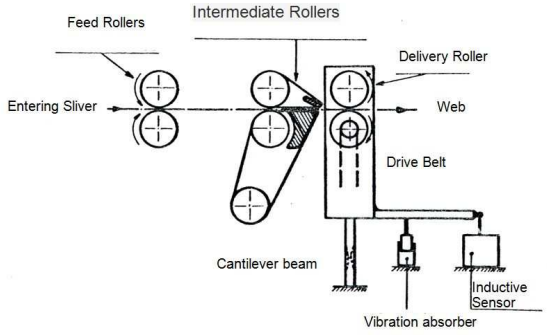

Figure 2-25. Spin Draft Tester

Audivert *et al*. [3] and Hannah [45] presented their study to overcome the problems of vibration and resonance couples. The problem was solved by introducing a compressive force sensor or a pressure sensor. On a

principle substantially identical, Plonsker [87] and Scardino [96] presented the American Viscose Instrument (Figure 2-26).

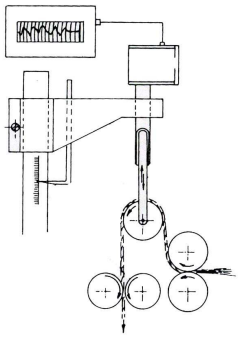

Figure 2-26. American Viscose Instrument

Lawson *et al.* [63] used another apparatus that has the problem of vibration and resonance couples. The instrument is shown in the (Figure 2-27). In this apparatus, the compression parameters of the ribbon in the drawing zone were more unclear. Indeed, when the drawing force on the sliver increased, the pressure on the roller guide also increased which increased the inter-fiber cohesion based on the resonance phenomenon of the drawing force.

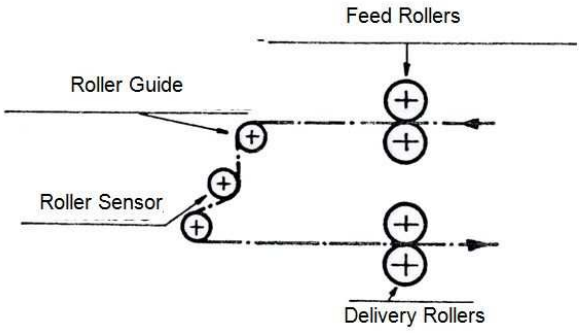

Figure 2-27. Lawson Friction Measuring Device

In addition, the roller guide created two drafting zones and the drafting zone spacing has no importance.

Nowrouzieh [80] observed that the results obtained by the measurement of the drawing forces are difficult to interpret and that the assessment of frictional forces is also difficult. Many factors affect the measured results particularly the sliver evenness. In some cases, the study of sliver load-elongation curve would be more useful than the drawing force measurement.

Basu [14]developed a sensor that can measure the force in horizontal and vertical directions by using two load cells S mounted on 2 plates at 90 as shown in the (Figure 2-28).

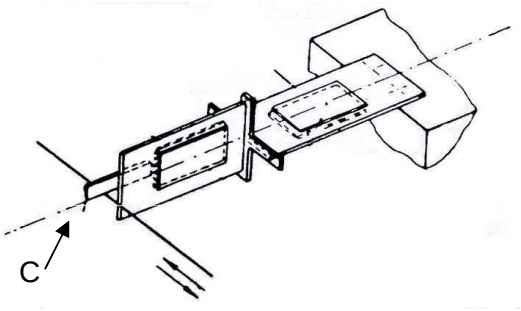

Figure 2-28. Basu Friction Measuring Device

Friction was measured by the plate C, which affects the fiber surface in one direction at a given velocity and normal force.

Anderson, Cox and Hardy [2] designed two instruments to measure the frictional force based on the principle of pulling a long single filament from a strand of fibres. In the first instrument, the static pulling force was measured of a single fiber from a strand of fibres held a vertical glass tube (Figure 2-29).The free end of the fiber was attached to a polyamide yarn wound around a disc. The extraction force of the fiber corresponds to the tangential point by the disc rotation.

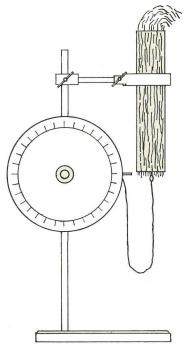

Figure 2-29. Anderson, Cox and Hardy Friction Measuring Device

The change in the diameter of the glass tube was used to vary the conditions of initial pressure.

In the second device, which was based on the principle of Wood [122], the only difference was the method of holding the fibre strand.

On the basis of principle used by Lord [69], Vernekar [113] described a methodology in which the carriage was pulled by a tensile testing machine (Figure 2-30).

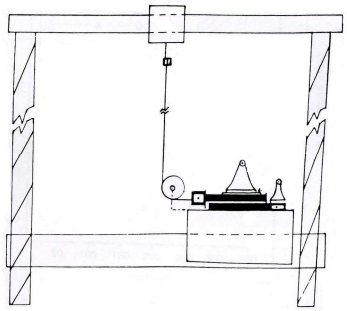

Figure 2-30. Anderson, Cox and Hardy Friction Measuring Device

A new cohesion and friction measuring method known as "Rotor Ring" was designed by Ghosh [40] and El Mogahzy [31]. This method was based on the principle of measuring the fibre opening energy. Ghosh used the conventional ”Rotor Ring" (Figure 2-31) to measure the energy while the El Mogahzy made a slight change and added a carding segment on the inner surface of the rotor (Figure 2-32).

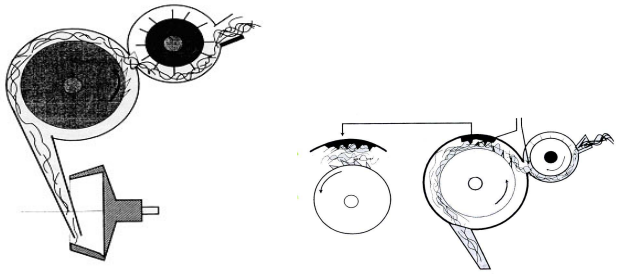

Figure 2-31. Ghosh Friction Measuring Device Figure 2-32. El Mogahzy Friction Measuring Device

Nowrouzieh [80] developed an instrument to measure inter-fibre friction which was know as Static Friction Tester (SFT). The SFT consists of two identical clamps (Figure 2-33). One of them is fixed, whereas the second is moving through a linear guide. The load type cell force sensor is attached with the fixed clamp. A piece of sliver is put down in the channel of the two clamps which are initially in zero gage position. The sliver is compressed with the upper clamp sides where two identical weights are loaded. The moving one is tracked with a constant speed, whereas the fixed one is attached, by the intermediate of a force sensor, to the frame. The distance between the two carriages is measured by displacement sensor.

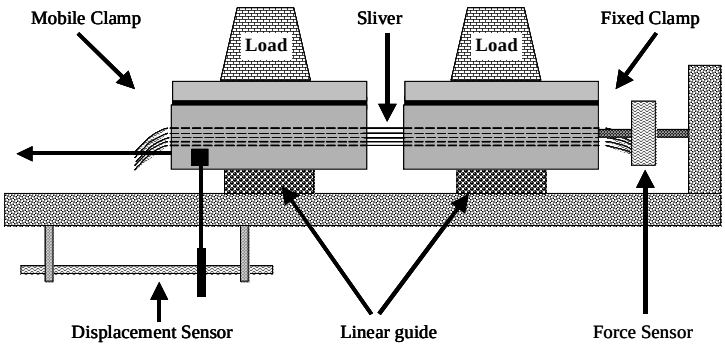

Figure 2-33. Static Friction Tester

The data obtained from SFT gives rise to the following equation to get the inter-fibre friction results:

$$F/N_F = k\,(W/\,N_F)^a \qquad (2\text{-}17)$$

Where:

F: the frictional resistance force,

N_F: the number of fibres in sliver cross-section,

W: the perpendicular compression force on fibre,

K, *a*: the coefficients that characterize friction.

2.6.2 Friction Measurement of Friction between different materials

In this group, the devices that measure friction between different materials will be discussed for example fibre to metal, fibre to plastic etc.

The instrument of Mercer and Makinson [74] was suitable for measuring the fiber friction between fiber and fibre or fiber against any solid material. The fibre F to be examined is mounted, under slight tension, by means of wax on a glass bow B on one arm of a balance A, which is damped by a mica vane V dipping into a dashpot of oil. A force is applied to the permanently magnetized needle N mounted at the opposite end of A, by passing a current through the solenoid I; when a fixed load is required a weight hung on the arm may replace the electromagnetic system. The fibre is thus pressed against a surface H which may be another fibre but in our experiments on wool was usually a cylindrical piece of polished horn, which is chemically very similar to wool and, as a rubbing surface, is much more convenient than a second fibre. The surface H is mounted on the end of a piece of clock spring S which also carries a mirror M. The fibre is moved forward against H by means of the hydraulic system, which drives the platform carrying the fibre at a velocity which can be varied between 0.01 cm/sec. and 0.1 cm/sec.

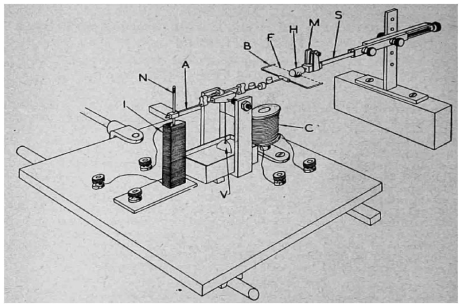

Figure 2-34. Mercer and Makinson Friction Measuring Device

As the fibre moves forward the surface H sticks to it and the spring was deflected until its elastic restoring force becomes equal to the maximum force of static friction.

Krumme [61] proposed another model to measure friction. In this method, a loop of yarn was wrapped around a cylinder of large diameter (Figure 2-35). The rotation of the cylinder results in a shift of the position x relative to its initial position vertically.

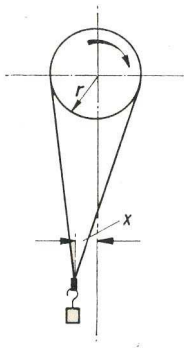

Figure 2-35. Krumme Friction Measuring Device

Krumme deduced the coefficient of friction by the following equation:

$$\mu = \frac{1}{\alpha} Ln \frac{r + x}{r - x} \qquad (2\text{-}18)$$

Where

x: horizontal displacement,

α : Contact angle between the line and the roll surface.

Speakman and Stott [105] were the first to apply inclined plane principle to measure the fibre frictional forces. They used a set of wool fibers stretched and fixed between two parallel ridges oriented in the same plane. The coefficient of friction between a fabric and fiber is determined by measuring the angle from which the whole system begins to slide (Figure 2-36).

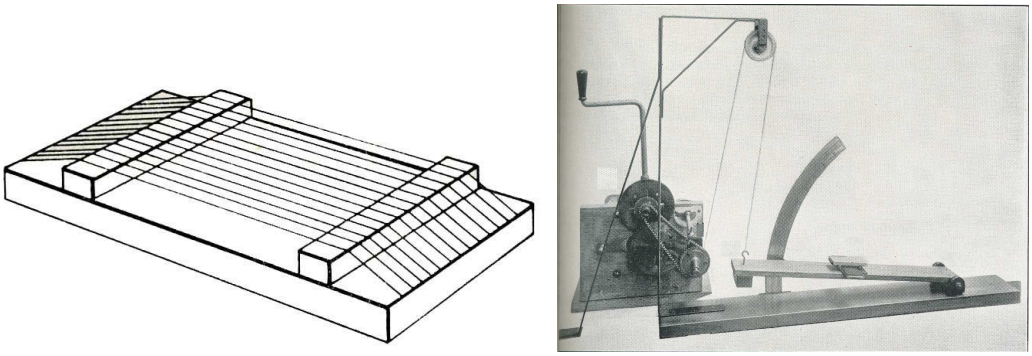

Figure 2-36. Speakman and Stott Friction Measuring Device

Kaidanovsky and Haykin [57] highlighted the phenomenon of stick-slip by using the device proposed by Mercer and Makinson [74]. This apparatus is suitable for measuring friction of a fiber against any other solid material which is positioned in place of the fiber K.

Saxl [94, 95] developed a measuring device based on the principle of Krumme's device (Figure 2-35). A loop yarn whose ends were connected to two horizontal levers D and G wound around a cylinder A (Figure 2-37). A rotation of the cylinder caused the tilting of levers D and G.

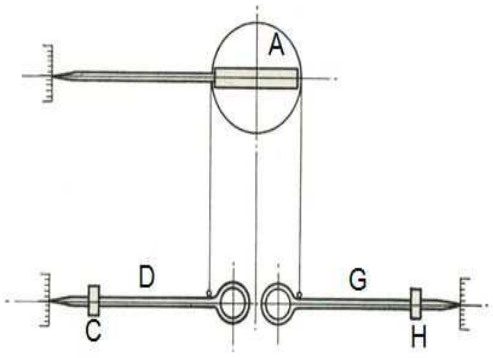

Figure 2-37. Saxl Friction Measuring Device

The tilt of the horizontal levers was recovered with the help of the two masses C and H. The coefficient of friction μ was then calculated using the law of Amontons.

Morrow [79] described an instrument for measuring the coefficient of kinetic friction of a yarn traveling at higher speed (Figure 2-38). The yarn passes over a large pulley against which the friction was measured. This pulley rotates around a point P off-center. During dynamic testing the assembly is held in equilibrium by the weight W mounted on a moving needle.

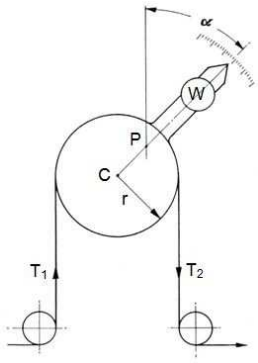

Figure 2-38. Morrow Friction Measuring Device

The coefficient of friction was calculated by the following equation:

$$e^{\mu\theta} = \frac{T_2}{T_1} = \frac{1 + N\sin\alpha}{1 - N\sin\alpha} \qquad (2\text{-}19)$$

With N = CP/r

By using the principle in which the yarn was fixed on a cylinder having a certain diameter. The cylinder was rotated at certain speed to measure the friction between yarn and the cylinder. Based on this principle, Mercer [75, 76 and 77], King [59] and Roder [91] developed three different measuring devices that differ only by the sensors used to measure the friction.

The first used an electrical measuring unit (Figure 2-39), the second used an optical system (Figure 2-40), and the third one used a torsion balance (Figure 2-41).

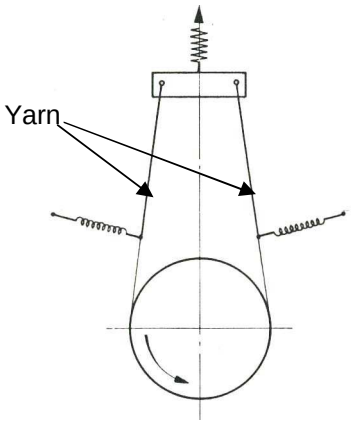

Figure 2-39. Mercer' Device

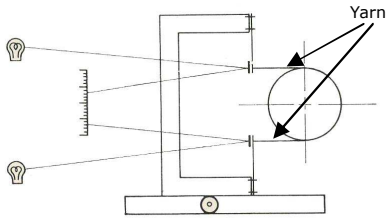

Figure 2-40. King's Device

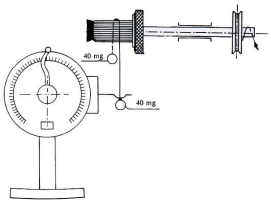

Figure 2-41. Roder' Device

Buckle and Pollitt [20] developed a device that gave the friction coefficient directly. The instrument consists of two unequal arms R1 and R2 (Figure 2-42) carrying the freely rotating pulleys C and D at each end (frictionless). This lever system rotates around the point O. A cylinder was fixed at point G. Friction was measured with respect to the fixed cylinder.

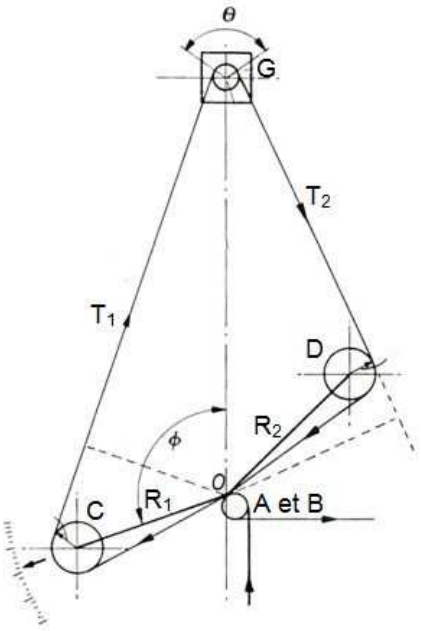

Figure 2-42. Buckle and Pollitt Friction Measuring Device

Sellers [100] described a method in which a yarn is clamped between a horizontal stretcher under a certain load (Figure 2-43). The weight W applied to the upper part of the clamp, yarn was pressed on the both sides. The tension T required to move the yarn at a constant speed was measured with a system of three pulleys (frictionless) by a dynamometer.

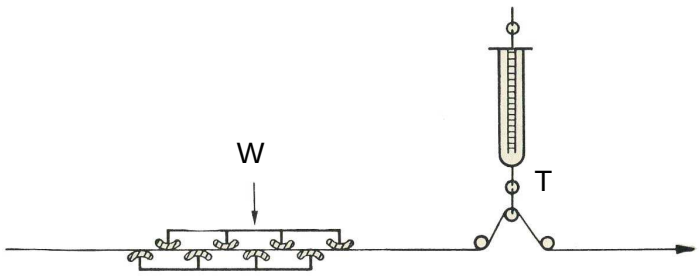

The following equation was used to calculate the friction:

$$\mu = \frac{T - C}{2W} \qquad (2\text{-}20)$$

The value of C corresponds to the yarn extraction force when W = 0.

A 2nd more complex apparatus was designed by Bartlett, Smith and Thompson using an electronic system. In this instrument the yarn was examined at a given tension that will produce friction on a piano wire at a constant speed (Figure 2-44).

Figure 2-44. Bartlett, Smith and Thompson Friction Measuring Device

The friction vibrates the piano wire and the vibrations were recorded using a piezoelectric sensor. However, this device was only suitable for continuous untwisted yarn or with very small amount of twist. Bartlett, Smith and Thompson [12] described a 3rd device called "slow-speed friction tester" in which the friction was measured using a load cell. The yarn was drawn on 5 steel cylinders of diameter of about 4.76 mm (Figure 2-45).

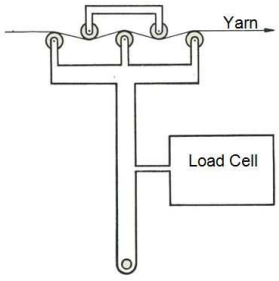

Figure 2-45. Bartlett, Smith and Thompson Friction Measuring Device

The system was made of three lower rollers and two top rollers. The authors hypothesized that the static frictional force was equal to the maximum deflection which was equal to the force just before the slippage. Roder [92] described a method in which a yarn was clamped between two plates under a certain load W (Figure 2-46).

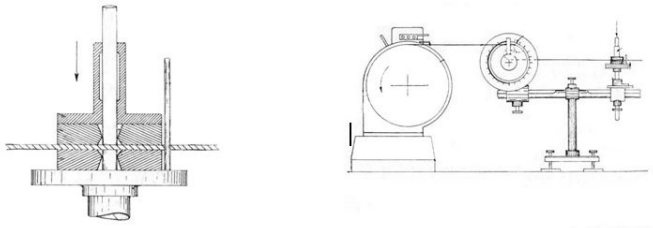

Figure 2-46. Roder Friction Measuring Device

The following equation was used to calculate the friction:

$$\mu = \frac{T}{2w} \qquad (2\text{-}21)$$

The Lepidometre instrument was developed for the measurement of wool fibres and other fibres creep. It was designed by Speakman, Chamberlain and Menkart [106]. The wool fiber was placed between two surfaces that were under a variable pressure vertically. The other end of the fiber was connected to a monitor. For every alternative motion of the friction device, the normal load on this device was increased. When the load was sufficient to cause fibre breakage, the value was recorded. The instrument consists of three main parts (Figure 2-47) (a) two frictional surfaces with a drive mechanism coupled to an electric motor at a constant speed, (b) a load measuring mechanism consisting of (c) a recording mechanism which automatically draws the load-time curve.

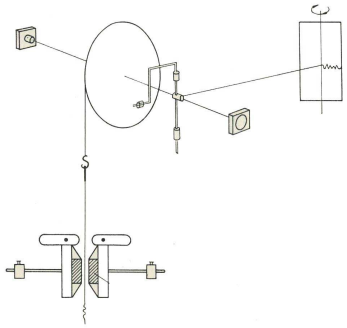

Figure 2-47. Speakman, Chamberlain and Menkart Friction Measuring Device

Chapter 3-Modified Static Friction Tester

3.1 Introduction

The purpose of this research is to improve the existing experimental device that was developed by Nowrouzieh (2007). The device is used to measure the inter-fibre friction. The purpose of this study is also to reveal possible relationships between the technological characteristics of fibres and the characteristics of the yarn spun from these fibres. In this chapter we will discuss the Static Friction Tester (SFT) and the problems faced while working on SFT. The modification made to the SFT protocol to run the modified SFT will also be discussed.

3.2 Static Friction Tester

The friction measuring device is based on the principle of measuring the force required to break a sliver. According to the studies related to the friction, it is necessary to control the normal force during relative movement of bodies in contact. Therefore the fibres in the sliver are tightened using a uniform normal load as shown schematically in Figure 3-1. Subsequently, the fibres in the sliver move relative to each other by simply pulling the sliver axially with two identical and opposite force (horizontal arrows in Figure 3-1). The force that the fibres develop to oppose their relative sliding force is the inter-fibre friction.

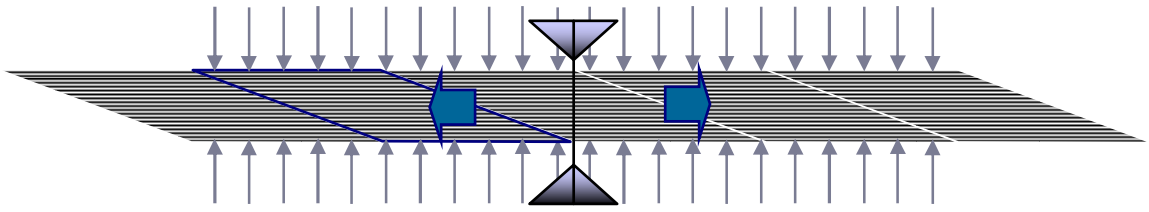

Figure 3-1. Measuring Principle

The Static Friction Tester consists of two identical little carriages (Figure 3-2). One of them (A) is fixed, whereas the second (B) is moved along a linear guide (C). A piece of sliver is put down in the channel (D) of the two carriages which are initially in zero displacement position, i.e. the two carriages are in contact. The sliver is compressed with the upper carriage sides (E) where two identical weights are loaded (W). The moving clamp is pulled by the cross head of the traction machine with a programmable constant speed, whereas the fixed one is attached, by the intermediate of a force sensor, to the frame.

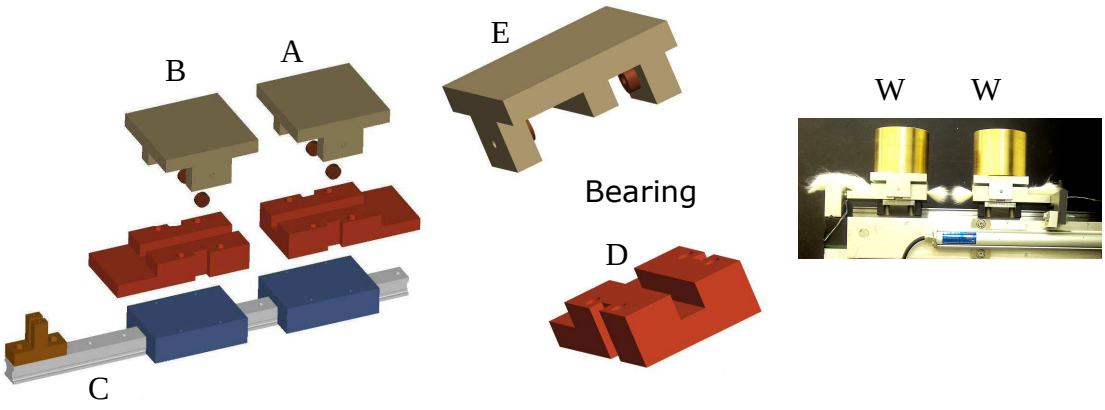

Figure 3-2. Components of Static Friction Tester [80]

The distance between the two carriages is periodically measured by displacement sensor during the test. Each clamp is composed of two parts, the cover and the body. The cover is T form supports the loads on its upper side, whereas the body is U form (Figure 3-3).

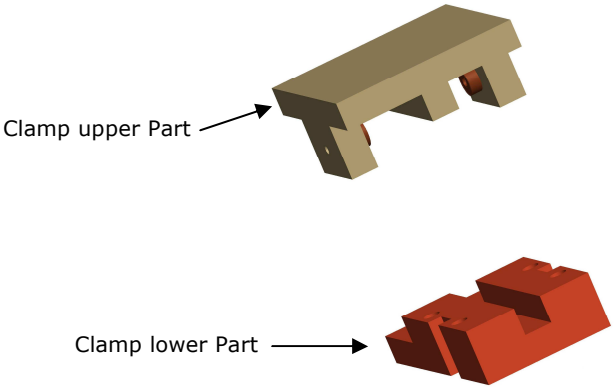

Figure 3-3. Clamps of Static Friction Tester [80]

These two parts fit together holding the sliver inside. In order to avoid an uncontrolled slippage between the sliver and the clamp inside walls, the upper and lower parts of the clamp are covered with a thin cotton layer with the help of a double sided tape as shown in figure 3-4.

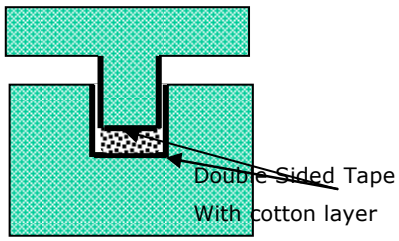

Figure 3-4. Cotton layer on the top and bottom of the clamp [80]

3.3 Shortcomings in Static Friction Tester (SFT)

The following problems were observed while working on the Static Friction Tester.

- The SFT was connected to dynamometer to apply pulling force to the moving carriage. A string was used to connect moving carriage with the dynamometer as shown in the Figure 3-5.

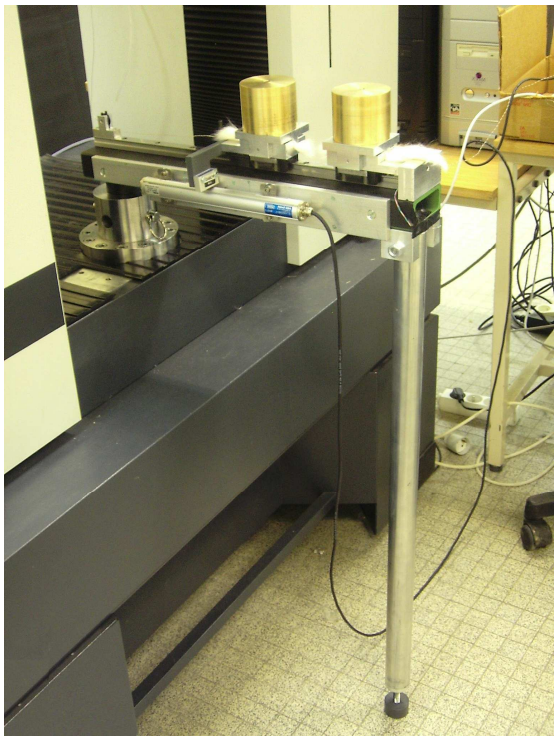

Figure 3-5. Static Friction Tester

Although the selection of the string was done carefully, it still had some effect is the obtained results. This string might be a cause of errors during the testing.

- The force sensor used was not highly accurate and sensitive enough as it only gave the accurate values to first decimal point.
- While the SFT should be properly levelled to get accurate result, this was not easily possible with this version.
- The portability of the SFT was not easy as a traction machine was needed to conduct test.
- The fixed clamp should be moved after some tests and a small amount of oil or grease should be put on the linear guide to avoid any friction produced between fix clamp and linear guide. The demounting of the fixed clamp was difficult in this version.

The SFT was modified to solve the above mentioned problems.

3.4 Modified Static Friction Tester (SFT)

The measuring principle is the same as the earlier version. There were small mechanical modifications made to the apparatus. The modified Static Friction Tester consists of two parts:

- Control Unit
- Measuring Unit

3.4.1 Control Unit

The control unit (Figure 3-6) is a fully secured electricity supplying system which was incorporated with the modified static friction tester to make it safe and secured to operate. It is also equipped with data acquisition cards that are used to collect the analogue signal from the two sensors. The acquisition cards also help to control the SFT and to do the testing semi-automatically.

Figure 3-6. Control Unit Interior

The control unit consists of following parts:

- SCON Controller
- Transformer
- USB Hub and Power Supply for USB Hub
- 24V Power Supply

- Force Sensor Conditioner
- Interface for PIO Cable
- Circuit Breakers
- Contactor and Relay
- Fuse for Transformer
- Data Acquisition Cards
- Cable Ducts and Cable Connecters

All technical details are given in annex A, while important features of the devices are described hereafter.

3.4.1.1 SCON Controller

The SCON is a single-axis AC servo controller capable of controlling actuators in the positioner mode or the pulse-train input mode.This is the control unit for the linear actuator used in the improved SFT. It is used to control the movement and speed of the linear actuator. The SCON is equipped with following main parts:

- LED indicators: These LEDs indicate the condition of the controller.
- System I/O connector: This connector is used to connect the emergency stop switch, etc.
- Motor connector: This connector is used to connect the motor power cable of the actuator.
- Power connector: This power connector accepts a 100/200-VAC single-phase power supply.
- PIO connector: This connector is used to connect to the host controller (PLC, etc.) via the PIO (parallel input/output) cable. It consists of a 40-pin flat connector and constitutes a DIO group of 16 inputs and 16 outputs.
- Encoder/sensor connector: This connector is used to connect the encoder/sensor cables of the actuator.

3.4.1.2 Transformer

A transformer is a device that transfers electrical energy from one circuit to another through inductively coupled conductors—the transformer's coils. By appropriate selection of the ratio of turns, a transformer thus enables an alternating current (AC) voltage to be "stepped up" or "stepped down". The control unit is equipped with a step down

transformer. This is used to step down voltage to be used for the data acquisition cards and other components of the control unit.

3.4.1.3 USB Hub and Power Supply for USB Hub

A USB hub is a device that expands a single USB port into several so that there are more ports available to connect devices to a host system. As the data acquisition card and the SCON controller has USB connecters. The USB hub is used to in the control unit to connect all the USB connecters to the host unit. As the hub requires 5V so a power supply with an adapter is also incorporated with the control unit.

3.4.1.4 24V Power Supply

There are two 24V supplies are used in the control unit. One 24V supply is used to supply current to the force and displacement sensors. While the other one used to supply PIO interface.

3.4.1.5 Force Sensor Conditioner

Conditioner is an electronic circuit for processing the signal from a sensor. It is used to simplify the interface with the sensor data acquisition system. In a measurement chain, the conditioner is made between the sensor and the interface. It formats the measured signal to translate it into a size allowing the processing (e.g. voltage, current, frequency). The control unit has a conditioner for the force sensor.

3.4.1.6 Interface for PIO Cable

The interface components are used as an alternative to the point-to-point wiring system in order to reduce costs and to simplify the setup of the electrical cabinets. The main function of this interface is as an adapter between the control devices and field elements. The interfaces consist of standard connectors for connection to the control devices and easy to install in electrical cabinets. The advantages of the interface system are as follows: saves time during the installation, no risk of wiring mistakes, improved order in the electrical cabinet and saves space in the cable ducts. The two passive 20 pole are used in the control unit. Theses interface are used to control the SCON controller with the help of software. The interfaces are based on the one-to-one electrical connection between SCON controller and the data acquisition card connections. The digital signals are transferred to control the linear actuator.

3.4.1.7 Circuit Breakers

A circuit breaker is an automatically operated electrical switch designed to protect an electrical circuit from damage caused by overload or short circuit. Its basic function is to detect a fault condition and, by interrupting continuity, to immediately discontinue electrical flow. The control unit is equipped with Residual Current Device for the overall security and safety. Residual Current Device is a generic term used for Residual Current Circuit Breaker with Overload protection (RCBO). A Residual Current Circuit Breaker with Overload protection (RCBO) is an electrical wiring device that disconnects a circuit whenever it detects that the electric current is not balanced between the energized conductor and the return neutral conductor. It combines the functions of over current protection and leakage detection. The control unit is also equipped with three simple circuit breakers. These are used for the safety of the 24V power supply, force sensor, displacement sensor etc.

3.4.1.8 Contactor and Relay

A contactor is an electrically controlled switch used for switching a power circuit, similar to a relay except with higher current ratings. A contactor is controlled by a circuit which has a much lower power level than the switched circuit. This is used in the control unit to control the current for the linear actuator.

3.4.1.9 Fuse for Transformer

A fuse is a type of low resistance resistor that acts as a sacrificial device to provide over current protection, of either the load or source circuit. This is used for the safety of the step-down transformer used in the circuit.

3.4.1.10 Data Acquisition Cards

Data acquisition is the process of sampling signals from the sensors and converting the resulting signals into digital numeric values that can be manipulated by a computer. Data acquisition systems (abbreviated with the acronym DAS or DAQ) typically convert analog waveforms into digital values for processing. The components of data acquisition systems include sensors that convert physical parameters to electrical signals, the signal conditioning circuits to convert sensor signals into a form that can be converted to digital values and the analog-to-digital converters, which convert conditioned sensor signals to digital values. The control unit is

equipped with one data acquisition card (NI USB-6210). This card is used to acquire the analogue signals of force and displacement sensors. The NI USB-6210 is a multifunction data acquisition (DAQ) module for USB that is optimized for superior accuracy at fast sampling rates. It has 16 analog inputs, four digital input lines, four digital output lines and four programmable input ranges. This card does not require external power. The control unit also has a bus-powered USB device (NI USB-6525). This is used to control the linear actuator by using digital signal. Data acquisition applications are controlled by software programs. In this case the Labview software is used.

3.4.1.11 Cable Ducts and Cable Connecters

The cable ducts are used to hold the wires that were used to connect different components of the control unit. The cable connecters are used to connect the control unit to the main supply, the linear actuator, the force sensor etc.

The control unit is fully independent electrical cabinet. You just have to connect it to an external power supply for the electric current and to a PC by a USB cable to control the linear actuator (Figure 3-7).

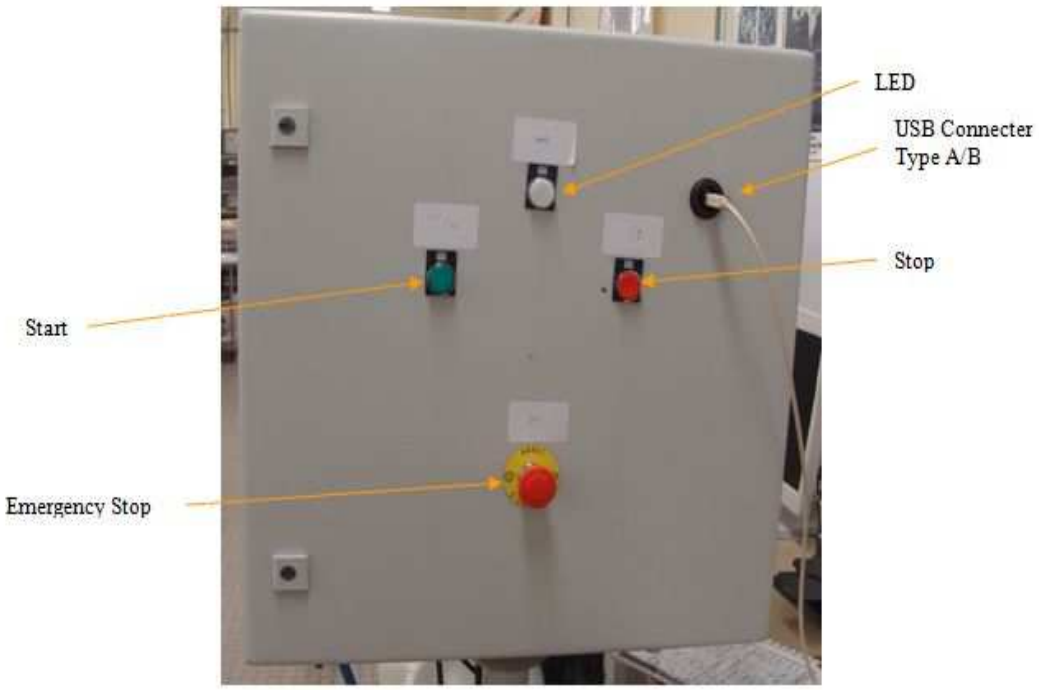

Figure 3-7. Control Unit Exterior

The door of the control unit (electrical cabinet) consists of a LED, start, stop and emergency buttons. There is also a USB connecter to connect the control unit to a computer. The detailed circuit diagram of the control unit can be found in Annex A.

3.4.2 Measuring Unit

The mechanical structure of the modified SFT is similar to the earlier version and the measuring principle also remains the same. The following new components are added to the earlier version (Figure 3-8).

- Linear Actuator
- Force Sensor
- Mechanical Linkage Liaison

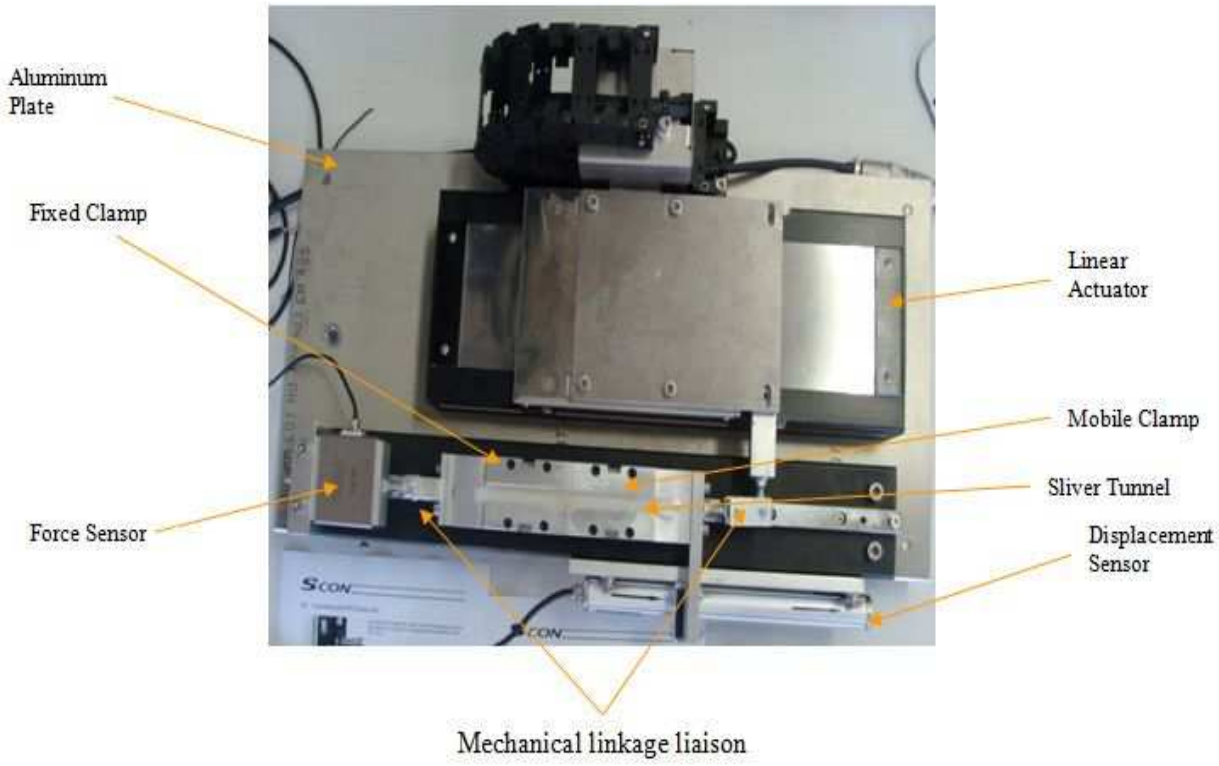

Figure 3-8. Measuring Unit

3.4.2.1 Linear Actuator

A linear actuator is an actuator that creates motion in a straight line. As for the friction testing we also require motion in a straight line so that a linear actuator is used. It has moving range from 0 to 100mm. The line diagram of the linear actuator is shown in the Figure 3-9. The 'slider' part of the actuator moves in a straight line. The moving clamp of SFT is

attached to the slider. By using the linear actuator, the problem posed by the string has been solved. The use of linear actuator also helps in easy portability of the SFT as we do not need a traction machine for friction measurement.

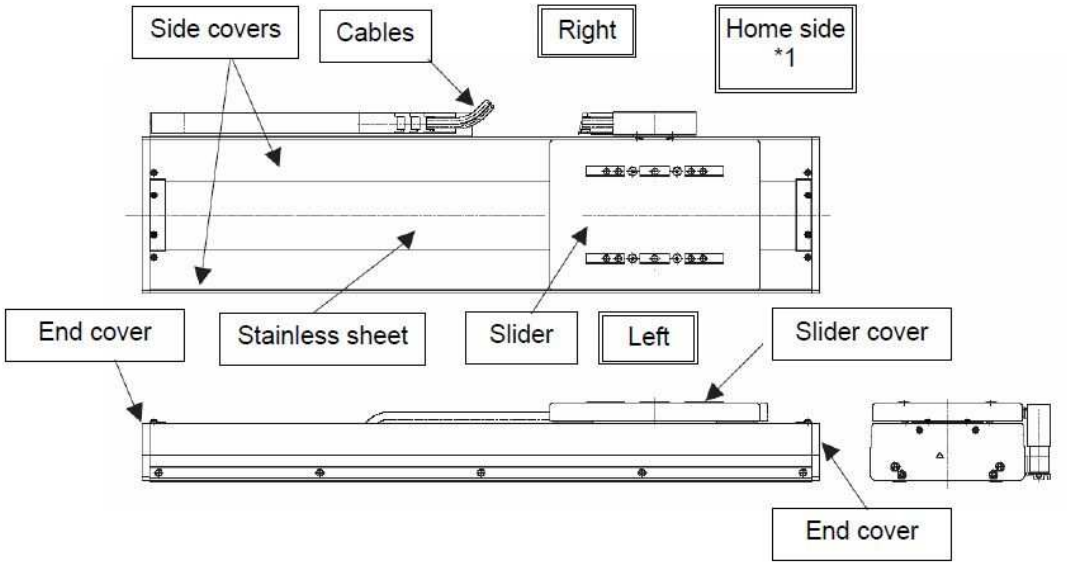

Figure 3-9. Linear Actuator

3.4.2.2 Force Sensor

The measuring unit is equipped with a more precise force sensor (FN3148) which is load cell type sensor. The load cell gave accurate value up to three decimal points. A load cell is a transducer that is used to convert a force into electrical signal. This conversion is indirect and happens in two stages. Through a mechanical arrangement, the force being sensed deforms a strain gauge. The strain gauge measures the deformation (strain) as an electrical signal, because the strain changes the effective electrical resistance of the wire. The FN3148 is a high precision load cell features accuracy of 0.05% F.S. It has high accuracy. It can measure compression as well as tension. The measurement range is from 0 to 100N. By using the more accurate force sensor, the problem of low accurate force sensor in the earlier version is also solved.

3.4.2.3 Mechanical Linkage Liaison

The force sensor is connected with fixed carriage using the mechanical linkage liaison (spherical). This is also used to connect slider of the linear actuator with the moving carriage to apply the pulling force. A mechanical

linkage is an assembly of bodies connected to manage forces and movement. Mechanical linkages are usually designed to transform a given input force and movement into a desired output force and movement. The two linkage used are shown in Figure 3-10.

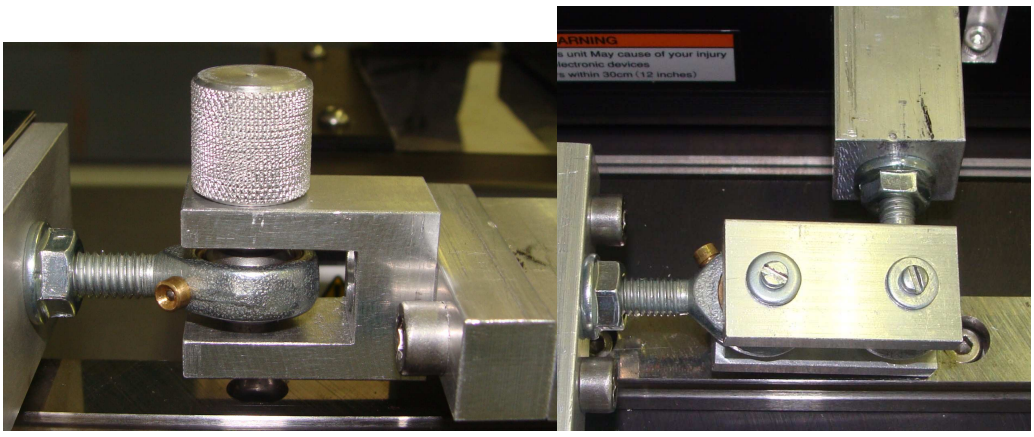

Figure 3-10. Mechanical Linkage Liaison

The purpose of this type of linkage that the actual force is transformed not the couple produced. The heim joint is used for these linkages. A heim joint, also known as a rod end bearing is a mechanical articulating joint. Such joints are used on the ends of control rods, steering links, tie rods, or anywhere a precision articulating joint is required. A ball swivel with an opening through which a bolt or other attaching hardware may pass is pressed into a circular casing with a threaded shaft attached (Figure 3-11).

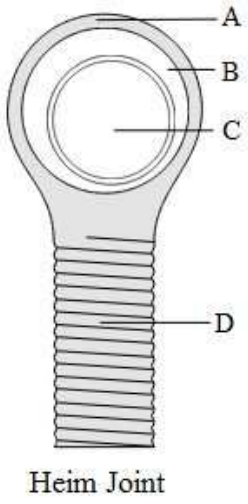

Figure 3-11. Heim Joint

Where A is the casing, B is the ball swivel, C is the opening for attaching other parts and D is the threaded shaft. The threaded portion may be either male or female. The demounting of fixed clamp is easy due to the

use of this linkage. So oil can be put easily between the fix clamp and the linear guide so this solved the problem present in the earlier version. The improved SFT is mounted on an aluminium plate that is equipped with four adjustable feet so that SFT could be levelled easily.

3.5 Mechanical Play/backlash Problem

The initial experiments on the improved Static Friction Tester showed some problems in the measured force values. The close observation of the apparatus showed that the cause of this problem is the "play". The Play or backlash is defined as the maximum distance through which one part of something can be moved without moving a connected part. Theoretically, the backlash should be zero, but in actual practice some backlash must be allowed to prevent jamming. It is unavoidable for nearly all reversing mechanical couplings, although its effects can be negated. Depending on the application it may or may not be desirable. The source of this play is the mechanical linkages used in the modifications. The problem can be shown if we plot a graph of the force values Figure 3-12.

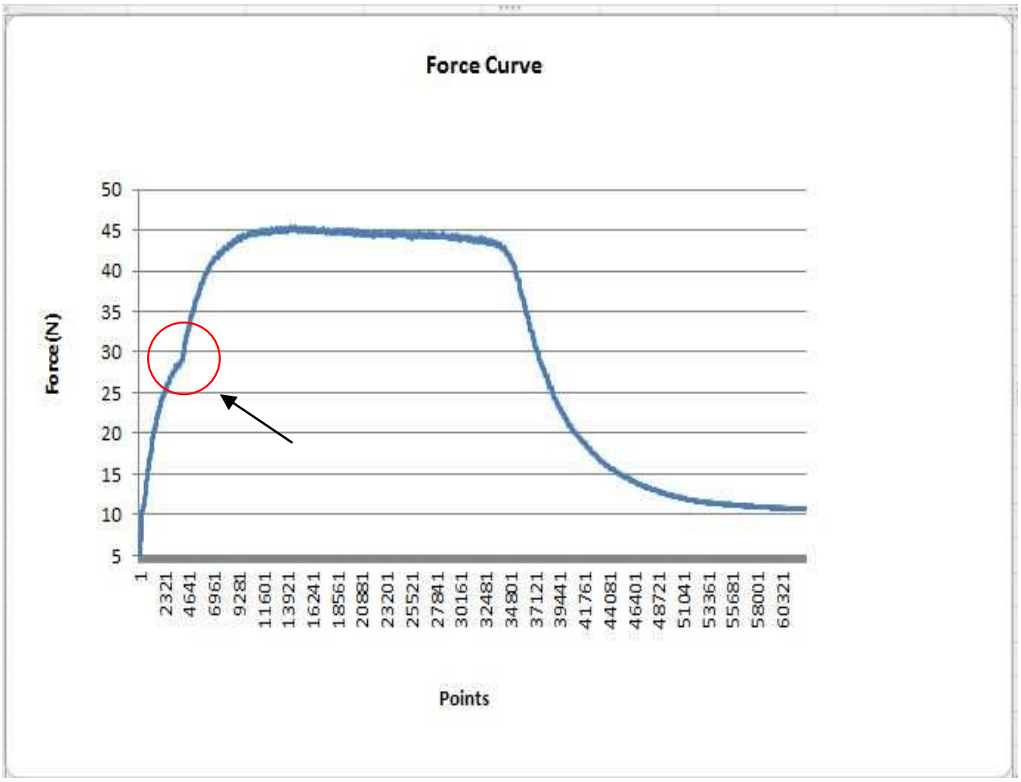

Figure 3-12. Force Curve

The value of the force should increase gradually, but there is some decrease in the values at a certain point shown by the circle in the figure. To solve this problem, further mechanical modifications are made to the

apparatus. The springs are added on the both side with the mechanical linkage. The springs will absorb the small amount of play present in the mechanical set up and we will get the smooth curve. These mechanical modifications are shown in the Figure 3-13.

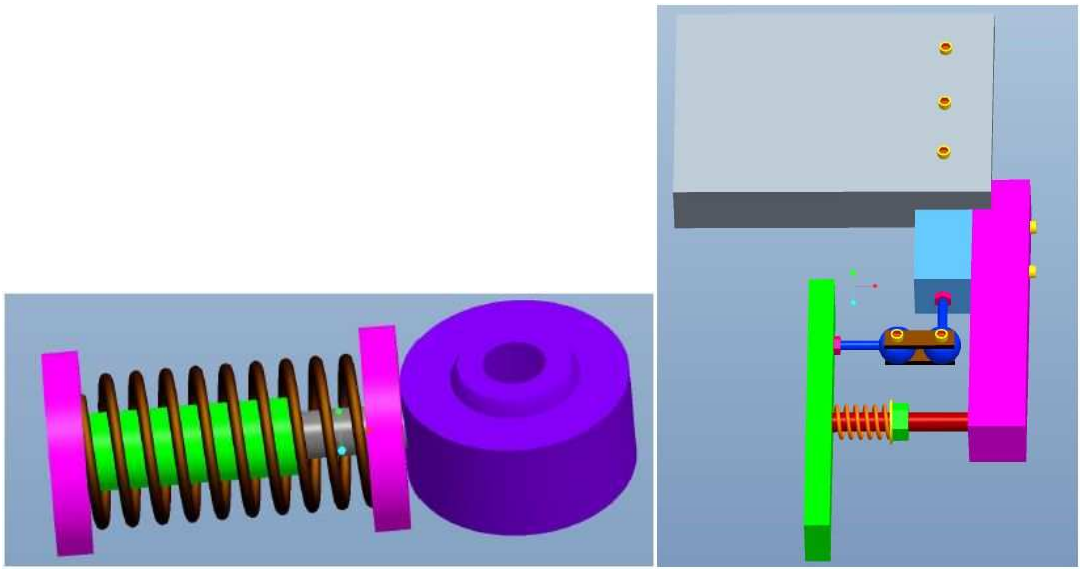

Figure 3-13. Modified Mechanical Linkage

The further experiments confirmed the solution of the mechanical play problem.

3.6 Static Friction Tester Operating programme

The data acquisition card is used to acquire the analogue signals from the force and displacement sensors. As the data acquisition cards are controlled by the software, Labview software is used to perform all the activities. Labview programs are called virtual instruments (VIs). Each VI has two components: a block diagram and a front panel. Controls and indicators on the front panel allow an operator to input data into or extract data from a running virtual instrument. However, the front panel can also serve as a programmatic interface. We have written a small program in Labview to control the SFT and acquire data simultaneously. The program is called as SFT VI. The block diagram of the program is shown in the Figure 3-14.

We have used two while loops as we will be performing two tasks simultaneously. One while loop is for the linear actuator control. The SCON controller is connected to NI USB-6526, through an interface, which is then connected to the computer. The SCON controller can be programmed for 36 different functions. But we have only chosen six basic

functions. PC1 and PC2 functions are used to configure the positions of the linear actuator. There is possibility of configuring 256 different positions. Pause function is to stop the linear actuator while start function is to start the movement of the actuator. An alarm is reset when the reset function is in operation. The linear actuator remains ON while this servo on function is ON.

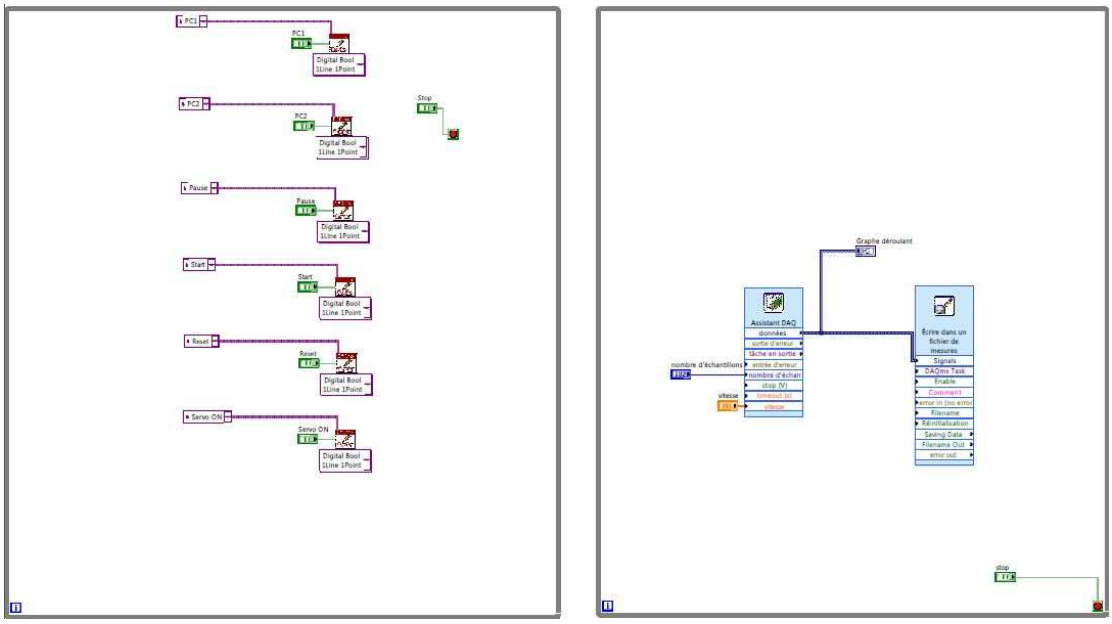

Figure 3-14. Block Diagram

The linear actuator remains OFF while this signal is OFF. The other while loop is used to acquire data from the force and displacement sensors. Two data inputs are configured in a pre-programmed DAQ Assistant. The DAQ assistant is small programme, already written in the Labview to help the new users who are not familiar with more complex programming, to collect data from the data acquisition card. The output from the DAQ assistant is stored in a file and also as a form of continuous graph on the front panel. The two loops can be stopped separately at any time while the VI is running. The two while loops are integrated in one VI. The front panel of the SFT VI is shown in Figure 3-15.

The front panel consists of the controls for the six function of the linear actuator. The graphical representation show the data acquired in the form of continuous graph. The frequency and number of test can also be changed by the front panel. However in case friction measurement continuous testing is performed. The small stop button is to stop the control while loop whereas the large stop button is to stop the data

acquisition. The SFT VI can be used to perform friction measurement in a semi-automatic manner.

The detailed measurement protocol is given in annex B.

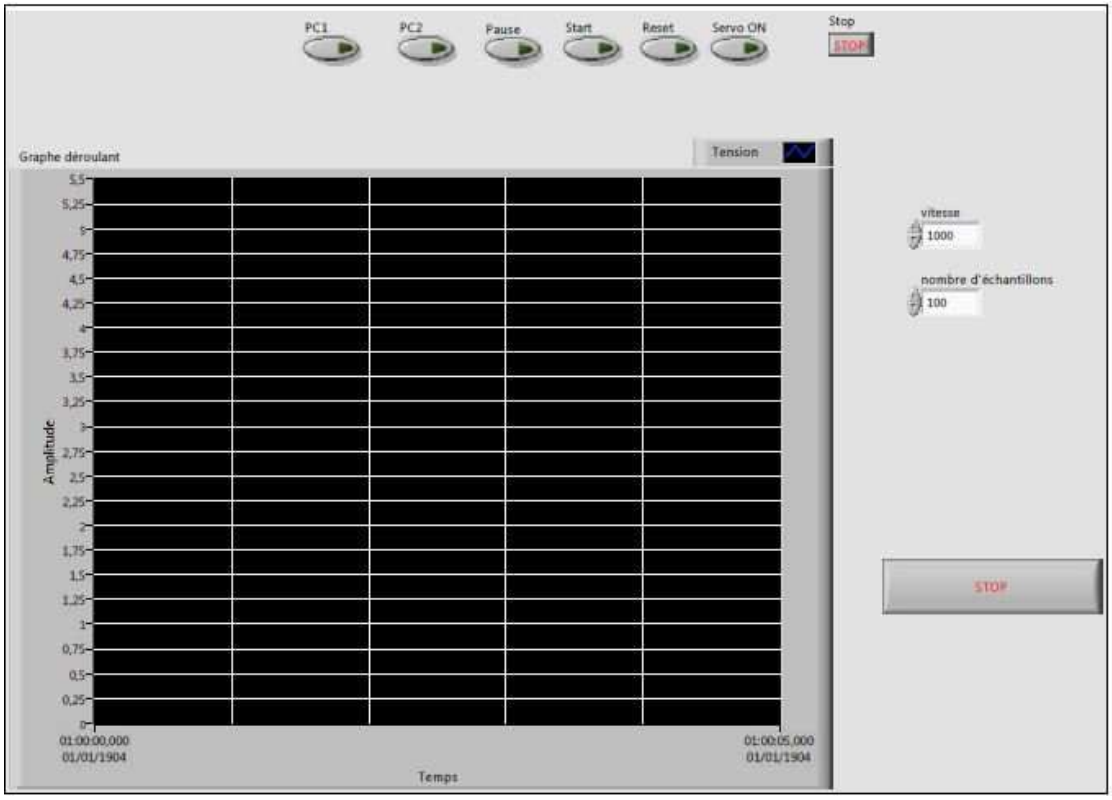

Figure 3-15. Front Panel

3.7 Conclusion

The earlier version of SFT was discussed and some shortcoming in that version also discussed. An improved Static Friction Tester was developed and the problems faced in the earlier version were solved. A simple and complete protocol to operate the modified SFT was also established.

Chapter 4-Materials and Methods

4.1 Introduction

In this chapter, we will discuss the selection of a panel of cottons, measurement of fibre properties, sampling at different stages of processing, inter-fibre friction measurement, processing of fibre into yarn, and measurement of yarn properties. We will also discuss the instruments used to measure all the fibre and yarn properties and its operating procedure. All the fibre and yarn testing is carried out at standard atmospheric conditions i.e. 20°C ± 2°C and RH 65% ± 2%.

4.2 Selection of Cottons

A panel of 30 cottons was selected randomly from the available stock of CIRAD. The detailed description of selected cotton is given in the following table:

No.	Cotton Name	Origin	No.	Cotton Name	Origin
1	Irma BLT	CIRAD	16	07 Nere	Mali
2	C2	CMR	17	07 Sigal/s	Senegal
3	C5	C1 Greek	18	Short 33080	USDA
4	C6	PRY-P288	19	Ac2	Soudan
5	C9	CMR-1243	20	RAW01	Soudan
6	C11	PRY-Gauz	21	RAW04	Soudan
7	C12	TCD	22	RAW05	Soudan
8	C18	MLI	23	RAW06	Soudan
9	C22	MLI	24	RAW07	Soudan
10	C33	TUR	25	Ian338	Paraguay
11	AZ3281001	Azerbaijan	26	DPL90Upper Awash lot222	Ethiopia
12	2 E.G	Benin	27	24013 IM 4,80	Brazil
13	3331/31	Cameroun	28	DM 14	ICCS 3.98
14	4144/11	Cameroun	29	IM 43	ICCS 5.02
15	3257006	Tajikistan	30	ISA 268A	CIV

Table 4-1. Panel of Cottons

These cottons were chosen to cover a wide range in each of the main fiber characteristics.

Subsequently, the randomly selected cottons were collected from the cotton storage of CIRAD. From each one of the cotton, around 800-850 grams of sample was taken and put in a carton for further testing and processing.

4.3 Fibre Opening and Blending

The fibre opening and blending is carried out on a semi-automatic blending machine which is called the Fibre Blending Machine (Figure 4-1). It consists of a feed plate, four pair of rollers, suction pipe and plastic bag

to collect the opened fibres. The tufts of fibres are fed, by the help of feed plate, to the four pair of rollers which are rotating at different speeds. The upper roller have rubber cots while the bottom rollers are grooved, the purpose of rubber cot is to properly handle the passing material, the rollers are fitted with brushes to clean it of any foreign material.

Figure 4-1. Fibre Blending Machine

The pressure is also applied on the upper roller to properly grip the fibres. The roller gauges and pressure can be adjusted. The roller gauges are adjusted according to the estimated fibre length. At the end of fourth roller, a suction piper is mounted to suck the opened fibres and gather them in the plastic bags. The 800 grams of fibres from each cotton are divided in to two parts. These two halves of samples are opened and blended by using Blending machine. The opened and blended halves of fibres are superposed on one another and independent sampling is proceeded for fibre analysis (FMT+HVI-1000+H2SD).

4.3 Fibre Analysis

After opening and blending, two independent samples of 10 to 15 grams and 50 to 60 grams are taken respectively. The smaller sample is for cotton stickiness measurement (H2SD) while the larger one is used for the measurement of other fibre properties. The samples are conditioned for 24 hours in controlled standard atmospheric condition.

4.3.1 Fineness and Maturity Tester 3 (FMT-3)

The conditioned samples are then tested on FMT to measure fibre fineness and maturity. About 10 to 15 gram sample is passed through Shirley Fibre blender to remove any foreign impurities as these impurities may affect the results. The FMT-3 works on the air flow principle. It measures air porosity of the cotton fibres. The FMT-3 device measures the depression caused by the passage of two successive air flow (at different rates) through the fibrous layers that are subjected to two levels of mechanical compression in a measuring chamber. It is possible to apply the relationship established by Koseny, who says that the square of the specific surface of the material is proportional to the difference in air pressure between the inlet and outlet of the fibrous layers and inversely proportional the air flow [93].

Figure 4-2. Fineness and Maturity Tester 3 (FMT-3)

The device must be calibrated by reference cottons (ICCS - International Cotton Calibration Standard) before any testing. A sample of approximately 3.8 to 4.2 gram is taken and then put in a small tube that is fed to measuring chamber. Two repetitions per cotton are carried out for fineness and maturity measurement. The following fibre parameters are obtained from the FMT testing.

- MI - Micronaire Index: In practice, we define the fineness and maturity by a complex called micronaire index (MI). However, one must be cautious about interpreting the results of MI, knowing that

for the same micronaire value, it is possible to have different maturities since the finesse is a component,

- MR - Maturity Ratio: The maturity ratio that combines the percentages of normal and dead fibres,
- PM: the average percentage of mature fibres,
- H: the linear fineness (H in millitex) which corresponds to the actual linear density and the standard fineness (Hs millitex) corresponding to the linear density that would be obtained under ideal conditions of maturity.

4.3.2 High Volume Instrument 1000 (HVI-1000)

The HVI-1000 (Figure 4-3) device measures the fibre physical and mechanical characteristics simultaneously. It consist of three modules, one module is to measure fibre Micronaire, the other module is used to measure fibre length and its mechanical characteristics and the last module is to evaluate color characteristics.

Figure 4-3. High Volume Instrument 1000 (HVI-1000)

As the fibre Micronaire is measured by FMT-3, so its value is manually fed to HVI-1000. A sample of around 30 grams is put on a glass window to evaluate color characteristics. The same sample is then fed to auto sampler which automatically draws a comb of fibre for length and other mechanical properties measurement. The same procedure is repeated six times for each cotton in the panel. The HVI-1000 gives the following fibre parameters:

- UHML - Upper Half Mean Length in mm: the average length of the upper half of the fibers,

- ML - Mean Length in mm: the average length of all the fibers,
- UI - Uniformity Index is obtained by taking the ratio of the ML and UHML and provides a good indication of the cotton uniformity,
- SFI - short fiber index which gives an indication of the rate of short fibers shorter than 12.5 mm,
- SCI: Spinning Consistency Index. This index is calculated from parameters such as tenacity, medium length, UI and the MI,
- Strength (cN / tex): The fiber strength is usually expressed as specific breaking load, also known as "tenacity", that is defined as the breaking strength expressed in cN relative to the mass per unit length in tex,
- Elongation: The elongation % at break of fibers,
- Rd: degree of reflectance. This value is related to the level of whiteness of the sample and corresponds to the reflectance (%) of the light reflected by the sample.
- -b: Degree of yellowness

4.3.3 Advanced Fibre Information System (AFIS)

The AFIS (Figure 4-4) device is based on the single fibre measurement principle. The measuring principle is the separation of the sample into individual fibers by using aero-mechanical unit. An electro-optical sensor counts the number of impurities and the distinction between the fibers and neps.

Figure 4-4. Advanced Fibre Information System (AFIS)

It analyzes the fibers and impurities. Cotton fibers are flat ribbon-shaped spiral and have kidney-shaped cross-sections. In the optical measuring unit each fiber is projected with the help of light emitter on the receiver. The length of the fiber and its average diameter is calculated from this image. For AFIS testing, the cotton fibre samples after third drawing passage is collected and conditioned for 24 hours. A sample of about 5 grams is weighed with the help of weighing balance and made into a sliver of about 30 cm. The sliver is then fed to measuring unit. Five repetitions are carried out for each cotton. The AFIS gives following fibre parameters:

- L (w), L (n) (mm): average fiber length by the weight (w) or by the number (n),
- L (w) CV %, L (n) CV %: the coefficient of variation of the average fiber length by the weight (w) or by the number (n),
- Neps (Cnt/g): number of fiber neps,
- Neps (microns ²): average size of fiber neps,
- SCN - Seed Coat Neps (Cnt/g): number of fragments of shell seeds entangled with fibers,
- SFC (w), SFC (n) in % : Short Fibre Content - Share of short fiber lengths of less than 12.7mm, by weight (w) or number (n),
- UQL (w) in mm: Upper Quartile Length - 25% by exceeded length of the fibers on the weighted cumulative distribution by mass,
- 5.0% (mm): length exceeded by only 5% of fibers on the weighted cumulative distribution by mass,
- Fineness in mtex: fibre fineness,
- IFC (%): Immature fiber content - percentage of immature fibers,
- Mat. Ratio: Maturity Ratio ,
- Total (Cnt/g): number of impurities per gram,
- Mean Size: average size of impurities in microns square,
- Dust (Cnt/g): number of dust particles per gram,
- Trash (Cnt/g): number of trash particles per gram,
- VFM (%) - Visible Foreign Matter: proportion of impurities.

4.3.4 High Speed Stickiness Detector (H2SD) – Stickiness Measurement

The stickiness tester H2SD (Figure 4-6) is used to measure cotton stickiness. It plays a part during processing of fibres into yarn. The test is

performed in a conditioned atmosphere. A cotton sample (3 to 3.4 grams) prepared as a pad using a rotor is placed on an aluminium support which is passed through the four positions (Figure 4-5). At first, a hot pressure is applied to the sample. The combination of cotton moisture content, temperature differential between the heat applied and the aluminium sheet, produces a thin layer of moisture on the aluminium foil [35, 36].

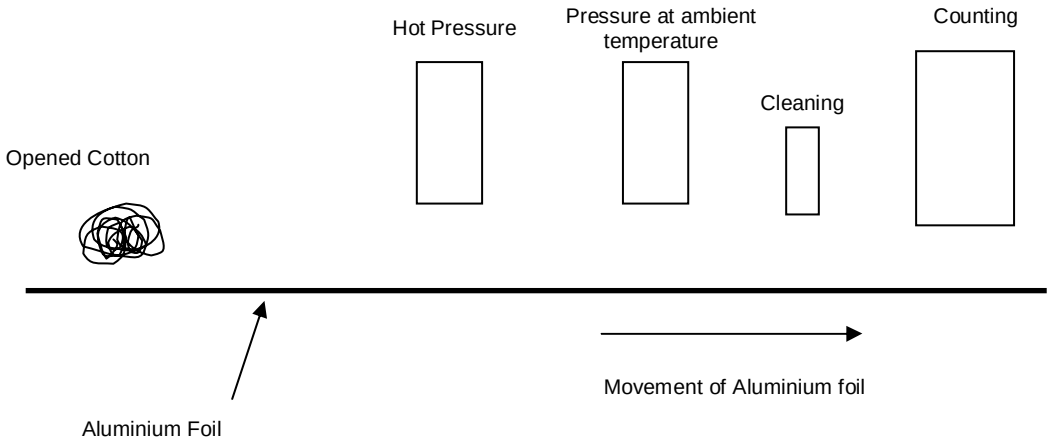

Figure 4-5. H2SD Operating Diagram

The sticky points located in contact with the support get stuck to the aluminium foil and are fixed by a second room temperature pressure. The cotton is then removed and the fibre sticky points are counted and analyzed by image analysis.

Figure 4-6. High Speed Stickiness Detector (H2SD)

The degree of cotton stickiness is evaluated by counting the honeydew insects stuck to the fibres. These are composed of honeydew sugars that come from the insects. During the development of H2SD, the sticky points were divided into small (up to 9 mm²), medium (9-18 mm²) and large (>

18 mm²). There is no unit because it is a counting of the sticky points. Three tests are performed to get the average stickiness value.

4.3.5 TRASHCAM - Measuring the amount of impurities

This device is used to measure the percentage of trash and seed coat fragments in the cotton fibers (Figure 4-7). The measuring principle is as follows: a cotton web of approximately 100g is prepared with the mini card (Figure) and is placed on a scanner specifically to cover an area of 22×35cm. The scanner detects all foreign materials on the surface and counts and categorizes the object by their sizes [39]. The two sides on the each end of the web are scanned. The average of these four tests gives us value of trash and seed coat fragments.

Figure 4-7. TRASHCAM

4.4 Micro Spinning for Cotton Fibres

The micro-spinning technology at CIRAD is used mainly to develop new of cotton varieties by spinning very small amount of fibres, 50 grams of fibre [24], but larger amounts can also be spun from 500 to 700 g , amounts necessary for researchers and spinners to evaluate the behavior of cotton spinning. Frydrych and Drean [33] presented techniques for spinning the yarn of 20, 27 and 37 tex count and making fabrics with a certain amount of fibers, ranging from 50 to 500 g (Figure 4.8). The Cotton Technology Laboratory of CIRAD-CA uses micro-spinning equipment (Platt) that consists of a mini-card, a drawing frame and a ring spinning machine with 8 spindles. The detailed description of finalized plan of experimentation for this research work and the sampling procedure for different fibre and yarn tests is as follows:

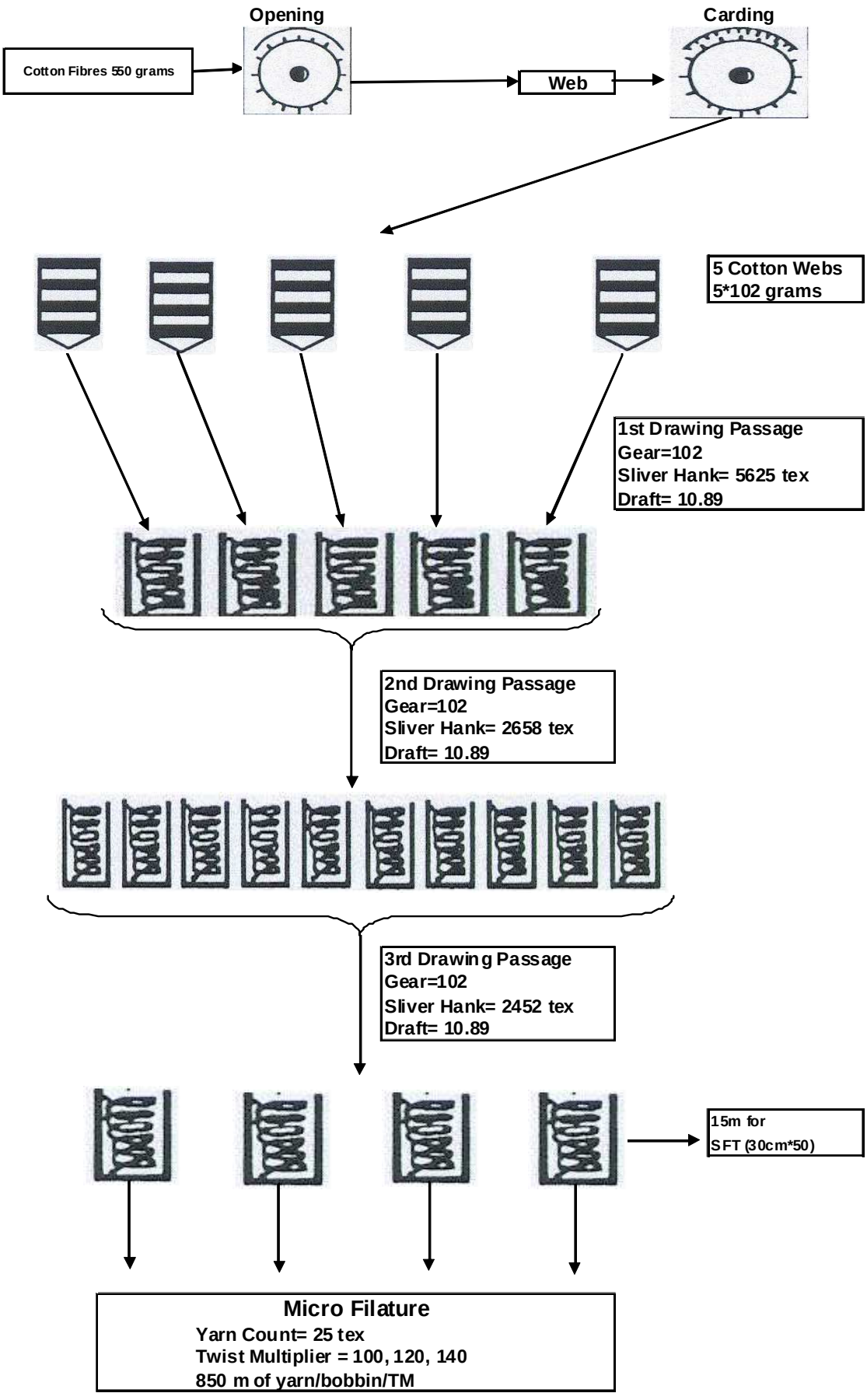

Figure 4-8. Spin Plan

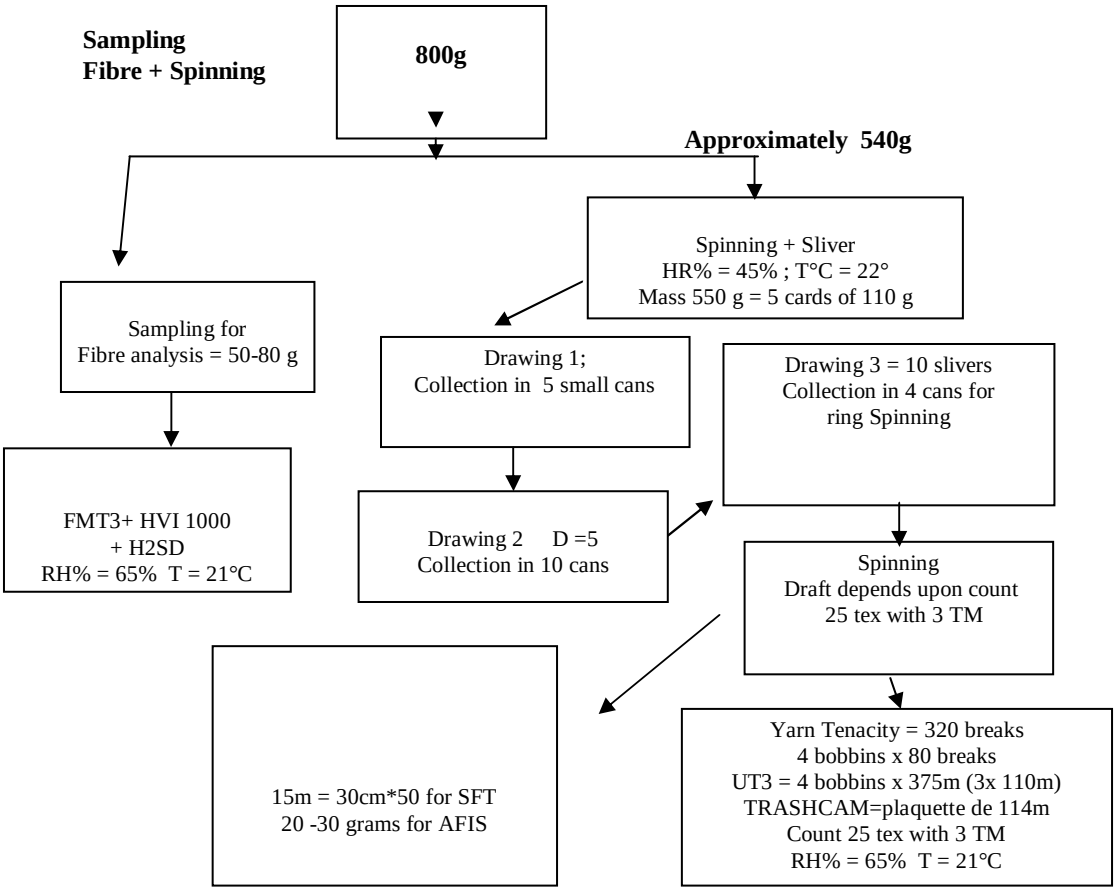

Figure 4-9. Sampling Plan

The randomization was done for the order of cotton at which it will be processed and also the three twist multiplier as it will be applied on each cotton during its spinning on small ring machine. The different processes of micro spinning will be discussed in detail below.

4.4.1 Opening and Homogenization of the sample

This process is carried out by using plain cover instead of using wired surface on the cylinder of the mini-card. During this operation, the cotton undergoes a first disentanglement to remove heavier impurities. The obtained output in the form of web is wound on a cylinder, which ensures a fibre blending and obtaining a regular cotton web to optimize the following carding operation. The 550 grams of sample is divided into five equal parts of 110 grams and passed through the mini card without using the wired surface on the large cylinder (Figure 4-10). This process is known as the opening. The amount of trash removal ranges from 1 to 5

%. This percentage depends upon the amount of trash present in the raw cotton.

4.4.2 Carding

Carding provides cleaning, combing, individualized fibres and removes a fraction of short fibres and neps. The web obtained after the previous phase of opening, weighing about 280 g / m² is usually separated from the receiving cylinder and divided in half lengthwise. These two parts are then superposed to form a doubling of two which are then fed to the card by placing it on the feed plate. For this operation, the large cylinder is covered with the needle cap. As the Mini card has no automatic cleaning system the top wired surface is cleaned after processing 50 grams of cotton. This cleaning is necessary to have a better carding process. Thus, for a sample of 100 g, an additional intermediary cleaning is necessary. The percentage of trash, neps and short fibre removal ranges from 3 to 6%.

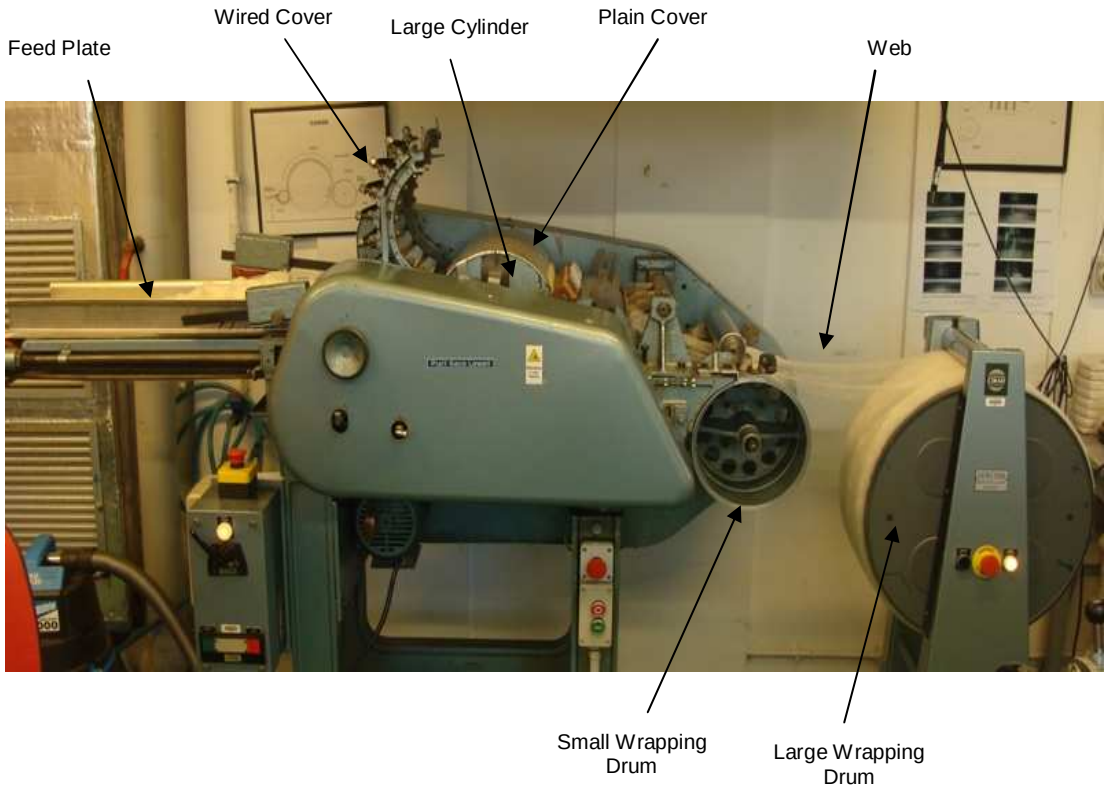

Figure 4-10. Mini Card

The material is fed through the feed plate to the large cylinder which is moving at a high speed. The material is cleaned due to "point to point"

operation between cylinder and the wired top surface. The material is then transferred to the doffer due "to point to point" transfer operation between the cylinder and the doffer. The material is then collected from the doffer and form a web which is collected on a large wrapping drum. The five opened samples are passed separately through the carding process. The operating principle is shown in Figure 4-11.

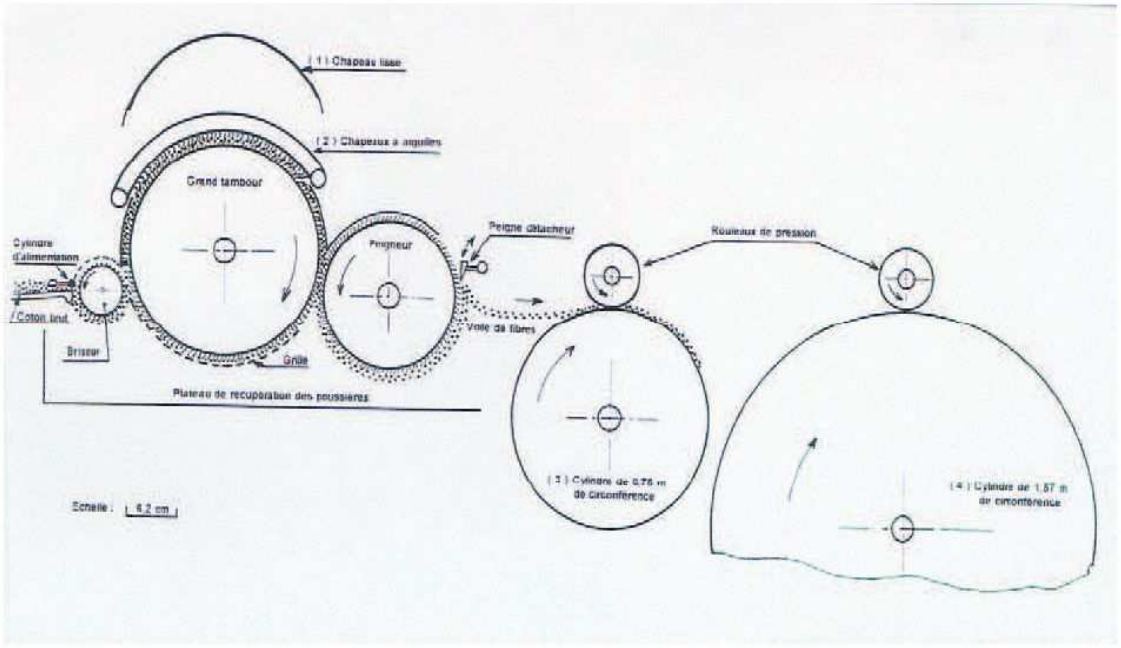

Figure 4-11. Card Operating Principle

4.4.3 Drawing

The purpose of drawing frame (Figure 4-12) is to align the fibres and also reduce the material count by repeated drafting. The drawing frame is equipped with 4/4 drafting system. The drafting zone gauges are adjusted according to UHML of the cotton fibres. The cotton fibres are passed through three drawing passages. The total amount of draft is 10.98. The same amount of draft is applied on all three passages.

The carded web is passed through the first drawing passage to a sliver. As the material is divided into five parts so we have five slivers after the first passage. For the 2nd passage, all five slivers are used and a doubling of five is applied. The resulting sliver is collected in ten small can. For the 3rd drawing passage a doubling of 10 is applied, and the material is collected in 4 small can which are then used to feed material to four spindles on the ring spinning frame. The operational principle of the mini drawing frame is shown in the Figure 4-13.

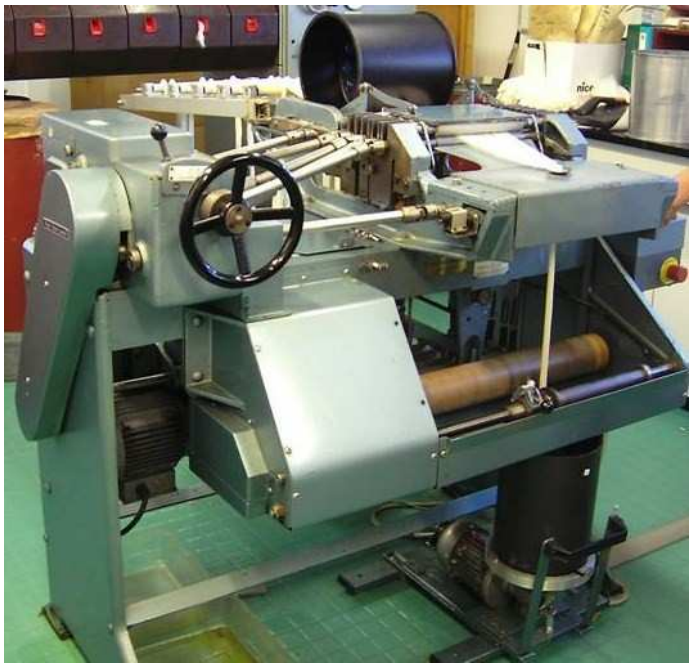

Figure 4-12. Mini Drawing Frame

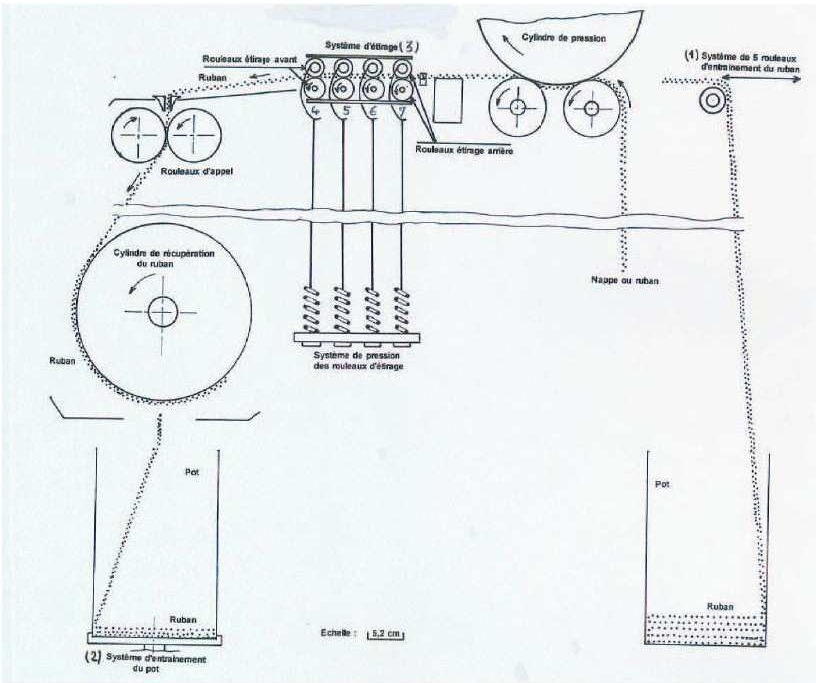

Figure 4-13. Operational Principle of Mini Drawing Frame

4.4.4 Spinning

The process of converting a strand of fibres into yarn is called spinning. In this process, fibres are aligned along its axis and a certain amount of twist is imparted to the fibre flow to give it strength. The spinning frame (Figure 4-14) is composed of a two drafting zones, the back and the front drafting

zone to obtain a high amount of drafting and this helps in eliminating the phase of the roving frame. The yarn can be spun from the sliver of last drawing frame. The sliver collected in four small cans after the third drawing passage are fed to four spindles on the small ring frame. The spindles rotate at 9100 rpm. The yarn count of 25tex is spun for each cotton by using three different twist multipliers i.e. 100, 120 and 140. The amount of total draft varies and it depends upon the sliver count fed to the ring spinning machine.

Figure 4-14. Mini Ring Spinning Frame

For each twist multiplier, approximately 800m of yarn is spun to perform all the yarn analysis.

4.5 Yarn Analysis

The spun yarn is tested for its regularity and tensile properties by using different testing machines.

4.5.1 UT-3: Yarn Evenness, Imperfections and Hairiness

Yarn evenness is determined by measuring the variation in capacity occurring as yarn pass through the condenser and recorded in terms of mean linear irregularity (U%) and the coefficient of variation in yarn mass (CV%). The Uster Evenness Tester (UT-3) device was employed which simultaneously measures the imperfection viz., thin, thick places and neps per thousand meters of yarn [123].

Figure 4-15. UT-3

The hairiness module of the UT-3 consists of an electronic optical sensor which converts the scattered light reflection of the peripheral fibres into a corresponding electrons signal while the solid yarn body is eclipsed. Yarn hairiness is expressed in the form of hairiness value H, which is an indirect measure for the number of cumulative length of all fibres protruding from the yarn surface. The testing speed is 50 m/min. Each bobbin is tested three times for a length of 125 meters. The same test is performed on the yarn produced by using different twist multipliers.

4.5.2 Tensile Properties of Yarn

Tensile properties viz., single yarn strength, elongation and breaking length calculated with Uster Tensorapid, which applies the principle of constant rate of extension (CRE) for testing [124]. CRE describes the simple fact that the moving clamp is displaced at the constant velocity. As a result the specimen between the stationary and moving clamp extended by a constant distance per unit time and the force is measured. The breaking tenacity is calculated from the peak force, which occurs normally just before the final rupture of the specimen. The breaking elongation is calculated from the clamp displacement at the point of peak force. The breaking length (RKM) value is calculated by applying the following formula.

RKM = Single yarn strength x 0.00169 x actual count

Figure 4-16. USTER Tensorapid

The apparatus consists of two pneumatic jaws, one is fixed and the other moves downwardly. The clamp moves with a linear guide at constant speed. The testing speed is 82 mm/min. The initial difference between the two clamps is 0.5m. Statistically, 40 tests are required for reliable results. We conducted 80 trials per bobbin, or 320 tests per twist multiplier (4 bobbins). This device is programmable and can test continuously in the absence of the operator.

4.5.3 TRASHCAM for Yarn

This device can also be used to measure the percentage of seed coat fragments in the yarn. In this case, the yarn is wound on a white rigid plate. Then both sides of this plate are scanned. The yarn wound on the plate is approximately 114m in length.

Figure 4-17. TRASHCAM for Yarn

4.6 Inter-fibre Friction Measurement

The samples collected after the 3rd drawing passage is tested for fibre to fibre friction. As noted by Nowrouzieh [80], the sliver count should be between 4.5 to 5 Ktex for a better frictional measurement. Therefore the slivers are doubled to perform the measurement. The mass applied on the two carriages are 2000, 3000, 4000 and 5000 grams. Six repetitions are performed for each mass applied. This results in 24 tests of fibre to fibre friction measurement for each cotton.

Chapter 5-Results and Discussion

5.1 Introduction

In this chapter we will discuss the results obtained by using different testing apparatus and testing methods. The simple and complex statistical analyses were employed to establish relation between different properties of fibre and yarn. The used statistical analyses include regression, correlation and principle component analysis. We will start with statistical analysis of fibre properties, yarn properties and frictional properties. The different frictional models were employed to the results obtained from inter-fibre friction testing.

5.1 Statistical Analysis of Fibre Properties

The fibre properties analyses were performed in standardized atmospheric conditions i.e. RH 65% and temperature 21°C. Several measuring devices were used:

- FMT3 to measure the fineness, maturity and micronaire of raw cotton
- HVI-1000 to measure UHML, Fibre length, elongation, tenacity, colour of raw cotton
- H2SD to measure stickiness of raw cotton
- AFIS to measure length, short fibre content, by number and weight

The HVI-1000 is a device that measures the fibre properties as bulk whereas AFIS measures the individual fibres.

The fibre properties are grouped according to the instrument used to measure these properties.

AFIS: Neps (cnt/g), Neps (microns²), SCN (cnt/g), SCN (microns²), L(w), L (w)CV%, SFC (w), UQL (w), L (n), L (n)CV%, SFC (n), Fineness, IFC, Maturity, Total foreign particle, Mean size, Dust particle, Trash particles, VFM etc.,

FMT3: MI, MR, PM, H, HS,

HVI-1000: UHML, Uniformity, SFI, Strength, Elongation, Rd, - b,

Trashcam: The number and the size distribution of seed coat fragments in cotton fibres,

H2SD: The level of cotton stickiness is evaluated by counting the honeydew spots stuck on an aluminium foil.

The statistical tests used were comparison of means and Student's t test on the different fibre properties. The Figure 5.1 shows graphical

representation of the Means test and Student's t test for the fibre tenacity of a panel of 30 cottons. The individual means values are given in the Table 5-1.

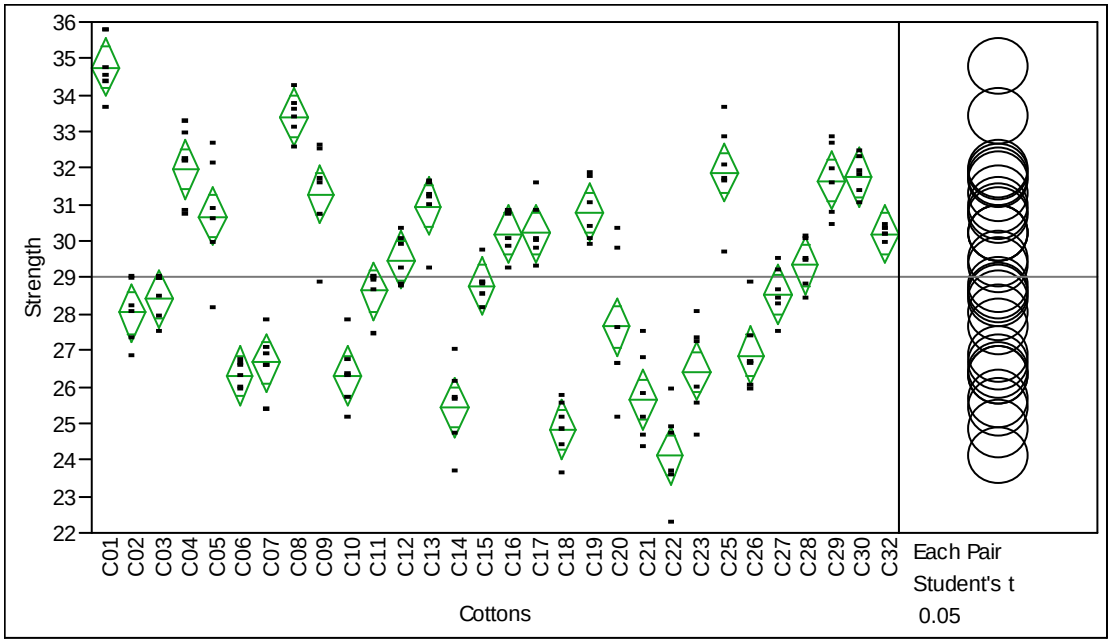

Figure 5-1. Graphical Representation of Fibre Tenacity

Level	Cotton Groups based on Fibre Strength																											Mean	Std Dev
C01	A																											34.761903	0.83572
C08		B																										33.398220	0.56695
C04			C																									31.968212	1.07506
C25			C	D																								31.870193	1.34755
C30			C	D	E																							31.755120	0.52885
C29			C	D	E																							31.656843	0.97701
C09			C	D	E	F																						31.273947	1.37962
C13			C	D	E	F																						30.950487	0.88938
C19				D	E	F																						30.778340	0.85029
C05					E	F																						30.680362	1.62546
C17						F	G																					30.210557	0.82353
C16						F	G																					30.191925	0.64786
C32						F	G																					30.183333	0.18348
C12							G	H																				29.468308	0.67046
C28							G	H																				29.336128	0.66200
C15								H	I																			28.767540	0.52646
C11								H	I																			28.624972	0.62947
C27								H	I																			28.539768	0.71246
C03								H	I																			28.419217	0.64263
C02									I																			28.028870	0.87822
C20									I	J																		27.648425	2.00257
C26										J	K																	26.865285	1.09002
C07										J	K	L																26.668020	0.80812
C23											K	L	M															26.419288	1.26821
C06											K	L	M															26.301678	0.34714
C10											K	L	M															26.299053	0.90707
C21												L	M	N														25.650945	1.22865
C14													M	N														25.433930	1.14190
C18														N	O													24.830020	0.78522
C22															O													24.117972	1.26042

Table 5-1. Fibre Tenacity

The cottons are divided into groups that are statistically different based on the values of fibre tenacity as shown in the above table.

The cotton C01 has the highest value (34.76 g/tex) of fibre tenacity and the cotton C22 has the lowest amount of fibre tenacity (24.11 g/tex). The

range of fibre tenacity shows that the panel of cotton is well distributed as a function of fibre tenacity.

The graphical representation of fibre length is shown in the Figure 5-2. The individual means values are given in the following Table 5-2. The fibre length given below is measure by AFIS and it is fibre length by number.

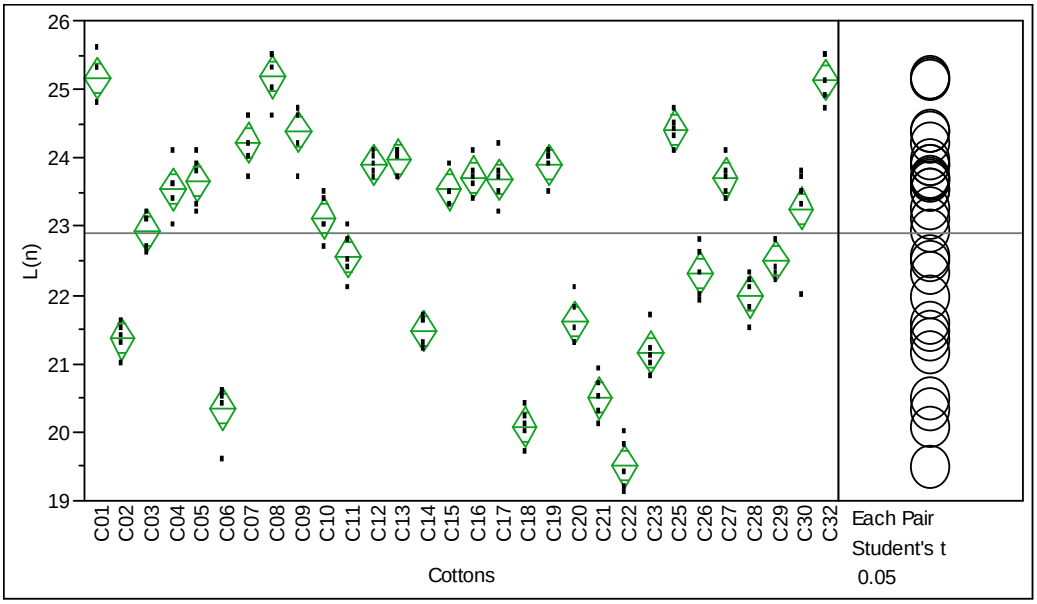

Figure 5-2. Graphical Representation of Fibre Length (n)

Level	Cotton Groups based on Fibre Length (n)																												Mean	Std Dev
C08	A																												25.180000	0.383406
C01	A																												25.160000	0.350714
C32	A																												25.140000	0.357771
C25		B																											24.400000	0.223607
C09		B																											24.380000	0.432435
C07		B	C																										24.220000	0.389872
C13		B	C	D																									23.980000	0.164317
C19			C	D	E																								23.900000	0.234521
C12			C	D	E																								23.900000	0.158114
C16				D	E																								23.720000	0.258844
C27				D	E																								23.700000	0.273861
C17				D	E	F																							23.680000	0.370135
C05				D	E	F																							23.660000	0.391152
C04					E	F	G																						23.540000	0.397492
C15					E	F	G																						23.540000	0.219089
C30						F	G	H																					23.260000	0.730068
C10							G	H																					23.120000	0.327109
C03								H	I																				22.940000	0.270185
C11									I	J																			22.560000	0.350714
C29										J																			22.500000	0.282843
C26										J	K																		22.320000	0.383406
C28											K	L																	21.980000	0.327109
C20												L	M																21.600000	0.346410
C14													M	N															21.480000	0.216795
C02													M	N															21.360000	0.230217
C23														N															21.160000	0.336155
C21															O														20.500000	0.316228
C06															O														20.340000	0.421900
C18															O														20.080000	0.258844
C22																P													19.500000	0.387298

Table 5-2. Fibre Length (n)

The table of mean values indicates that the panel has wide range of cotton fibres having different level fibre length. The panel of cottons is divided

into 16 groups that are statistically different based on the fibre length by number.

The table of mean values and graphical representation of means values and Student t test for short fibre content is given in Table 5-3 and Figure 5-3 respectively.

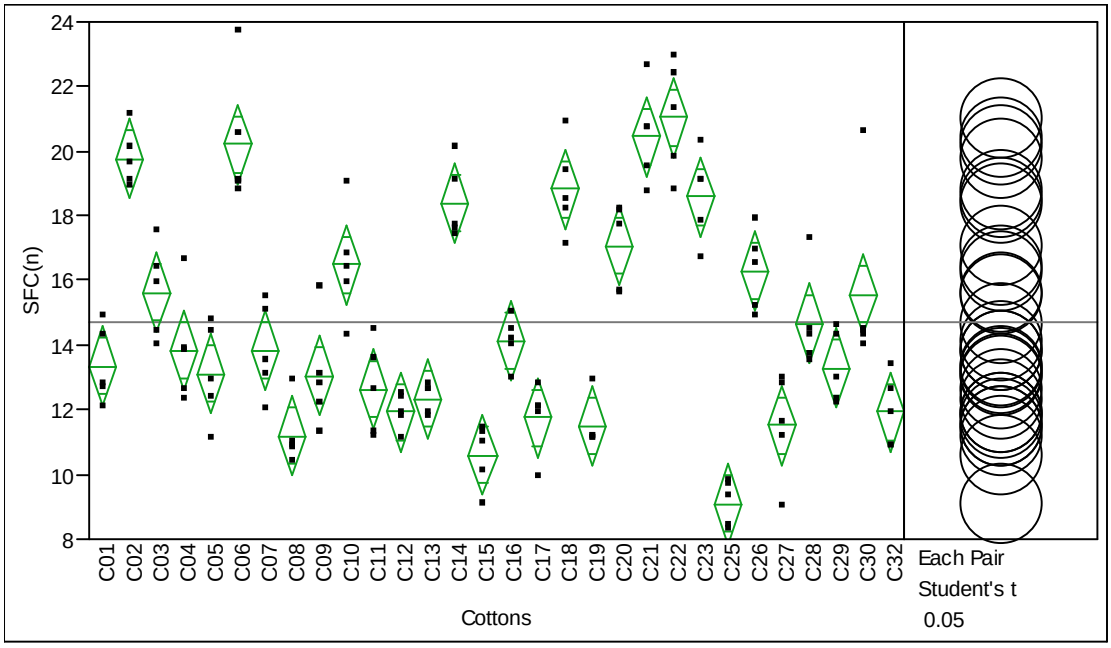

Figure 5-3. Graphical Representation of Short Fibre Content (n)

Level	Cotton Groups based on Short Fibre Content (n)	Mean	Std Dev
C22	A	21.040000	1.72714
C21	A B	20.440000	1.47580
C06	A B C	20.220000	2.05840
C02	A B C D	19.760000	0.88204
C18	B C D	18.820000	1.42373
C23	C D E	18.600000	1.38203
C14	D E	18.380000	1.17346
C20	E F	17.060000	1.30115
C10	F	16.480000	1.69912
C26	F G	16.280000	1.23774
C03	F G H	15.640000	1.44326
C30	F G H I	15.560000	2.82365
C28	G H I J	14.660000	1.53232
C16	H I J K	14.140000	0.74027
C07	I J K L	13.840000	1.44845
C04	I J K L	13.840000	1.69794
C01	J K L M	13.360000	1.18237
C29	J K L M	13.280000	1.11669
C05	J K L M N	13.120000	1.50897
C09	J K L M N	13.040000	1.68908
C11	K L M N O	12.640000	1.43631
C13	L M N O	12.340000	0.45607
C32	M N O P	11.940000	1.08766
C12	M N O P	11.940000	0.55946
C17	M N O P	11.760000	1.09453
C27	N O P	11.520000	1.60375
C19	N O P	11.500000	0.78422
C08	O P	11.200000	0.97724
C15	P Q	10.580000	0.97314
C25	Q	9.100000	0.71063

Table 5-3. Short Fibre Content (n)

According to above table, the cotton C22 has highest amount of short fibre content. It also has the shortest fibre length and lowest fibre

tenacity. The range of short fibre content is from 9.10 to 21.04 percent. The cottons are classified into 17 groups that are statistically different based on the short fibre content values.

The Figure 5.4 shows graphical representation of the Means test and Student's t test for the Rd value of a panel of 30 cottons. The individual means values are given in the Table 5-4.

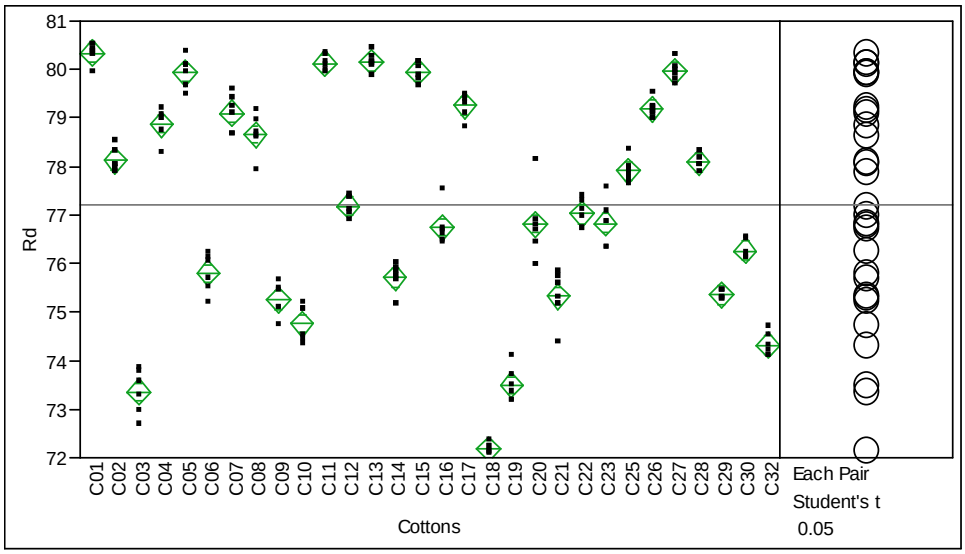

Figure 5-4. Graphical Representation of Rd Values

Level	Cotton Groups based on Rd Values																												Mean	Std Dev
C01	A																												80.334688	0.214787
C13	A	B																											80.150347	0.187639
C11	A	B																											80.119228	0.157532
C27		B																											79.956368	0.200647
C15		B																											79.943862	0.211405
C05		B																											79.932995	0.321837
C17			C																										79.255507	0.255960
C26			C	D																									79.187405	0.185721
C07			C	D																									79.098523	0.382327
C04				D	E																								78.871513	0.324641
C08					E																								78.657972	0.418214
C02						F																							78.113477	0.240667
C28						F																							78.081243	0.147773
C25						F																							77.903705	0.243357
C12							G																						77.188223	0.210333
C22							G	H																					77.021247	0.287977
C23							G	H																					76.829977	0.473709
C20								H																					76.812188	0.726692
C16								H																					76.743692	0.406905
C30									I																				76.267438	0.198106
C06										J																			75.796652	0.399619
C14										J	K																		75.706938	0.299894
C29											K	L																	75.351032	0.083139
C21												L																	75.328370	0.528009
C09												L																	75.251542	0.339141
C10													M																74.761933	0.366282
C32														N															74.316667	0.240139
C19															O														73.494282	0.349911
C03															O														73.351790	0.463128
C18																P													72.174230	0.110262

Table 5-4. Fibre Rd Values

The cottons are divided into groups that are statistically different based on the values of fibre tenacity as shown in the above table. The cotton C01

has the highest Rd value (80.33%) and the cotton C18 has the lowest Rd value (72.17). Note that the reflectance index can be used to compare the fibre surface. The fibre having smoother surfaces should have the highest Rd. But the Rd value is also affected by the amount of trash present in the raw cotton.

The graphical representation of fibre fineness is shown in the Figure 5-5. The individual means values are given in the following Table 5-5.

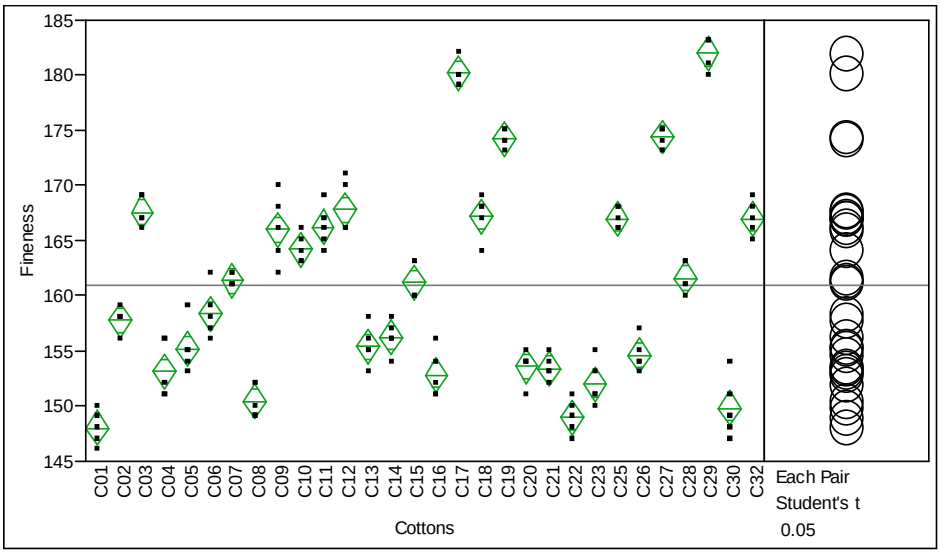

Figure 5-5. Graphical Representation of Fibre Fineness

Level	Cotton Groups based on Fibre Fineness													Mean	Std Dev
C29	A													182.00000	1.41421
C17	A													180.20000	1.09545
C27		B												174.40000	0.89443
C19		B												174.20000	0.83666
C12			C											167.80000	2.48998
C03			C											167.60000	1.34164
C18			C											167.20000	1.92354
C32			C											167.00000	1.58114
C25			C											167.00000	1.00000
C11			C	D										166.20000	1.92354
C09			C	D										166.00000	3.16228
C10				D										164.20000	1.30384
C28					E									161.60000	1.34164
C07					E									161.40000	0.54772
C15					E									161.20000	1.64317
C06						F								158.40000	2.30217
C02						F								157.80000	1.09545
C14						F	G							156.20000	1.48324
C13							G	H						155.40000	1.81659
C05							G	H						155.20000	2.28035
C26							G	H	I					154.60000	1.51658
C20								H	I	J				153.60000	1.51658
C21								H	I	J				153.40000	1.14018
C04								H	I	J				153.20000	2.58844
C16									I	J				152.80000	2.16795
C23										J	K			152.00000	2.00000
C08											K	L		150.40000	1.51658
C30											K	L	M	149.80000	2.77489
C22												L	M	149.00000	1.58114
C01													M	148.00000	1.58114

Table 5-5. Fibre Fineness

The table of mean values indicates that the panel has cotton samples having a wide range of fibre fineness. The panel of cottons is divided into 13 groups that are statistically different based on the fibre fineness values.

The table of mean values and graphical representation of means values and Student t test for fibre maturity (AFIS) is given in Table 5-6 and Figure 5-6 respectively.

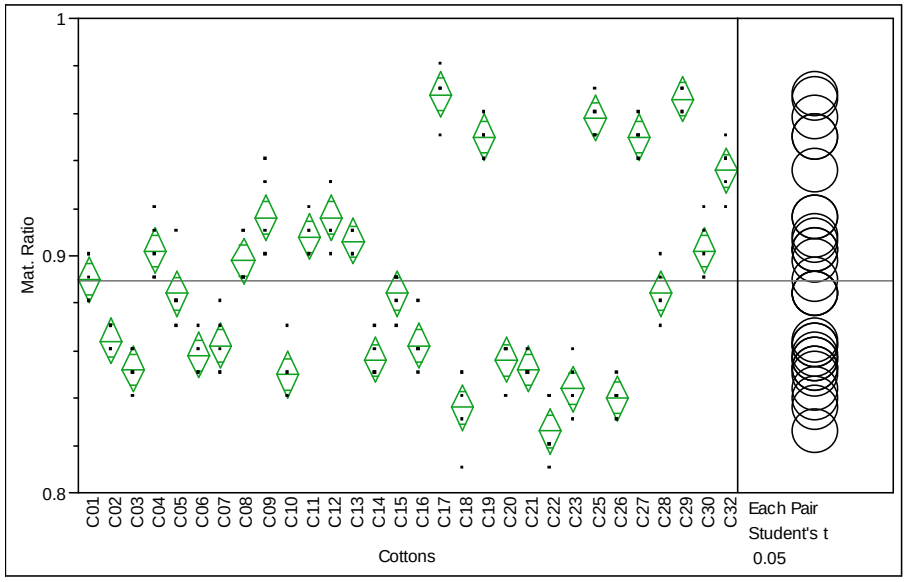

Figure 5-6. Graphical Representation of Fibre Maturity

Level	Cotton Groups based on Fibre Maturity													Mean	Std Dev
C17	A													0.96800000	0.010954
C29	A													0.96600000	0.005477
C25	A	B												0.95800000	0.008367
C19		B												0.95000000	0.007071
C27		B												0.95000000	0.007071
C32			C											0.93600000	0.011402
C12				D										0.91600000	0.013416
C09				D										0.91600000	0.018166
C11				D	E									0.90800000	0.008367
C13				D	E									0.90600000	0.005477
C04					E	F								0.90200000	0.013038
C30					E	F								0.90200000	0.013038
C08					E	F								0.89800000	0.010954
C01						F	G							0.89000000	0.010000
C28							G							0.88400000	0.011402
C15							G							0.88400000	0.008944
C05							G							0.88400000	0.015166
C02								H						0.86400000	0.005477
C07								H	I					0.86200000	0.013038
C16								H	I					0.86200000	0.010954
C06								H	I					0.85800000	0.008367
C20								H	I	J				0.85600000	0.008944
C14								H	I	J				0.85600000	0.008944
C21								H	I	J	K			0.85200000	0.004472
C03								H	I	J	K			0.85200000	0.008367
C10									I	J	K			0.85000000	0.012247
C23										J	K	L		0.84400000	0.011402
C26											K	L		0.84000000	0.007071
C18												L	M	0.83600000	0.016733
C22													M	0.82600000	0.013416

Table 5-6. Fibre Maturity

The cotton maturity indicates the degree of secondary wall development in the cotton fibres. The table shows that the panel of cottons has a reasonable fibre maturity values. The maturity ratio of C17 is highest and the maturity ratio of C22 is lowest. As noted earlier the C22 has low amount of fibre tenacity, shorter in length and highest amount of short fibre content. As the main purpose of this research is the study of inter-fibre friction and the cotton stickiness can play a part in the fibre friction. The cotton stickiness values were analyzed statistically and are shown in Figure 5-7 and Table 5-7.

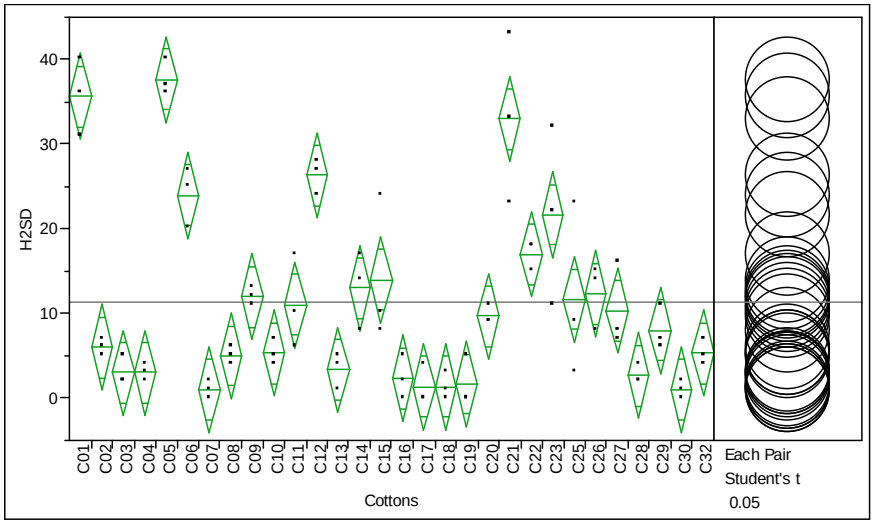

Figure 5-7. Graphical Representation of Cotton Stickiness

Level	Cotton Groups based on Cotton Stickiness												Mean	Std Dev
C05	A												37.666667	2.0817
C01	A												35.666667	4.5092
C21	A	B											33.000000	10.0000
C12		B	C										26.333333	2.0817
C06			C	D									24.000000	3.6056
C23			C	D									21.666667	10.5040
C22				D	E								17.000000	1.7321
C15					E	F							14.000000	8.7178
C14					E	F	G						13.000000	4.5826
C26					E	F	G	H					12.333333	3.7859
C09					E	F	G	H	I				12.000000	1.0000
C25					E	F	G	H	I				11.666667	10.2632
C11					E	F	G	H	I				11.000000	5.5678
C27					E	F	G	H	I	J			10.333333	4.9329
C20						F	G	H	I	J	K		9.666667	1.1547
C29						F	G	H	I	J	K	L	8.000000	2.6458
C02							G	H	I	J	K	L	6.000000	1.0000
C10								H	I	J	K	L	5.333333	1.5275
C32								H	I	J	K	L	5.333333	1.5275
C08									I	J	K	L	5.000000	1.0000
C13										J	K	L	3.333333	2.0817
C04											K	L	3.000000	1.0000
C03											K	L	3.000000	1.7321
C28											K	L	2.666667	1.1547
C16												L	2.333333	2.5166
C19												L	1.666667	2.8868
C18												L	1.333333	1.5275
C17												L	1.333333	2.3094
C07												L	1.000000	1.0000
C30												L	1.000000	1.0000

Table 5-7. Cotton Stickiness

The above table indicates that the most of the selected cottons have low stickiness.

It is very important to note that the cotton groups not connected by same letter are significantly different. All the statistical analyses are conducted at 95% confidence level. The statistical analyses of other fibre properties are given in the Annex-C.

5.2 Statistical Analysis of Yarn Properties

The panel of cotton was processed into yarn by using lab scale spinning machines at CIRAD Montpellier (23°C and RH 55%). The detailed description of the spinning process is given in chapter 4. The yarn count spun was 25tex by using three different twist multipliers i.e. T_1=100, T_2=120 and T_3=140. The length of spun yarn is approximately 850 meter per bobbin for each twist multiplier. The Table 5-8 shows the average count for the panel of cotton for all the twist multipliers.

Cotton	T_1	T_2	T_3	Cotton	T_1	T_2	T_3	Cotton	T_1	T_2	T_3
C01	25.95	26.08	25.70	**C11**	24.98	25.65	25.63	**C21**	24.43	25.38	25.05
C02	25.15	26.15	26.23	**C12**	25.00	24.90	26.23	**C22**	24.48	24.88	25.33
C03	25.48	25.80	26.00	**C13**	25.48	25.65	26.10	**C23**	24.80	25.05	25.83
C04	25.63	26.15	26.35	**C14**	24.98	25.35	25.73	**C25**	25.23	26.30	26.18
C05	25.88	25.08	26.40	**C15**	25.03	25.30	25.58	**C26**	25.90	25.88	26.48
C06	24.80	23.95	25.05	**C16**	25.40	25.93	26.73	**C27**	25.73	25.58	26.33
C07	25.55	25.88	26.28	**C17**	25.32	25.48	26.08	**C28**	25.35	25.85	26.35
C08	25.48	26.28	26.93	**C18**	24.83	24.43	25.33	**C29**	24.68	24.73	25.80
C09	26.00	25.94	26.00	**C19**	24.15	25.38	26.28	**C30**	25.95	26.30	26.35
C10	24.78	26.18	26.38	**C20**	23.40	23.75	23.95	**C32**	23.18	23.63	23.93

Table 5-8. Average Yarn Count

The slight variation in yarn count may be due to processing at the lab scale spinning machines. The micro spinning machines were not equipped with auto levelers to compensate any variation in the sliver during drawing process.

All the yarn tests were carried out at RH 65% and 21°C. Yarn evenness and imperfections measurement tests were performed on USTER UT-3, the yarn tenacity tests were performed on USTER Tensorapid and TRASHCAM was used to measure seed coat fragments in the yarn. For UT-3, 125 meter yarn was tested three times for each bobbin and each twist multiplier. For Yarn tenacity test, 80 breaks per bobbin per twist multiplier per cotton were performed. For the measurement of seed coat fragments,

114 m yarn was wound on a small white rigid plate and subsequently scanned to complete the test.

The list of measured parameters is given below:

UT3: U%, CV%, Index, Thin Places -30%, Thin Places -40%, Thin Places -50%, Thin Places -60%, Thick Places +35%, Thick Places +50%, Thick Places +70%, Thick Places +100%, Neps +140%, Neps +200%, Neps +280%, Neps +400%, Hairiness, Sh1, Sh2,

USTER Tensorapid: Tenacity, Max Force, Elongation, Rupture per KM.

The statistical analyses of UT-3 measurements results are large in quantity. For this reason, we will give a brief overview in the form of figures and tables and only the results for twist multiplier T_2 will be discussed. The remaining statistical analyses are given in Annex-D. As the twist multiplier will affect the yarn tensile properties so the statistical analysis of tensile properties for all the twist multipliers will be discussed. The means values and quantiles statistical test were applied on the yarn properties. The statistical analysis for yarn evenness is given in Figure 5-8 and the mean values are given in Table 5-9.

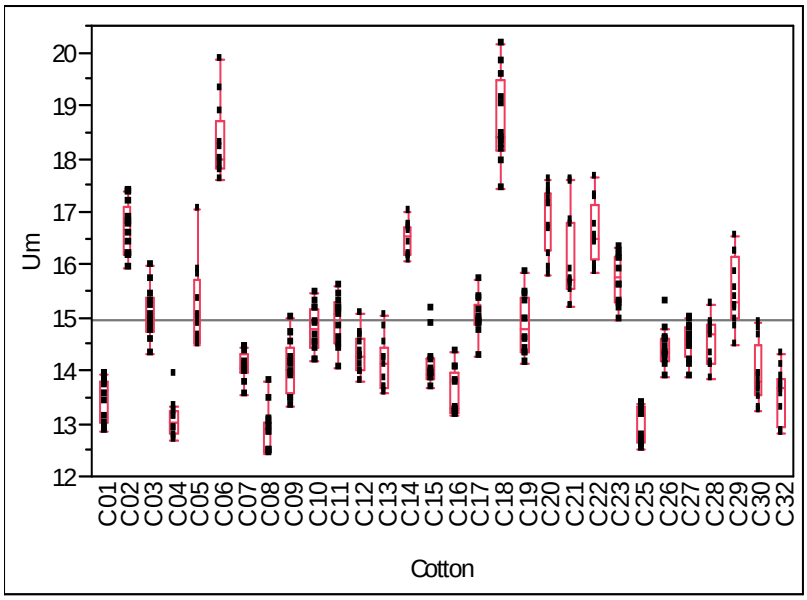

Figure 5-8. Yarn Evenness

Cottons	Mean	Std Dev
C01	13.4758	0.410974
C02	16.6392	0.483613
C03	15.0717	0.481453
C04	13.0633	0.346996
C05	15.1408	0.774895
C06	18.2892	0.700227
C07	14.0675	0.266974
C08	12.8883	0.420732
C09	14.0533	0.505503
C10	14.7708	0.429068
C11	14.9300	0.456548
C12	14.3183	0.359945
C13	14.1217	0.484258
C14	16.4700	0.312846
C15	14.1225	0.449082
C16	13.5375	0.427022
C17	15.0000	0.357873
C18	18.7133	0.822693
C19	14.8558	0.552407
C20	16.8742	0.617951
C21	16.0950	0.855692
C22	16.5800	0.564801
C23	15.7225	0.474593
C25	13.0108	0.335870
C26	14.4342	0.358873
C27	14.5408	0.340813
C28	14.5400	0.430961
C29	15.4683	0.629052
C30	13.9275	0.558832
C32	13.5283	0.496988

Table 5-9. Yarn Evenness

The high amount of yarn unevenness may be due to the usage of lab scale spinning machines which are not equipped with auto levelers. The range of U% is from 12.88% to 16.63%.

The yarn index is shown as graphical form in Figure 5-9. The individual mean values and standard deviation is given in Table 5-10.

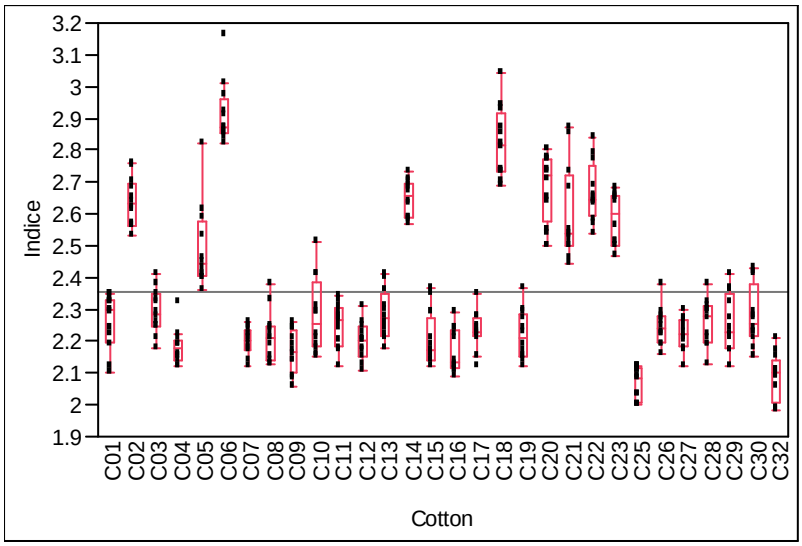

Figure 5-9. Yarn Index

Cotton	Mean	Std Dev
C01	2.26083	0.086808
C02	2.63583	0.075493
C03	2.29250	0.068241
C04	2.18000	0.055103
C05	2.48917	0.130346
C06	2.91083	0.096338
C07	2.20000	0.042640
C08	2.21583	0.078330
C09	2.16500	0.066127
C10	2.27750	0.115059
C11	2.24917	0.068684
C12	2.20000	0.057208
C13	2.28167	0.076495
C14	2.64833	0.055895
C15	2.20500	0.084692
C16	2.16833	0.066992
C17	2.23167	0.059518
C18	2.82083	0.109665
C19	2.21833	0.077675
C20	2.68167	0.103996
C21	2.59750	0.148086
C22	2.66667	0.091685
C23	2.58333	0.081389
C25	2.06750	0.051368
C26	2.24500	0.058075
C27	2.22167	0.050602
C28	2.25917	0.071026
C29	2.25667	0.090487
C30	2.27833	0.094179
C32	2.08833	0.072967

Table 5-10. Yarn Index

The variation in yarn index for the panel of cotton is not very significant. And the values range between 0.90 of each other.

The yarn imperfections, thin places, thick places and neps plays very important role in determining the yarn quality. The UT3 give thin, thick and neps at different levels. According to researchers, the most important of these are thin place at -30% and -50% of the yarn diameter and having length of approximately fibre length. While for the thick places +35% and +50% of yarn diameter are more important as a function of yarn quality. The neps discussed are the ones having diameter of +140 and 200% of yarn diameter and having a length of 1 mm or 2 mm. The yarn hairiness also plays important role during knitting process and more hairiness cause faults during knitting process. The statistical analysis of

these yarn parameters are given in graphical form (Figure 5-10 to 5-16) and tabulated form (Table 5-11 to 5-17).

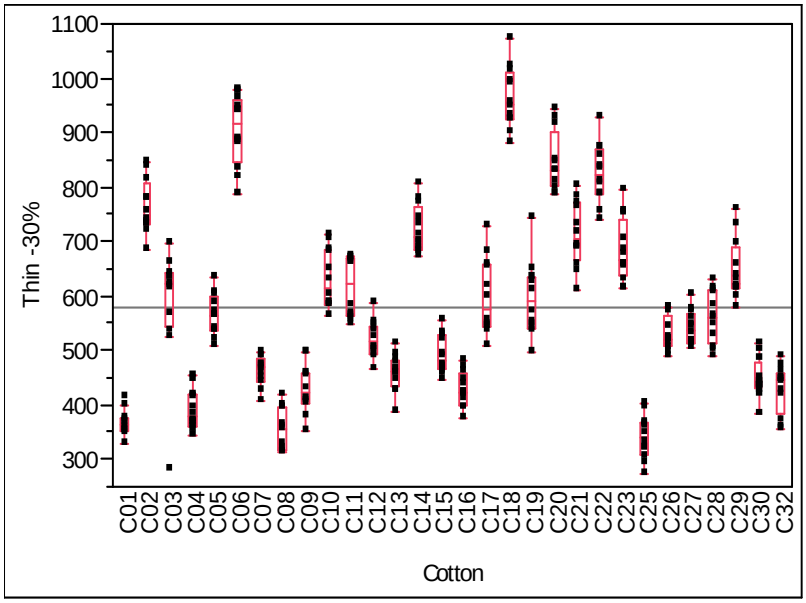

Figure 5-10. Yarn Thin Places -30%

Cotton	Mean	Std Dev
C01	365.833	22.731
C02	762.917	49.314
C03	586.083	107.481
C04	389.583	36.405
C05	563.667	37.919
C06	903.000	64.796
C07	461.250	26.697
C08	356.083	38.529
C09	429.250	43.681
C10	630.000	54.123
C11	615.083	54.745
C12	519.917	33.857
C13	458.417	33.886
C14	722.167	43.915
C15	491.083	35.362
C16	428.250	31.924
C17	597.583	69.541
C18	962.667	56.519
C19	594.750	67.227
C20	846.000	54.331
C21	712.917	59.703
C22	824.250	53.995
C23	683.000	57.741
C25	339.583	39.590
C26	530.083	31.271
C27	541.083	30.918
C28	561.250	48.664
C29	646.250	55.217
C30	446.167	36.025
C32	428.417	44.164

Table 5-11. Yarn Thin Places -30%

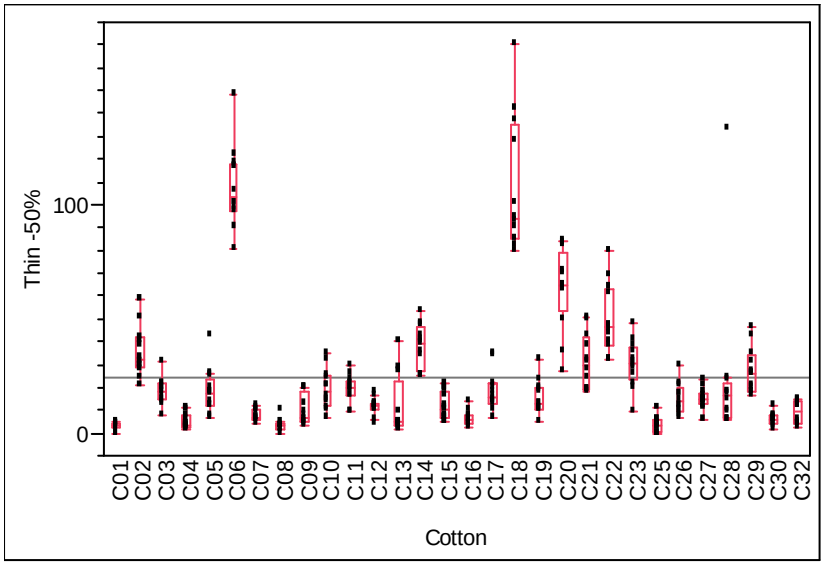

Figure 5-11. Yarn Thin Places -50%

Cotton	Mean	Std Dev
C01	2.917	1.7299
C02	35.583	11.0656
C03	18.167	5.7498
C04	4.750	3.2787
C05	18.333	9.7732
C06	108.000	17.6687
C07	8.000	2.3741
C08	3.167	2.6572
C09	9.917	6.6121
C10	19.250	8.6982
C11	19.250	6.1957
C12	11.417	3.8009
C13	11.167	13.0581
C14	38.000	9.4002
C15	11.833	6.0126
C16	6.417	3.3155
C17	18.167	8.6322
C18	107.333	29.4196
C19	15.417	7.3294
C20	63.250	17.8790
C21	31.000	12.1131
C22	49.917	15.2223
C23	30.167	10.3206
C25	3.500	3.1766
C26	15.000	6.8091
C27	15.000	4.4518
C28	23.750	35.0016
C29	27.250	9.8454
C30	6.000	2.8284
C32	8.750	4.9749

Table 5-12. Yarn Thin Places -50%

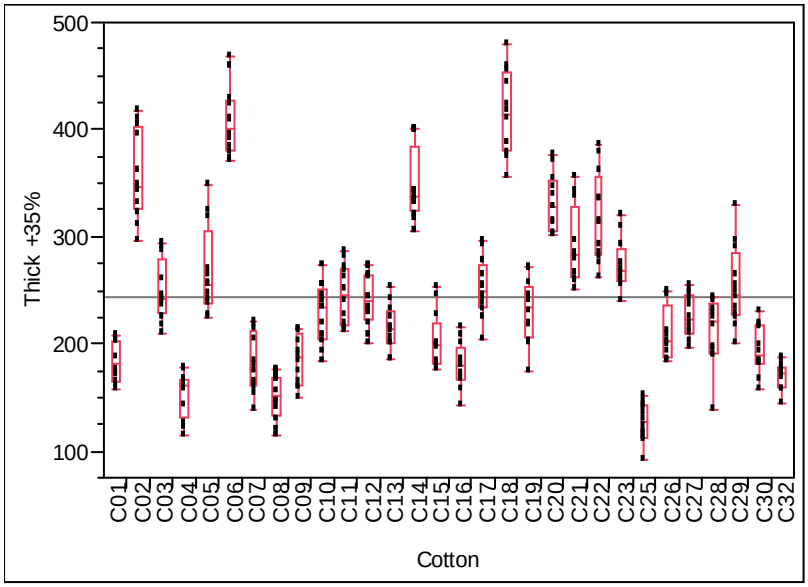

Figure 5-12. Yarn Thick Places +35%

Cotton	Mean	Std Dev
C01	184.083	19.1095
C02	357.250	40.9259
C03	249.250	28.2622
C04	153.333	21.5926
C05	267.667	40.8085
C06	407.167	32.1921
C07	181.250	27.1833
C08	150.500	21.5048
C09	184.583	23.2358
C10	228.583	27.4904
C11	245.417	27.5894
C12	240.167	24.2481
C13	214.333	21.1288
C14	346.917	33.3043
C15	203.083	25.3465
C16	179.917	20.6330
C17	252.000	27.0488
C18	414.333	38.7494
C19	230.833	29.2259
C20	331.167	26.3157
C21	292.333	35.1499
C22	318.417	41.3202
C23	274.167	23.2685
C25	126.333	17.7883
C26	209.167	24.8334
C27	225.750	19.3585
C28	211.250	30.4605
C29	252.583	36.9384
C30	194.000	22.6996
C32	170.500	12.2437

Table 5-13. Yarn Thick Places +35%

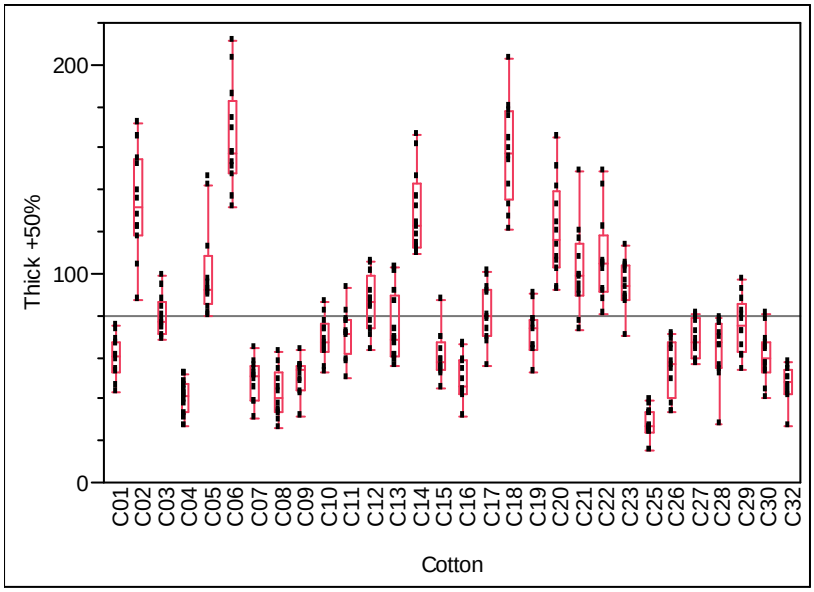

Figure 5-13. Yarn Thick Places +50%

Cotton	Mean	Std Dev
C01	60.417	10.0042
C02	133.167	25.0630
C03	79.333	9.9026
C04	41.000	8.0114
C05	100.000	22.2057
C06	164.750	24.7685
C07	48.917	9.4336
C08	42.167	11.5902
C09	50.583	8.3607
C10	68.583	10.0676
C11	71.500	11.5955
C12	85.750	13.6590
C13	74.500	16.5502
C14	129.333	19.3829
C15	60.167	10.8948
C16	49.833	10.5299
C17	81.333	13.7862
C18	157.667	24.2425
C19	72.417	10.9416
C20	120.667	23.0270
C21	101.083	20.4693
C22	107.167	20.9190
C23	94.583	11.5322
C25	28.583	6.7616
C26	54.917	13.7077
C27	68.750	9.0164
C28	64.083	14.7368
C29	75.083	13.3175
C30	60.417	12.2360
C32	47.167	8.5263

Table 5-14. Yarn Thick Places +50%

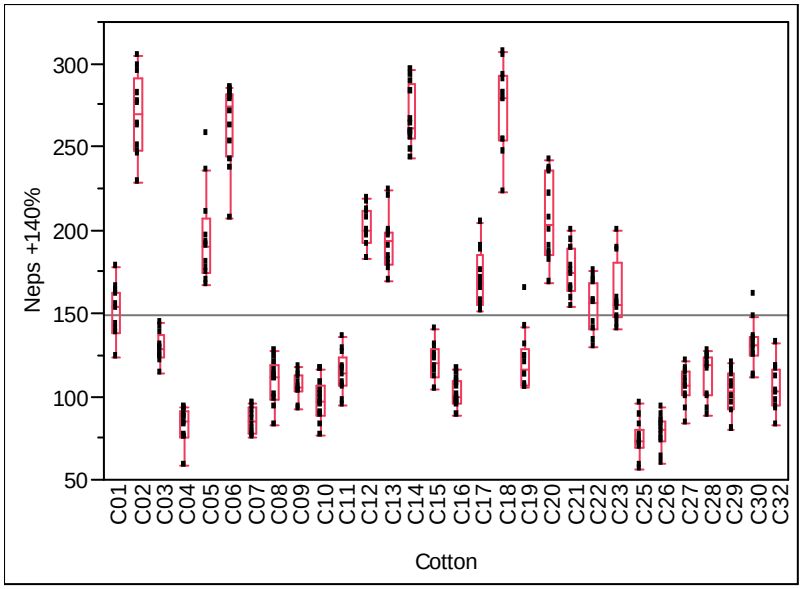

Figure 5-14. Yarn Neps +140%

Cotton	Mean	Std Dev
C01	151.667	15.4939
C02	269.167	23.7212
C03	129.167	8.7265
C04	82.667	10.1295
C05	195.000	27.3030
C06	263.333	24.2537
C07	85.083	7.8562
C08	108.833	12.7553
C09	105.833	7.8258
C10	97.500	12.3030
C11	113.917	12.3469
C12	201.083	11.9883
C13	192.833	16.6178
C14	267.667	18.0168
C15	120.000	11.0289
C16	102.083	8.5116
C17	170.417	16.4065
C18	274.083	25.1702
C19	121.167	17.5749
C20	207.250	25.7863
C21	175.333	14.8712
C22	153.500	15.6292
C23	160.833	19.4928
C25	74.167	11.1586
C26	78.417	9.8669
C27	106.083	10.5784
C28	112.917	13.8003
C29	102.083	13.5811
C30	131.417	13.4601
C32	105.500	13.5881

Table 5-15. Yarn Neps +140%

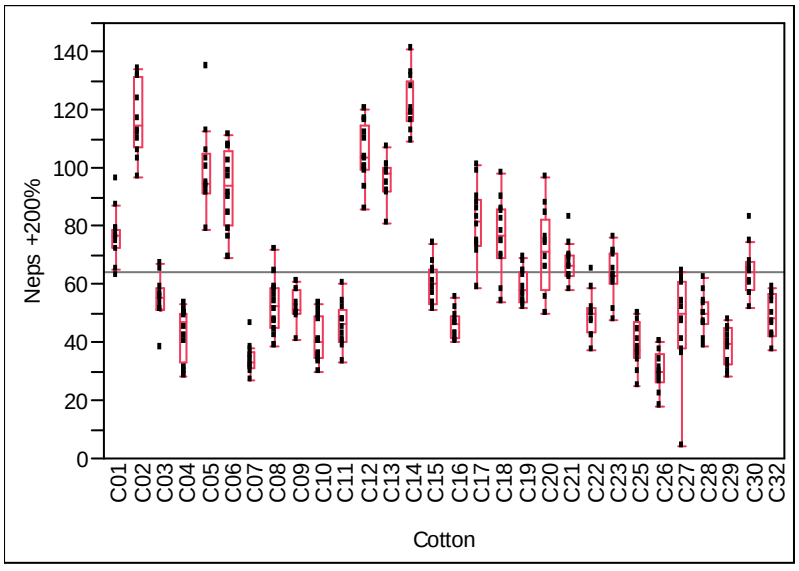

Figure 5-15. Yarn Neps +200%

Cotton	Mean	Std Dev
C01	77.000	8.7594
C02	117.500	12.6455
C03	54.833	7.4203
C04	43.250	9.0365
C05	99.417	14.1322
C06	92.750	13.5923
C07	34.167	4.8021
C08	52.833	9.6090
C09	52.750	5.8329
C10	40.833	7.7087
C11	45.917	7.3665
C12	105.000	10.2691
C13	96.250	6.6350
C14	122.000	9.3030
C15	60.083	7.2043
C16	45.917	4.6213
C17	81.583	12.1090
C18	76.667	12.7588
C19	59.417	5.9766
C20	70.833	14.6959
C21	67.500	6.4597
C22	49.333	7.4752
C23	63.417	8.1515
C25	39.083	7.8446
C26	30.167	6.7667
C27	47.167	16.6779
C28	49.667	6.5690
C29	38.667	6.5690
C30	64.333	8.3594
C32	49.083	7.2671

Table 5-16. Yarn Neps +200%

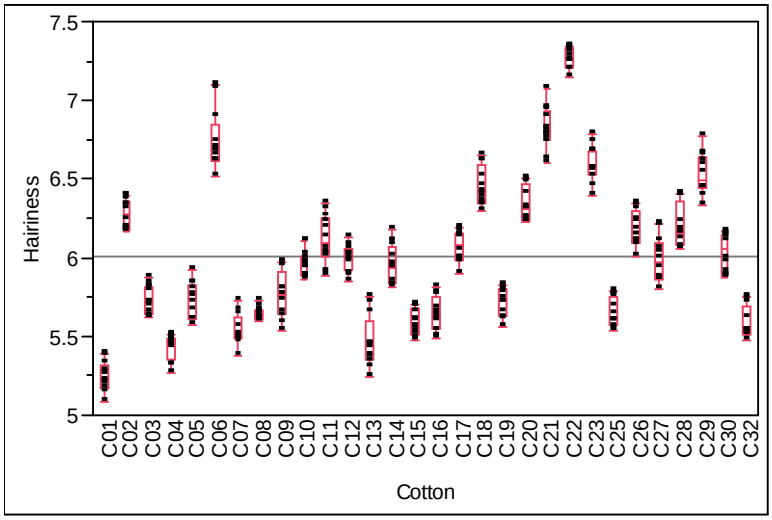

Figure 5-16. Yarn Hairiness

Cotton	Mean	Std Dev
C01	5.24333	0.092376
C02	6.27167	0.093501
C03	5.73083	0.090097
C04	5.42667	0.080491
C05	5.72500	0.112290
C06	6.74083	0.185299
C07	5.53500	0.098581
C08	5.64500	0.040339
C09	5.76250	0.147902
C10	5.96083	0.081180
C11	6.11500	0.151987
C12	5.99250	0.082916
C13	5.45917	0.161553
C14	5.95500	0.118590
C15	5.58667	0.084027
C16	5.64000	0.107450
C17	6.06917	0.098022
C18	6.45167	0.122536
C19	5.71833	0.089426
C20	6.33417	0.107489
C21	6.81500	0.133314
C22	7.26833	0.061767
C23	6.59583	0.112852
C25	5.65000	0.097421
C26	6.18083	0.109500
C27	5.98250	0.139878
C28	6.19833	0.133949
C29	6.52833	0.129041
C30	6.02833	0.121119
C32	5.57833	0.099894

Table 5-17. Yarn Hairiness

The yarn imperfection also has effect on the yarn tensile properties. As mentioned earlier, the panel of cotton is spun by using three different twist multipliers. The value of twist multiplier plays an important role in the amount of twist imparted to the yarn during spinning process. So the statistical analyses are applied to all the tensile results for all the twist multipliers. These analyses are shown in the following graphical figures and tables. The graphical representation of yarn elongation for twist multipliers T_1, T_2 and T_3 are shown in the Figure 5-17 to 5-19 respectively. The means values are given in the tabulated form in the following tables (Table 5-18 to 5-20). Similarly, the yarn tenacity is also given in graphical form and tabulated form for all the twist multipliers.

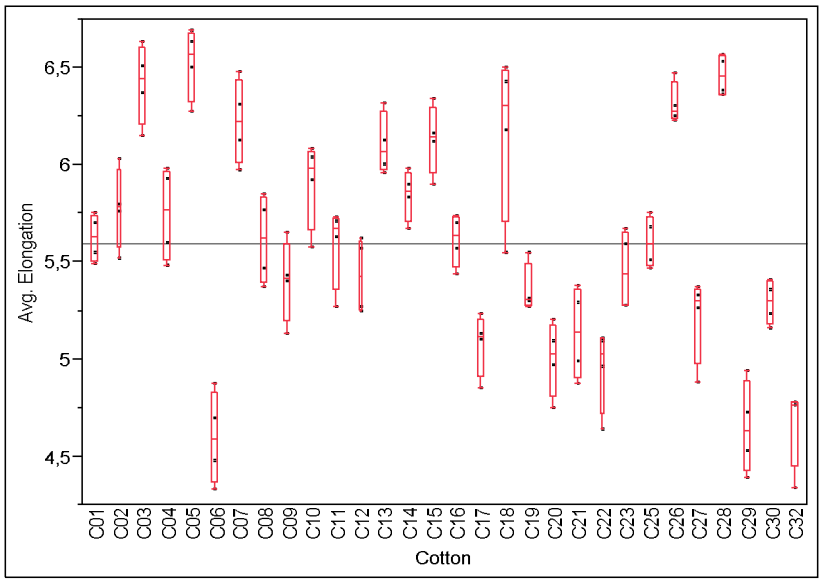

Figure 5-17. Yarn Elongation for T_1

Cotton	Mean	Std Dev
C01	5,62250	0,122577
C02	5,77750	0,208866
C03	6,41500	0,206155
C04	5,74750	0,245408
C05	6,52250	0,186078
C06	4,59500	0,238118
C07	6,22250	0,220813
C08	5,61500	0,231157
C09	5,40250	0,213131
C10	5,90500	0,227083
C11	5,58500	0,214398
C12	5,42750	0,194658
C13	6,10250	0,162147
C14	5,84500	0,131783
C15	6,13000	0,180739
C16	5,61250	0,135984
C17	5,07750	0,161529
C18	6,16500	0,432396
C19	5,35750	0,129454
C20	5,00250	0,192765
C21	5,13250	0,241713
C22	4,95000	0,217102
C23	5,45500	0,204695
C25	5,60250	0,134009
C26	6,31250	0,109049
C27	5,21000	0,224648
C28	6,46000	0,105515
C29	4,64750	0,239774
C30	5,29000	0,115181
C32	4,66250	0,215155

Table 5-18. Yarn Elongation for T_1

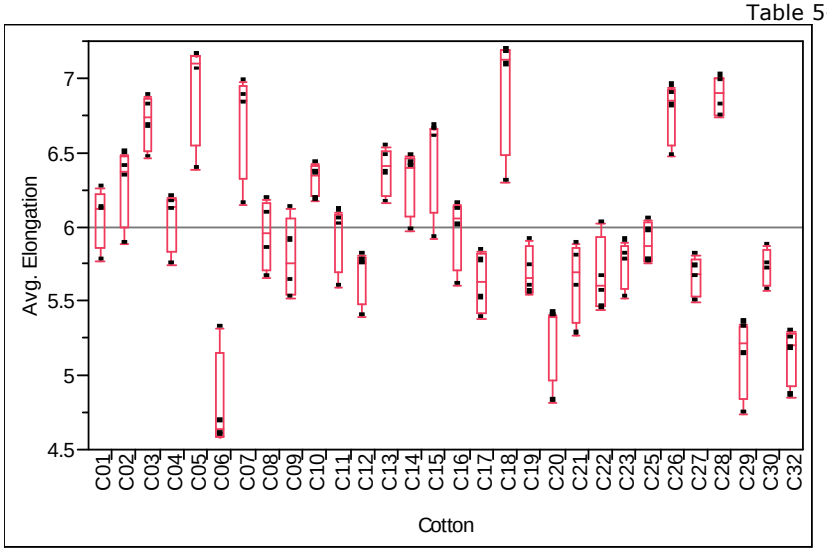

Figure 5-18. Yarn Elongation for T_2

Cotton	Mean	Std Dev
C01	6.06500	0.208247
C02	6.27500	0.271355
C03	6.70000	0.182757
C04	6.05000	0.209284
C05	6.93250	0.371338
C06	4.79250	0.346831
C07	6.70250	0.373575
C08	5.94000	0.234947
C09	5.79000	0.269196
C10	6.32250	0.107199
C11	5.93500	0.233024
C12	5.67500	0.192267
C13	6.37750	0.163172
C14	6.31000	0.229202
C15	6.45750	0.359293
C16	5.96250	0.249048
C17	5.62000	0.210871
C18	6.93000	0.429185
C19	5.69250	0.165806
C20	5.25000	0.286705
C21	5.63250	0.270355
C22	5.66750	0.251578
C23	5.74500	0.158430
C25	5.88500	0.143411
C26	6.77500	0.211424
C27	5.66500	0.131783
C28	6.88000	0.131403
C29	5.13000	0.276043
C30	5.72000	0.123558
C32	5.13500	0.197400

Table 5-19. Yarn Elongation for T_2

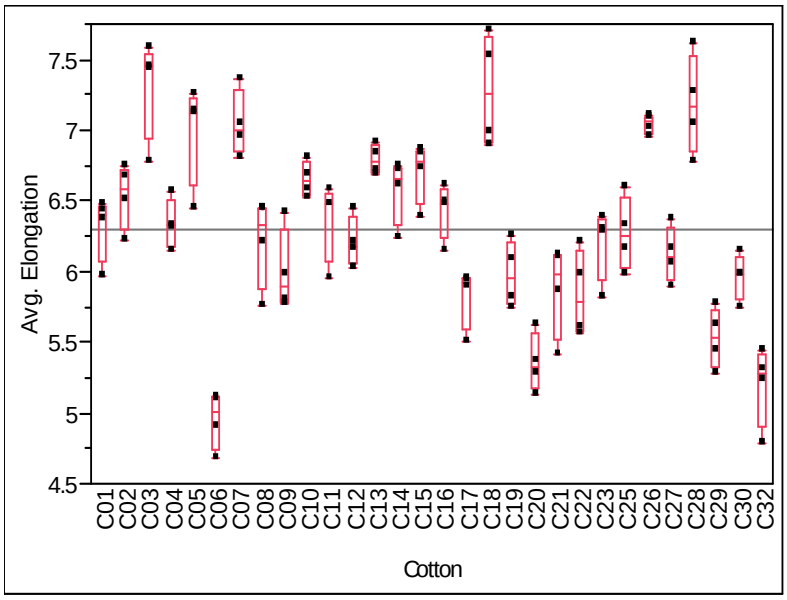

Figure 5-19. Yarn Elongation for T_3

Cotton	Mean	Std Dev
C01	6.31000	0.230362
C02	6.53250	0.231427
C03	7.31000	0.365605
C04	6.33750	0.176895
C05	6.98750	0.363169
C06	4.95250	0.204837
C07	7.04000	0.233381
C08	6.21250	0.320559
C09	5.99250	0.292504
C10	6.64750	0.123659
C11	6.37000	0.284371
C12	6.21000	0.175689
C13	6.79000	0.102956
C14	6.57250	0.235000
C15	6.70250	0.215619
C16	6.43000	0.196638
C17	5.82250	0.216083
C18	7.27500	0.401871
C19	5.97750	0.233435
C20	5.35000	0.205426
C21	5.87750	0.332403
C22	5.84000	0.302765
C23	6.19500	0.254886
C25	6.26500	0.259551
C26	7.04000	0.069761
C27	6.12000	0.200499
C28	7.17750	0.351129
C29	5.53000	0.214631
C30	5.96500	0.169017
C32	5.19750	0.285351

Table 5-20. Yarn Elongation for T_3

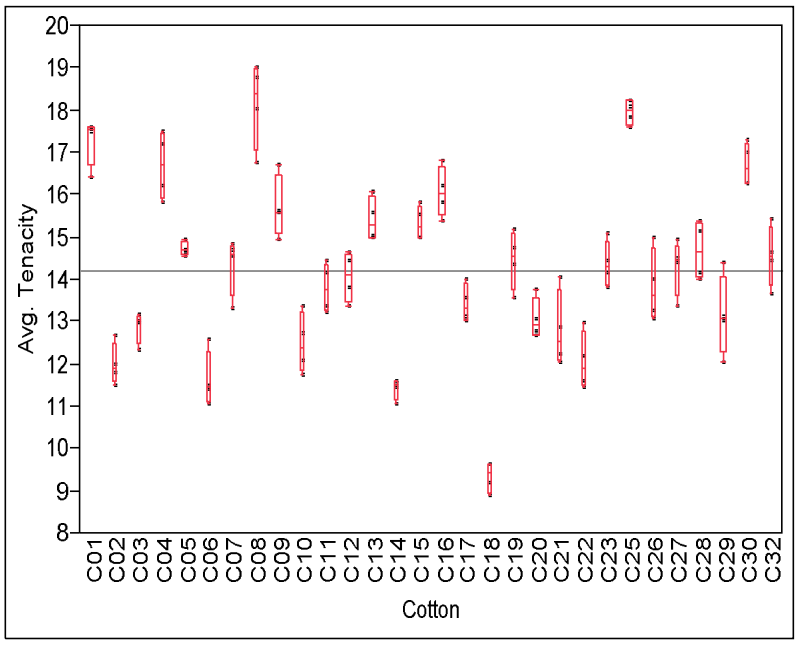

Figure 5-20. Yarn Tenacity for T_1

Cotton	Mean	Std Dev
C01	17,2775	0,57355
C02	11,9775	0,49426
C03	12,8650	0,36964
C04	16,6725	0,80897
C05	14,7025	0,16358
C06	11,6125	0,65566
C07	14,3400	0,68445
C08	18,1325	1,02233
C09	15,7050	0,74106
C10	12,4700	0,72032
C11	13,7975	0,59225
C12	14,0525	0,59416
C13	15,4150	0,51417
C14	11,4100	0,24125
C15	15,3175	0,41836
C16	16,0600	0,59537
C17	13,4100	0,45070
C18	9,3300	0,36341
C19	14,4550	0,68110
C20	13,0550	0,48611
C21	12,7900	0,90458
C22	12,0525	0,68563
C23	14,3550	0,54015
C25	17,9425	0,28964
C26	13,8250	0,87596
C27	14,2775	0,66865
C28	14,6625	0,69293
C29	13,1425	0,97079
C30	16,7000	0,51147
C32	14,5450	0,72592

Table 5-21. Yarn Tenacity for T_1

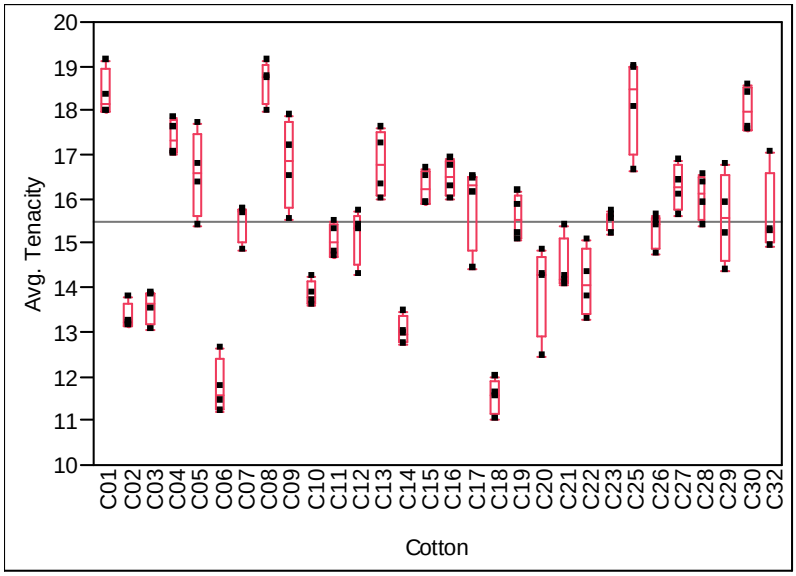

Figure 5-21. Yarn Tenacity for T_2

Cotton	Mean	Std Dev
C01	18.3375	0.55638
C02	13.3400	0.30995
C03	13.5650	0.37917
C04	17.3800	0.39858
C05	16.5525	0.95273
C06	11.7525	0.62888
C07	15.4975	0.44642
C08	18.6350	0.48363
C09	16.7875	1.00134
C10	13.8425	0.27512
C11	15.0625	0.38178
C12	15.1550	0.61701
C13	16.7800	0.75666
C14	13.0300	0.30800
C15	16.2400	0.39302
C16	16.4825	0.41532
C17	15.8725	0.98855
C18	11.5200	0.39251
C19	15.5725	0.52341
C20	13.9600	1.03772
C21	14.4600	0.63071
C22	14.1075	0.77168
C23	15.5075	0.20678
C25	18.1550	1.10543
C26	15.2950	0.38820
C27	16.2525	0.52684
C28	16.0500	0.52339
C29	15.5725	1.01454
C30	18.0175	0.51636
C32	15.6250	0.95158

Table 5-22. Yarn Tenacity for T_2

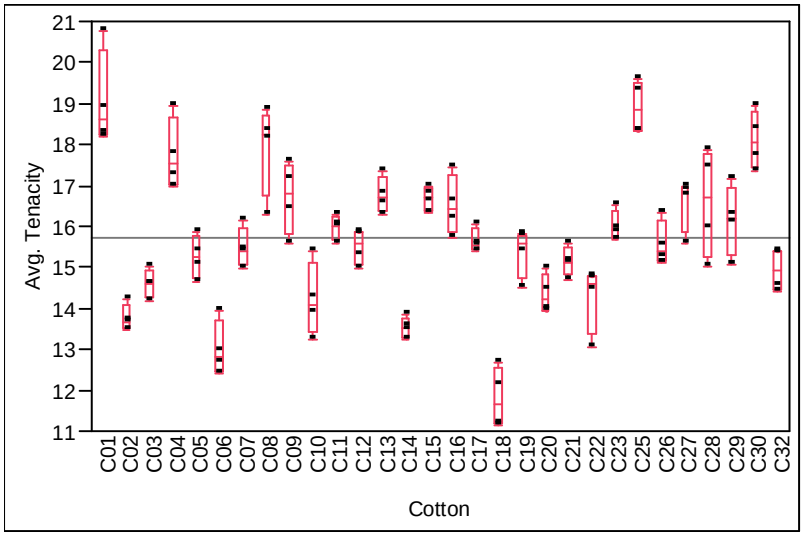

Figure 5-22. Yarn Tenacity for T_3

Cotton	Mean	Std Dev
C01	19.0425	1.18004
C02	13.7675	0.32837
C03	14.6075	0.34731
C04	17.7425	0.88013
C05	15.2450	0.52792
C06	13.0025	0.67756
C07	15.4700	0.48104
C08	17.9025	1.12373
C09	16.6975	0.88970
C10	14.2100	0.90602
C11	15.9700	0.30000
C12	15.4925	0.43370
C13	16.7525	0.45375
C14	13.5250	0.24624
C15	16.6725	0.28300
C16	16.4950	0.73894
C17	15.6450	0.29263
C18	11.7900	0.75158
C19	15.3650	0.58994
C20	14.3475	0.48699
C21	15.1350	0.35152
C22	14.2500	0.82069
C23	15.9975	0.37008
C25	18.9000	0.65401
C26	15.5550	0.54145
C27	16.5425	0.66289
C28	16.5800	1.33332
C29	16.1550	0.86277
C30	18.1050	0.69711
C32	14.9225	0.50947

Table 5-23. Yarn Tenacity for T_3

The above yarn tensile properties indicated that as the twist multiplier increases, the yarn elongation and tenacity also increase. So the twist

multiplier has significant effect on the yarn tensile properties. For example, the yarn elongation for C01 is 5.62%, 6.06% and 6.31% for T_1, T_2 and T_3 respectively. Similarly the yarn tenacity also increases gradually as the twist multiplier increases. This increase is due to the fact that as the twist multiplier increase, the amount of twist in the yarn also increases.

5.3 Statistical Analysis of Inter-fibre Friction

As described in the previous chapter, the cotton sliver after third drawing passage is tested for inter-fibre friction by using static friction tester. The loads applied on both carriages of SFT were 2000, 3000, 4000, and 5000 grams. The samples were tested six times for each of these loads. So that 24 test for fibre to fibre friction is performed for each cotton. The measurement performed at the SFT give a force displacement curve as shown in the Figure 5-23.

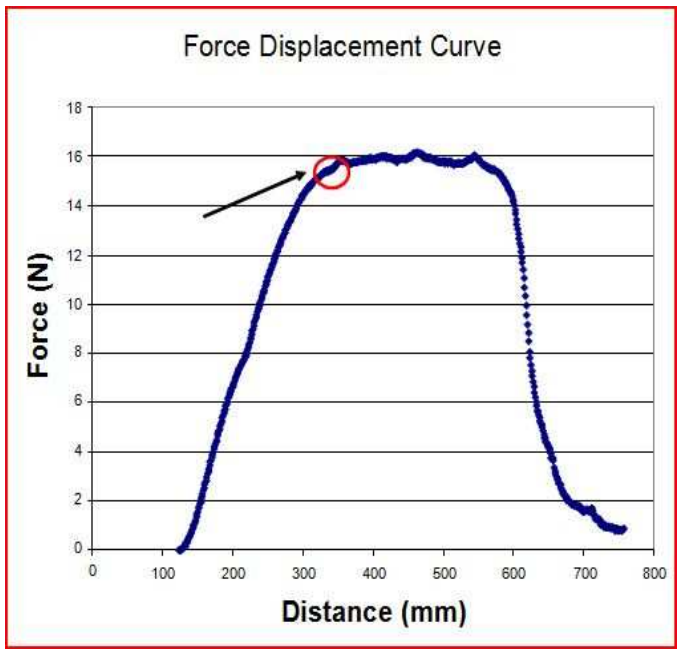

Figure 5-23. Force Displacement Curve

The force required to break the sliver is plotted against the distance travelled by the moving carriage. The distance is plotted against x-axis and is given in millimetres whereas the force is plotted against y-axis and the value is given in Newton. The force increases with the distance up to a certain level, after which the force decreases because the force applied to the sliver crosses the maximum resistive force. By analysing this curve, the value of force has been noted at the point where all the fibres are

contributing against the applied pulling force to break the sliver. The point is shown by the circle in the above figure.

5.3.1 Analysis of Force Displacement Curve

The analysis of the force displacement curve to select the point plays an important role in the fibre to fibre friction calculation. The curve analysis procedure with some example is given below:

The analog signals are acquired from the force sensor with the help of data acquisition cards. Tests are performed under the following conditions:

- Force is expressed in volt, with the following calibration: 1 volt = 10 newton;
- Mobile clamp is moving at 20 mm/min for around 2 minutes for each test;
- Force signal is acquired at 1 kHz frequency;
- In consequence, one record of data is taken at each 0.0005 mm.

The SFT measurement data for each step of displacement is recorded. Each test then produces around 70000 to 90000 lines of data (Figure 5-24, example of cotton 01, mass = 2000 during repetition 1).

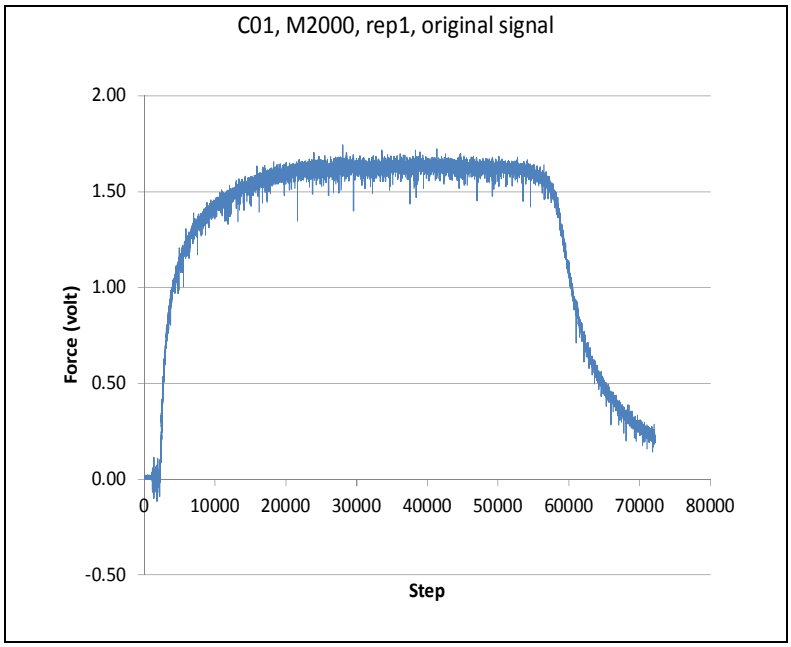

Figure 5-24. Analysis of Force Curve-1

The selection of the point, where all the fibres are contributing against the applied pulling force to break the sliver, on the curve involves several calculation steps which are explained as follows:

- The noise produced at the start of the test is removed, so that the curve starts at 0 as shown in Figure 5-25. The noise produced at the start is due to the fact that data acquisition starts immediately as the test start but the motor start after some seconds;

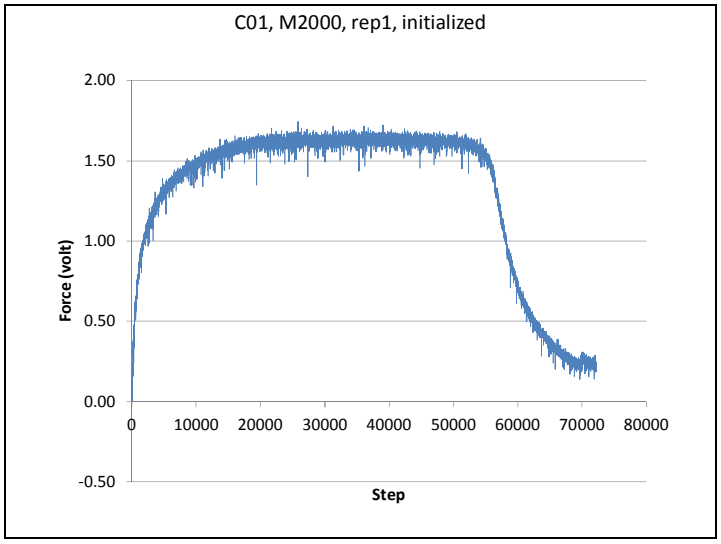

Figure 5-25. Analysis of Force Curve-2

- A moving average of 400 data lines is done up to a maximum of 40 000 lines in order to make the calculation simple in the Excel and also to remove noise in the signal (Figure 5-26);

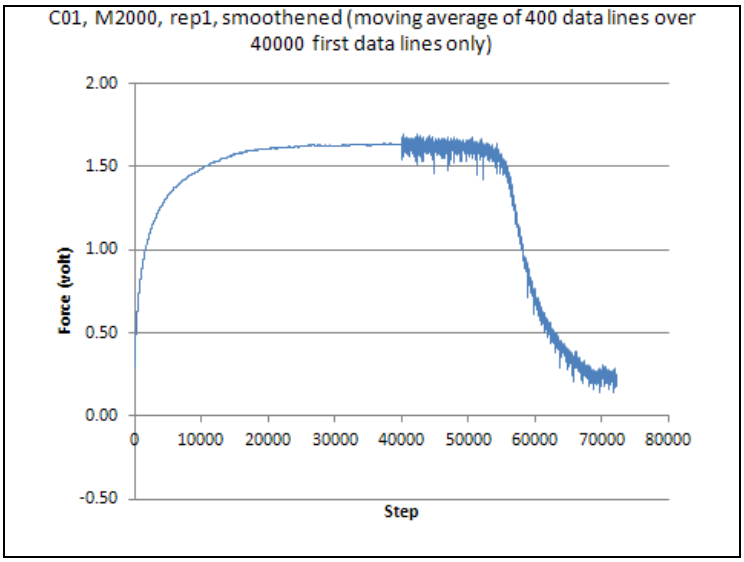

Figure 5-26. Analysis of Force Curve-3

- A further calculation step is performed to make the analysis simple and remove the noise. A line is selected out of 10 from 4000 data summary lines and calculating the slopes over 20 values along the 4000 data summary lines (Figure 5-27);

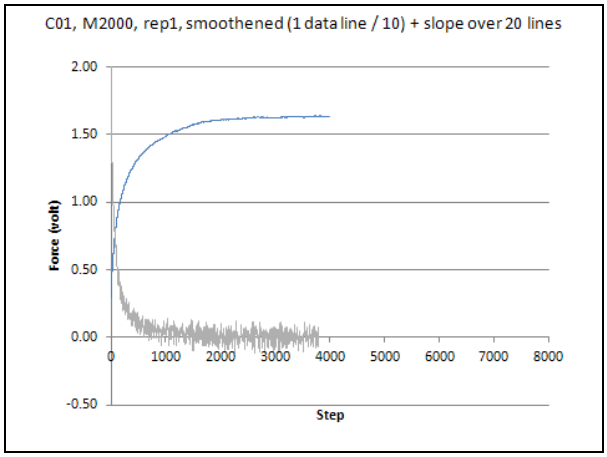

Figure 5-27. Analysis of Force Curve-4

- Smoothening of the slope signal with a moving average over 400 data lines up to a maximum of 4000 lines in order to remove noise in the signal (Figure 5-28);

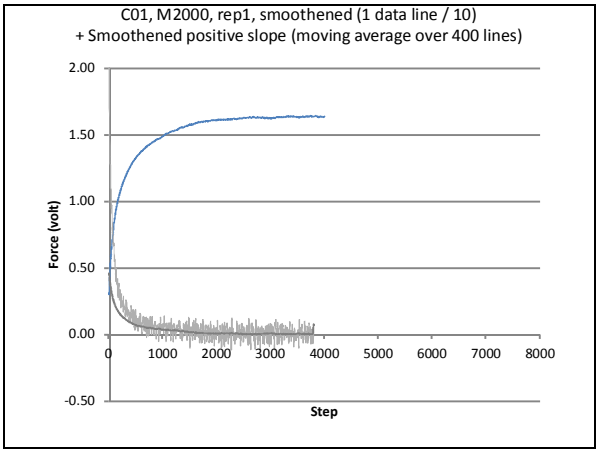

Figure 5-28. Analysis of Force Curve-5

- Calculation and detection of the smoothened first time slope which is equal to 0 to find the corresponding smoothened force (Figure 5-29).

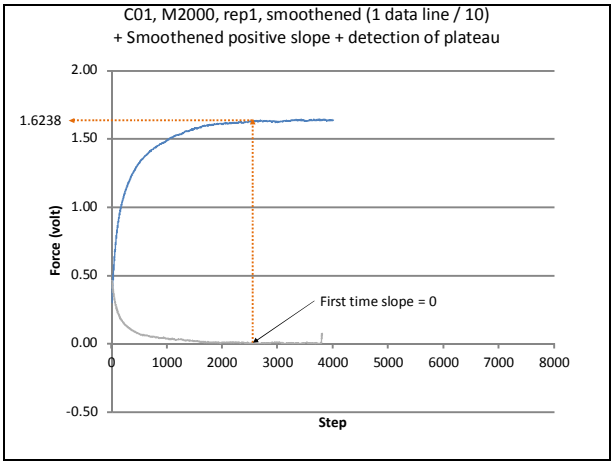

Figure 5-29. Analysis of Force Curve-6

The same force curve analysis has been used for 30 cottons * 4 masses * 6 replicates equivalent to 720 SFT data files.

5.3.2 Fibre Frictional Models

The data obtained from SFT gives rise to the following friction models to get the inter-fibre friction results. We have applied ten different fibre friction models in order to investigate which model is more descriptive. All these models are derived from the same model explained by Nowrouzieh [80]. The friction models with the corresponding equation are explained below:

Model 1: $(F/CFM) = k\,(W/CFM)^a$

Model 2: $(F/SC) = k\,(W/SC)^a$

Model 3: $(F/N_F) = k\,(W/N_F)^a$

Model 4: $(F/L^*) = k\,(W/L^*)^a$

Model 5: $(F/N^*) = k\,(W/N^*)^a$

Model 6: $(F/CFM) = k\,(W/CFM) + C$

Model 7: $(F/SC) = k\,(W/SC) + C$

Model 8: $(F/N_F) = k\,(W/N_F) + C$

Model 9: $(F/L^*) = k\,(W/L^*) + C$

Model 10: $(F/N^*) = k\,(W/N^*) + C$

where:

F is the frictional resistance force,

CFM is the mass of protruding fibres from the two clamps of SFT,

W is the perpendicular compression force on fibre,

SC is the sliver count or sliver hank,

N_F is the number of fibres in sliver cross section,

L* is the total length of the CFM fibres,

N* is total number of fibres present in the CFM,

K, *a* are the coefficients that characterize friction.

The L* and N* is calculated by the following equations

$$L^* = (CFM/\text{Fibre Fineness}) * 10^6$$

$$N^* = (CFM * 10^9)/(\text{Fibre Fineness} * L(n))$$

where:

L (n) is the fibre length of the cotton by number measured by AFIS.

5.3.3 Calculation of Fibre to Fibre Frictional Coefficients

The friction coefficients *k* and *a* are then calculated for each cotton by using equations of each frictional model.

The resistive force along with other calculated values were analysed statistically. The regression analysis was applied and a line fit was applied on the data for all the models separately. The line fit gave the value of Ln*k* and *a* for each model. As we will have large amount of data and figures, so we will only discuss one example of model 1 for C01. The individual values of the coefficients that characterize friction are given in Annex-E. The calculated values of (F/CFM) and (W/CFM) for C01 are given in Table 5-24.

W(cN)	F(cN)	F/CFM	W/CFM	Ln F/CFM	Ln W/CFM
2145	1623.177	0.155327929	0.205263039	-1.86221673	-1.58346301
2145	1616.022	0.168511198	0.22367036	-1.78075307	-1.49758192
2145	1474.235	0.130463241	0.189822899	-2.03666377	-1.66166375
2145	1532.993	0.163432143	0.228677906	-1.8113574	-1.47544079
2145	1476.48	0.142931271	0.207647508	-1.94539139	-1.57191331
2145	1586.959	0.164111609	0.221819933	-1.80720854	-1.50588934
3126	2039.732	0.206241877	0.316042847	-1.57870564	-1.15187748
3126	2233.399	0.224236856	0.313821662	-1.49505239	-1.15893041
3126	2056.876	0.193133935	0.293489555	-1.64437137	-1.22591323
3126	2169.945	0.233578539	0.336454656	-1.4542369	-1.08929189
3126	2209.185	0.240390092	0.340115752	-1.42549229	-1.07846927
3126	2003.479	0.182966135	0.285448745	-1.6984542	-1.25369279
4106	3123.953	0.36752394	0.483097501	-1.00096682	-0.72753678
4106	2665.382	0.283853256	0.437308707	-1.25929788	-0.82711591
4106	2594.983	0.275768612	0.436379252	-1.28819313	-0.82924357
4106	2334.19	0.279543738	0.491775899	-1.27459651	-0.70973216
4106	2581.996	0.284674271	0.45273746	-1.25640966	-0.79244288
4106	2657.188	0.249501175	0.385570776	-1.38829165	-0.95303051
5087	3076.664	0.312351661	0.516446067	-1.16362561	-0.66078442
5087	2942.973	0.540987727	0.935109148	-0.61435869	-0.06709202
5087	3252.659	0.350880125	0.548758766	-1.04731064	-0.60009634
5087	3176.217	0.344866133	0.552333742	-1.06459896	-0.59360281
5087	3077.071	0.314950928	0.520674899	-1.15533844	-0.65262943
5087	3102.361	0.364554763	0.5977666	-1.0090785	-0.5145549

Table 5-24. Values of (F/CFM) and (W/CFM) for C01

The linear regression analysis is applied on the columns Ln F/CFM and Ln W/CFM. The figure 5-30 shows the line fit for the regression analysis applied on the values of the cotton type C01 for the frictional model M1. Similar statistical analysis is applied for all the frictional models and coefficients of frictions are calculated.

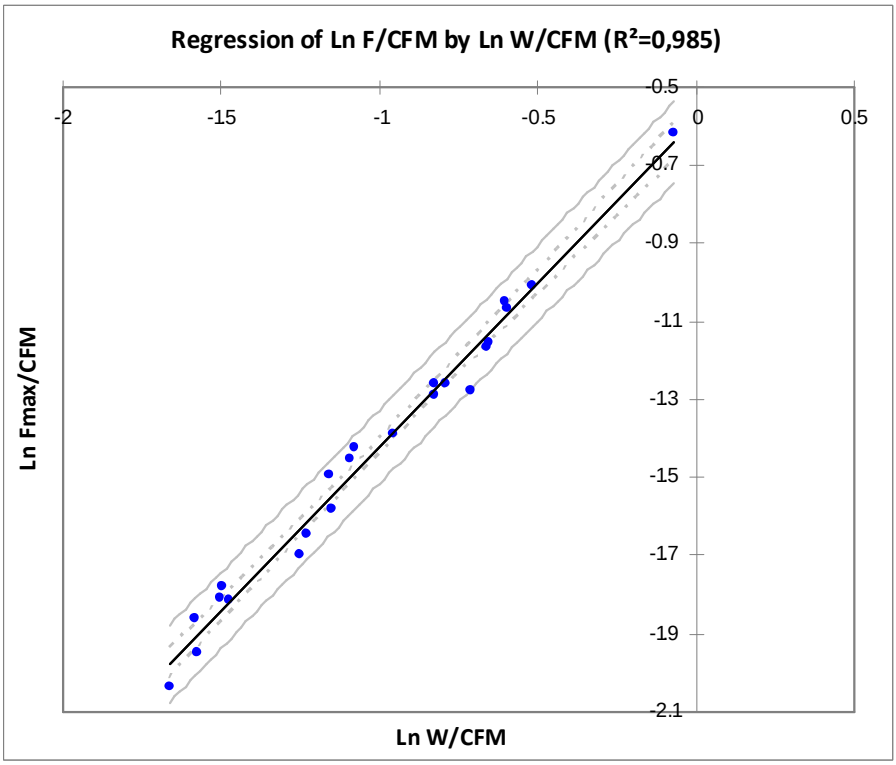

Figure 5-30. Line Fit regression analysis M1 for Cotton 01.

The coefficient of friction is given in the Table 5-25. The value of constant corresponds to coefficient friction Ln*k* and value of Ln W/CFM corresponds to coefficient friction *a*.

Source	Value	Standard Deviation	t	Pr > |t|
Constant	-0.583	0.025	-23.387	< 0,0001
Ln W/CFM	0.838	0.023	36.905	< 0,0001

Table 5-25. Values of Frictional coefficients

It is important to note that for Model 1 the values of F/CFM and W/CFM are divided by 10^5. Similarly the values of F/L* and W/L* for model 4 are divided by 10^4. This change for these two models is due to the fact that for all other models the values exist between -0.30 to -0.80 of the Ln curve. So in order to compare them we adjusted the values for these two models so that all the models have the values in the same zone of the curve.

5.3.4 Correlation Analysis of Frictional Models

The coefficients of friction for all models is calculated and put in table to apply correlation analysis. The graphical representation of the correlation analysis between different friction models is given in Figure 5-31. The correlation values are also given in the following Table 5-26.

	LnK1	a1	LnK2	a2	LnK3	a3	LnK4	a4	LnK5	a5	Constant 6	K6	Constant 7	K7	Constant 8	K8	Constant 9	K9	Constant 10	K10
LnK1	1																			
a1	0.6497	1																		
LnK2	0.9654	0.4884	1																	
a2	0.6377	0.9805	0.4803	1																
LnK3	0.8967	0.8811	0.8008	0.8975	1															
a3	0.6377	0.9805	0.4803	1.0000	0.8975	1														
LnK4	0.9588	0.4681	0.9462	0.4724	0.8054	0.4724	1													
a4	0.6497	1.0000	0.4884	0.9805	0.8811	0.9805	0.4681	1												
LnK5	0.9344	0.8465	0.8427	0.8463	0.9877	0.8463	0.8575	0.8465	1											
a5	0.6497	1.0000	0.4884	0.9805	0.8811	0.9805	0.4681	1.0000	0.8465	1										
Constant 6	-0.2410	-0.8377	-0.1023	-0.8171	-0.5685	-0.8171	-0.0269	-0.8377	-0.4958	-0.8377	1									
K6	0.9761	0.7298	0.9354	0.7162	0.9266	0.7162	0.9005	0.7298	0.9473	0.7298	-0.4123	1								
Constant 7	-0.4602	-0.9157	-0.2648	-0.9340	-0.7489	-0.9340	-0.2922	-0.9157	-0.6919	-0.9157	0.8750	-0.5708	1							
K7	0.9740	0.7450	0.9269	0.7442	0.9406	0.7442	0.8952	0.7450	0.9559	0.7450	-0.4167	0.9943	-0.6039	1						
Constant 8	-0.4481	-0.8676	-0.2966	-0.8630	-0.6682	-0.8630	-0.2158	-0.8676	-0.6144	-0.8676	0.8624	-0.5685	0.9173	-0.6007	1					
K8	0.9733	0.7468	0.9258	0.7458	0.9410	0.7458	0.8937	0.7468	0.9558	0.7468	-0.4204	0.9946	-0.6061	0.9999	-0.6028	1				
Constant 9	-0.2728	-0.7825	-0.1739	-0.7451	-0.5169	-0.7451	-0.0162	-0.7825	-0.4530	-0.7825	0.9440	-0.4432	0.7869	-0.4454	0.8969	-0.4490	1			
K9	0.9761	0.7298	0.9354	0.7162	0.9266	0.7162	0.9005	0.7298	0.9473	0.7298	-0.4123	1.0000	-0.5708	0.9943	-0.5685	0.9946	-0.4432	1		
Constant 10	-0.4631	-0.8409	-0.3497	-0.7989	-0.6416	-0.7989	-0.2182	-0.8409	-0.5922	-0.8409	0.8882	-0.6066	0.8205	-0.6070	0.9252	-0.6107	0.9571	-0.6066	1	
K10	0.9761	0.7298	0.9354	0.7162	0.9266	0.7162	0.9005	0.7298	0.9473	0.7298	-0.4123	1.0000	-0.5708	0.9943	-0.5685	0.9946	-0.4432	1.0000	-0.6066	1

Table 5-26. Correlation Analysis between Frictional Models

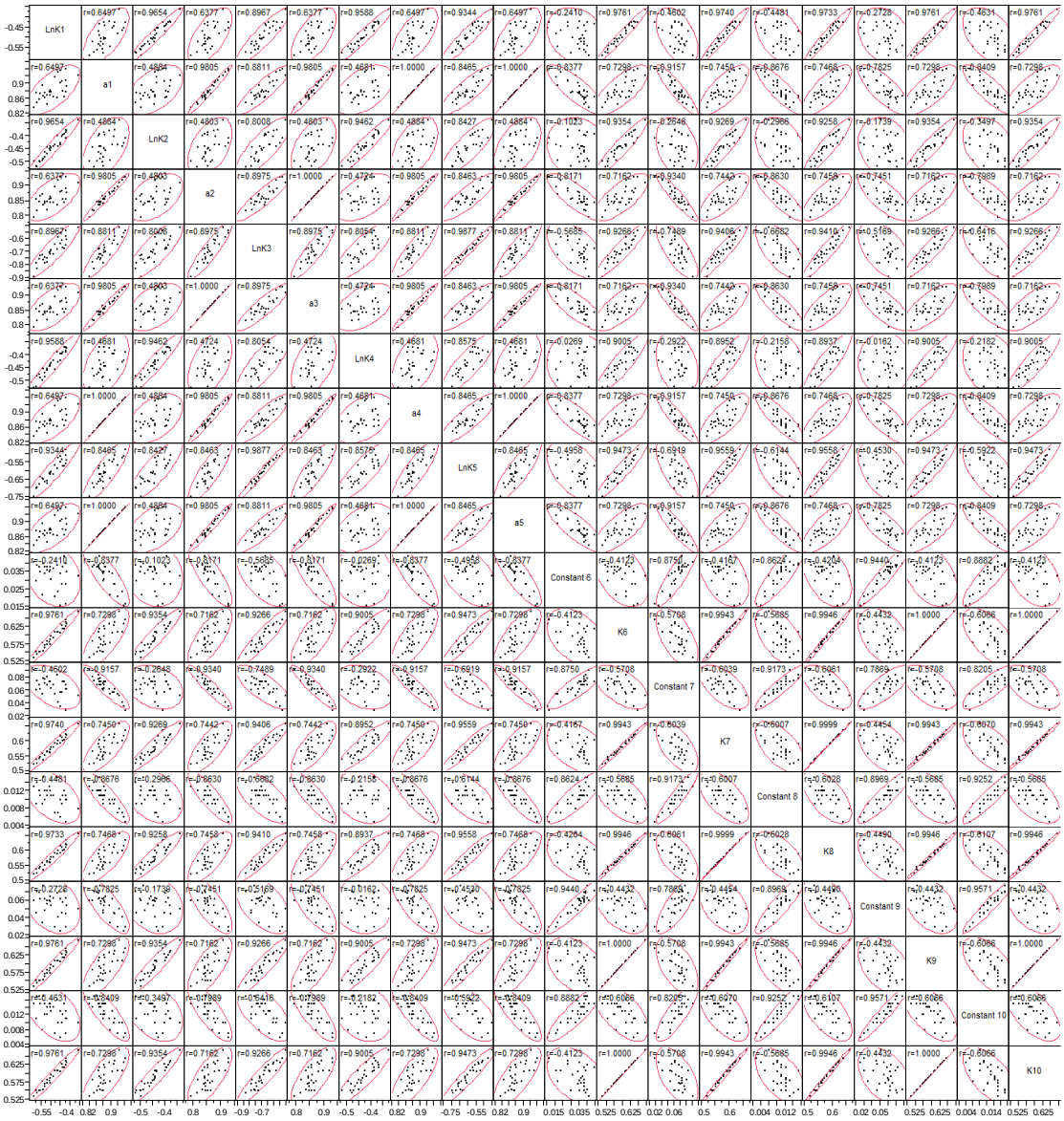

Figure 5-31. Correlation Analysis between Frictional Models

It can be seen from the above correlation analysis, the value of frictional coefficient *a* for model 1, model 4 and model 5 is identical. The value of *a* for model 2 and model 3 is also identical. Similarly the model 6, model 9 and model 10 also have same value as did the value of model 7 and model 8 is also identical. It is obvious that there is a good correlation between all the frictional coefficients. The constant involved in the linear frictional models (Model 6 to Model 10) also has a good correlation. The correlation between constant is not as strong as the correlation between lnk and k. The coefficient of friction *a* does not show any strong correlation with other frictional coefficients or the values of constant. The graphical representation of correlation analysis also gives a clear idea about the correlation between different friction models.

5.3.5 Differentiation between Cottons Based on Frictional Models

As different inter-fibre friction model are applied to the SFT data, it is important to find how the frictional models differentiate cottons. A panel of 30 cottons was tested. A procedure is developed to calculate the degree of differentiation for each model. The models 1 to 5 have two coefficients of friction. The models 6 to 10 have one coefficient of friction and a constant. The differentiation between cottons is carried out on the basis of all frictional coefficients. The differentiation procedure will be discussed for one coefficient only. For other coefficients, the values are given in Table 5-27. The detailed data for one coefficient, for which the differentiation procedure is explained, is given in Table 5-27. In this table, we have different DOF value (degree of freedom) because we have excluded some aberrant trials due to change of cotton.

Cotton	DOF	LnK1	Sigma Lnk	Confidence Interval 95%	Lower Limit	Upper Limit
C01	21	-0.583	0.025	0.01069248	-0.59369248	-0.57230752
C02	20	-0.451	0.023	0.010080009	-0.46108001	-0.440919991
C03	21	-0.498	0.024	0.010264781	-0.50826478	-0.487735219
C04	22	-0.529	0.012	0.005014389	-0.53401439	-0.523985611
C05	22	-0.519	0.013	0.005432254	-0.52443225	-0.513567746
C06	21	-0.425	0.008	0.003421594	-0.42842159	-0.421578406
C07	21	-0.502	0.015	0.006415488	-0.50841549	-0.495584512
C08	22	-0.48	0.022	0.009193046	-0.48919305	-0.470806954
C09	20	-0.507	0.017	0.007450442	-0.51445044	-0.499549558
C10	22	-0.466	0.008	0.003342926	-0.46934293	-0.462657074
C11	22	-0.425	0.011	0.004596523	-0.42959652	-0.420403477
C12	21	-0.555	0.016	0.006843187	-0.56184319	-0.548156813
C13	20	-0.542	0.013	0.005697397	-0.5476974	-0.536302603
C14	21	-0.518	0.009	0.003849293	-0.52184929	-0.514150707
C15	22	-0.504	0.015	0.006267986	-0.51026799	-0.497732014
C16	21	-0.425	0.015	0.006415488	-0.43141549	-0.418584512
C17	22	-0.558	0.018	0.007521583	-0.56552158	-0.550478417
C18	21	-0.453	0.01	0.004276992	-0.45727699	-0.448723008
C19	21	-0.569	0.012	0.00513239	-0.57413239	-0.56386761
C20	22	-0.433	0.014	0.00585012	-0.43885012	-0.42714988
C21	22	-0.419	0.008	0.003342926	-0.42234293	-0.415657074
C22	22	-0.361	0.012	0.005014389	-0.36601439	-0.355985611
C23	21	-0.438	0.015	0.006415488	-0.44441549	-0.431584512
C25	20	-0.531	0.012	0.005259135	-0.53625914	-0.525740865
C26	22	-0.442	0.012	0.005014389	-0.44701439	-0.436985611
C27	21	-0.463	0.013	0.00556009	-0.46856009	-0.45743991
C28	22	-0.488	0.014	0.00585012	-0.49385012	-0.48214988
C29	22	-0.537	0.012	0.005014389	-0.54201439	-0.531985611
C30	21	-0.574	0.015	0.006415488	-0.58041549	-0.567584512

Table 5-27. Differentiation Data for Lnk1

The value of DOF, Lnk1 and sigmaK1 is obtained from the linear regression analysis for model 1. The confidence interval at 95% is calculated by using the DOF value and sigma Lnk value. The upper limit and lower limit are calculated by adding and subtracting the confidence interval from Lnk value. By using the upper and lower limit values, a matrix was generated. A value of 1 is affected to a cotton couple if the confidence intervals are intersected; a 0 value if not. By adding all the values of the matrix so generated and dividing by two give the differentiation value for that case. It means how many cotton couples are different between (30x30-2)/2=435 couples at all. The differentiation matrix is given in Table 5-28. The graphical representation of Lnk1 with upper and lower limit of confidence interval is given Figure 5-32.

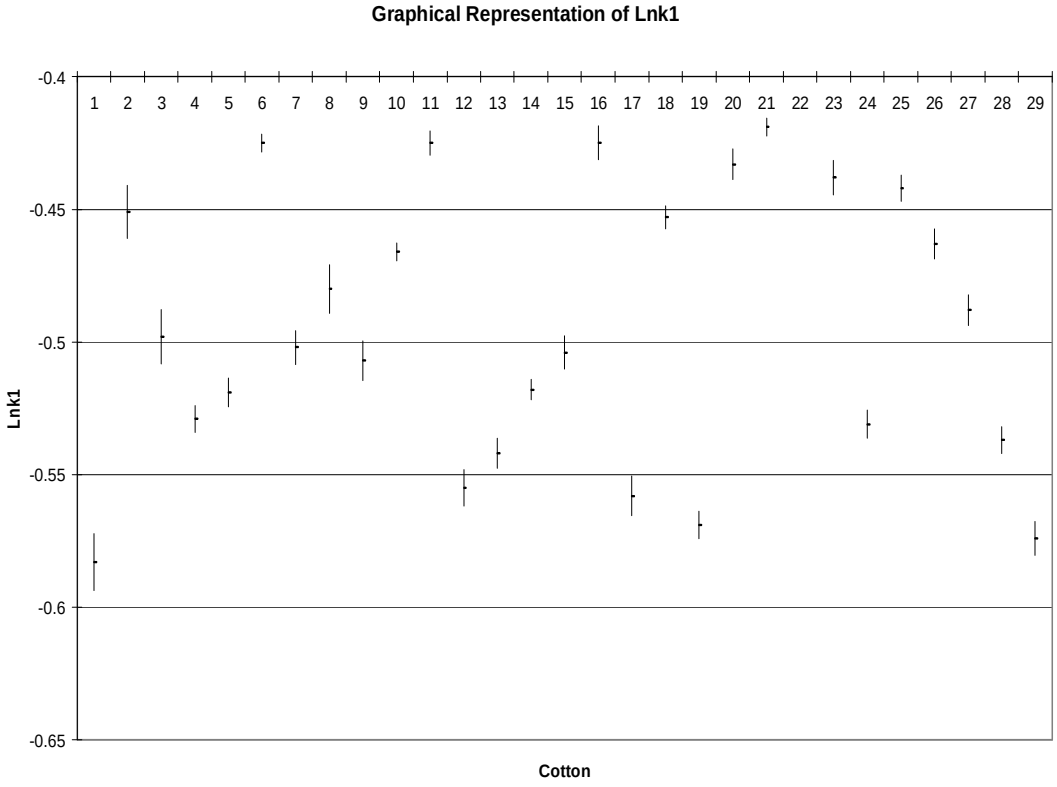

Figure 5-32. Graphical Representation of Lnk1

The individual differentiation values are given in Table 5.29. It is observed that the cottons are better differentiated by coefficients of friction than by constants C or *a*. The degree of differentiation seems to be similar for different frictional models.

Frictional Coefficient	Differentiation Value	Frictional Coefficient	Differentiation Value	Frictional Coefficient	Differentiation Value	Constant	Differentiation Value
LnK1	367	a1	292	K6	352	Constant6	232
LnK2	371	a2	298	K7	353	Constant7	267
LnK3	336	a3	298	K8	353	Constant8	279
LnK4	376	a4	292	K9	352	Constant9	264
LnK5	342	a5	292	K10	352	Constant10	270

Table 5-29. Differentiation Values for Frictional Coefficients

	C1	C2	C3	C4	C5	C6	C7	C8	C9	C10	C11	C12	C13	C14	C15	C16	C17	C18	C19	C20	C21	C22	C23	C25	C26	C27	C28	C29	C30
C1	0	1	1	1	1	1	1	1	1	1	1	1	1	1	1	1	1	1	0	1	1	1	1	1	1	1	1	1	0
C2	1	0	1	1	1	1	1	1	1	1	1	1	1	1	1	1	1	0	1	1	1	1	0	1	0	0	1	1	1
C3	1	1	0	1	1	1	0	0	0	1	1	1	1	1	0	1	1	1	1	1	1	1	1	1	1	1	0	1	1
C4	1	1	1	0	0	1	1	1	1	1	1	1	1	1	1	1	1	1	1	1	1	1	1	0	1	1	1	0	1
C5	1	1	1	0	0	1	1	1	0	1	1	1	1	0	1	1	1	1	1	1	1	1	1	1	1	1	1	1	1
C6	1	1	1	1	1	0	1	1	1	1	0	1	1	1	1	0	1	1	1	0	0	1	1	1	1	1	1	1	1
C7	1	1	0	1	1	1	0	1	0	1	1	1	1	1	0	1	1	1	1	1	1	1	1	1	1	1	1	1	1
C8	1	1	0	1	1	1	1	0	1	1	1	1	1	1	1	1	1	1	1	1	1	1	1	1	1	1	0	1	1
C9	1	1	0	1	0	1	0	1	0	1	1	1	1	0	0	1	1	1	1	1	1	1	1	1	1	1	1	1	1
C10	1	1	1	1	1	1	1	1	1	0	1	1	1	1	1	1	1	1	1	1	1	1	1	1	1	0	1	1	1
C11	1	1	1	1	1	0	1	1	1	1	0	1	1	1	1	0	1	1	1	0	0	1	1	1	1	1	1	1	1
C12	1	1	1	1	1	1	1	1	1	1	1	0	1	1	1	1	0	1	1	1	1	1	1	1	1	1	1	1	1
C13	1	1	1	1	1	1	1	1	1	1	1	1	0	1	1	1	1	1	1	1	1	1	1	1	1	1	1	0	1
C14	1	1	1	1	0	1	1	1	0	1	1	1	1	0	1	1	1	1	1	1	1	1	1	1	1	1	1	1	1
C15	1	1	0	1	1	1	0	1	0	1	1	1	1	1	0	1	1	1	1	1	1	1	1	1	1	1	1	1	1
C16	1	1	1	1	1	0	1	1	1	1	0	1	1	1	1	0	1	1	1	0	0	1	1	1	1	1	1	1	1
C17	1	1	1	1	1	1	1	1	1	1	1	0	1	1	1	1	0	1	0	1	1	1	1	1	1	1	1	1	1
C18	1	0	1	1	1	1	1	1	1	1	1	1	1	1	1	1	1	0	1	1	1	1	1	1	1	1	1	1	1
C19	0	1	1	1	1	1	1	1	1	1	1	1	1	1	1	1	0	1	0	1	1	1	1	1	1	1	1	1	0
C20	1	1	1	1	1	0	1	1	1	1	0	1	1	1	1	0	1	1	1	0	1	1	0	1	0	1	1	1	1
C21	1	1	1	1	1	0	1	1	1	1	0	1	1	1	1	0	1	1	1	1	0	1	1	1	1	1	1	1	1
C22	1	1	1	1	1	1	1	1	1	1	1	1	1	1	1	1	1	1	1	1	1	0	1	1	1	1	1	1	1
C23	1	0	1	1	1	1	1	1	1	1	1	1	1	1	1	1	1	1	1	0	1	1	0	1	0	1	1	1	1
C25	1	1	1	0	1	1	1	1	1	1	1	1	1	1	1	1	1	1	1	1	1	1	1	0	1	1	1	0	1
C26	1	0	1	1	1	1	1	1	1	1	1	1	1	1	1	1	1	1	1	0	1	1	0	1	0	1	1	1	1
C27	1	0	1	1	1	1	1	1	1	0	1	1	1	1	1	1	1	1	1	1	1	1	1	1	1	0	1	1	1
C28	1	1	0	1	1	1	1	0	1	1	1	1	1	1	1	1	1	1	1	1	1	1	1	1	1	1	0	1	1
C29	1	1	1	0	1	1	1	1	1	1	1	1	0	1	1	1	1	1	1	1	1	1	1	0	1	1	1	0	1
C30	0	1	1	1	1	1	1	1	1	1	1	1	1	1	1	1	1	1	0	1	1	1	1	1	1	1	1	1	0

Table 5-28. Differentiation Values Matrix for Frictional Coefficient Lnk1

5.4 Principle Component Analysis

The objective is to find a relationship between fibre, yarn and frictional properties of the cotton. The Principle Component Analysis (PCA) was applied to all the results and shown in the Figure 5-33.

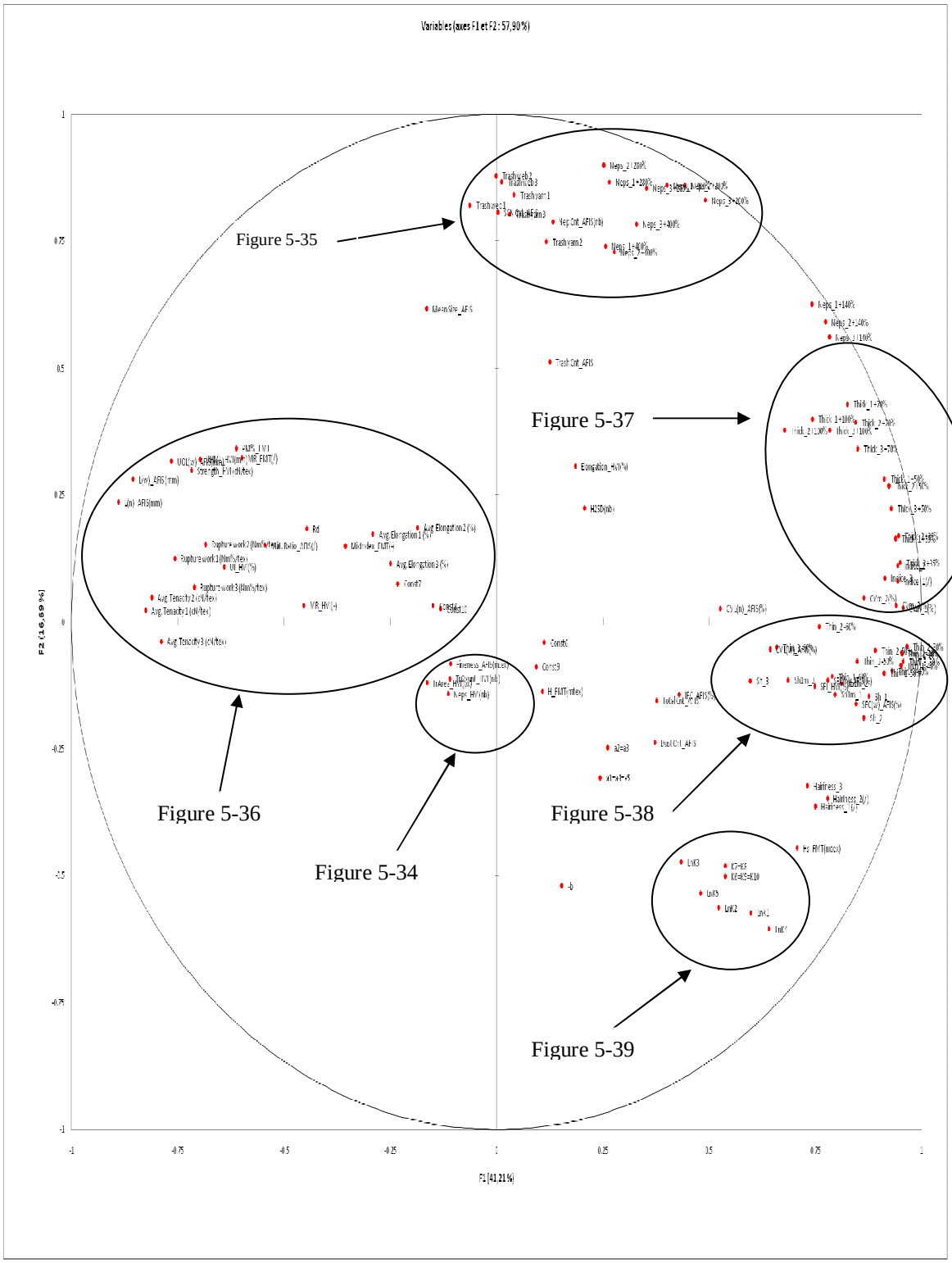

Figure 5-33. Principle Component Analysis

As it can be seen from the above PCA figure, there are a lot of parameters involved in the analysis. Different fibre and yarn parameters form groups. The groups thus formed are visualised in the figures below and discussed later. The fibre fineness and estimated trash content of cotton form a group during the principle component analysis shown in the Figure 5-34.

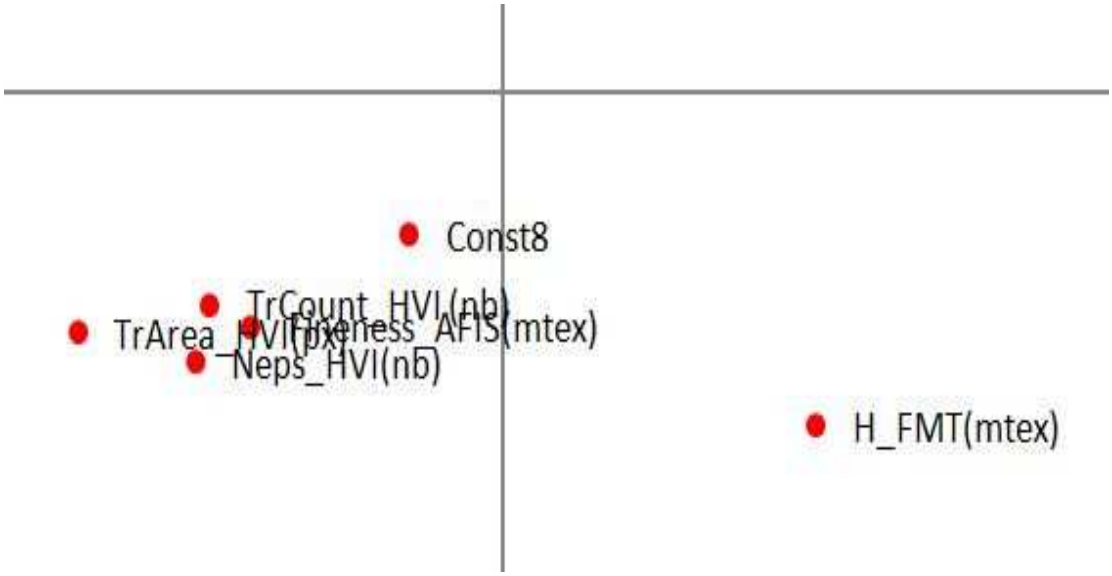

Figure 5-34. Fineness, Neps and Trash Content (HVI)

Another group is formed by the neps content (AFIS), SCN content (AFIS), yarn neps and TRASHCAM values for fibre and yarn. This group is shown in the Figure 5-35.

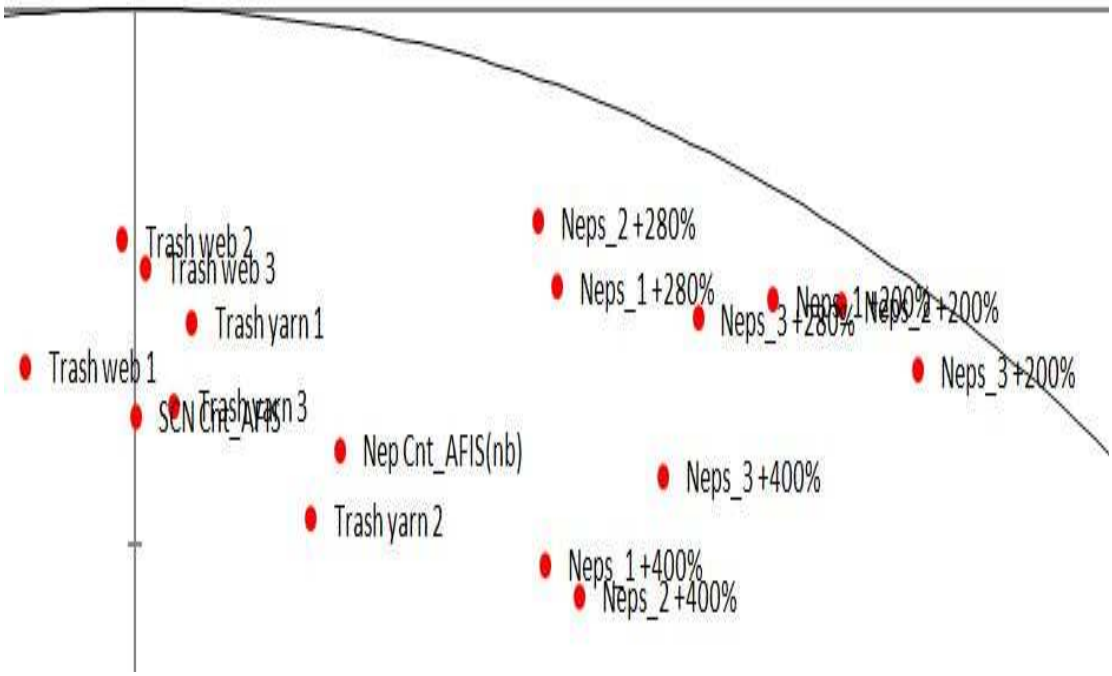

Figure 5-35. Neps content (AFIS), SCN content (AFIS), Yarn Neps and TRASHCAM values

The Figure 5-36 shows a group of yarn tensile properties, fibre tensile properties, maturity ratio, UHML, uniformity index, UQL (w) and fibre length by number and weight.

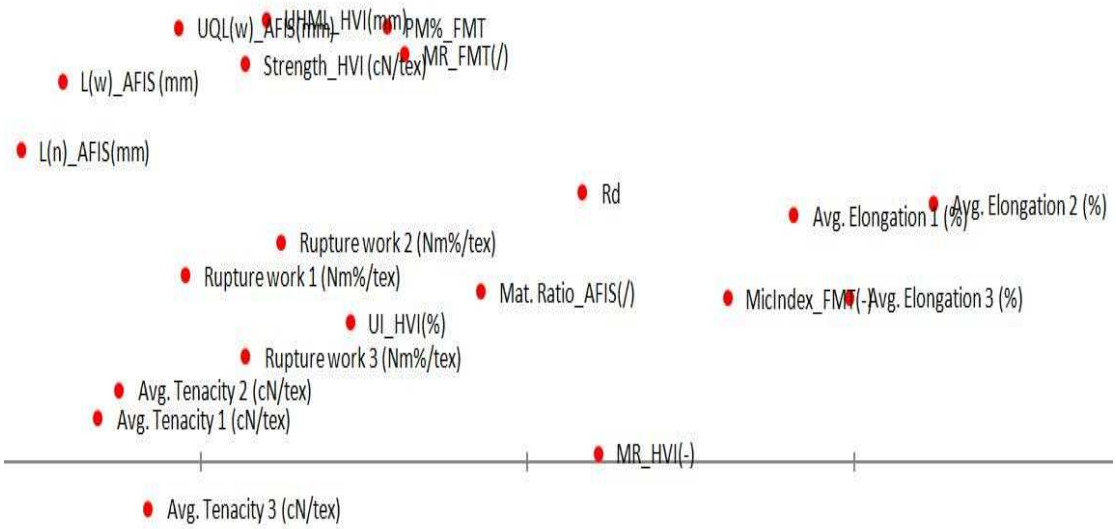

Figure 5-36. Fibre Length, Yarn Tensile Properties and Fibre Tensile Properties

The yarn thick places, yarn index and yarn CV% form a group during the principle component analysis shown in the Figure 5-37.

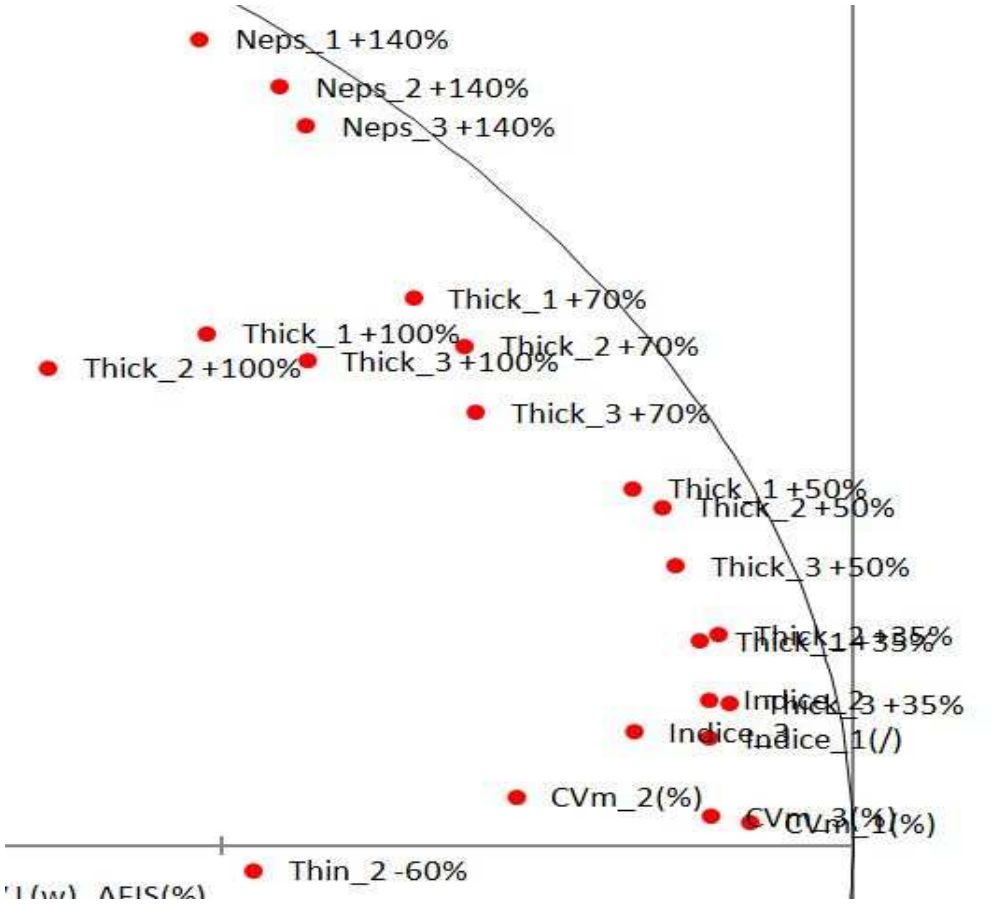

Figure 5-37. Yarn Thick Places and Yarn Index

Another group is also formed by yarn thin places and hairiness. This group is shown in the Figure 5-38.

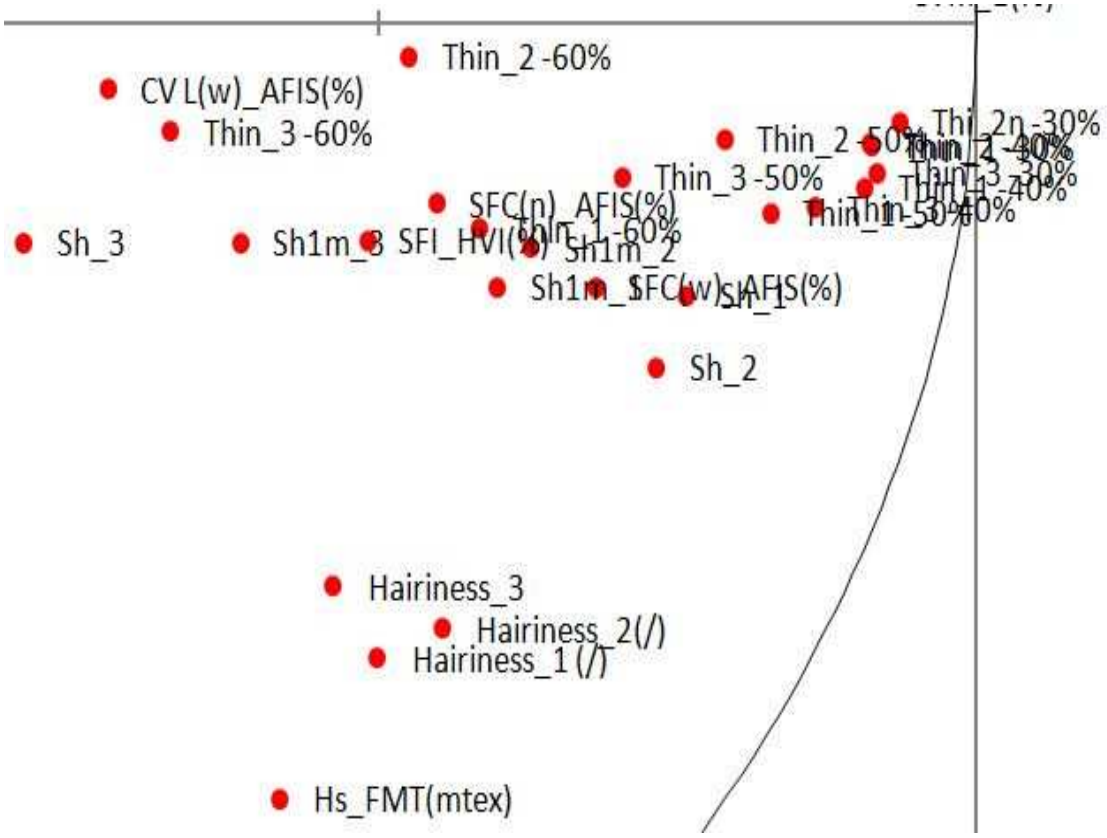

Figure 5-38. Yarn Thin Places and Yarn Hairiness

The fibre to fibre frictional parameters also form a group as shown in the Figure 5-38.

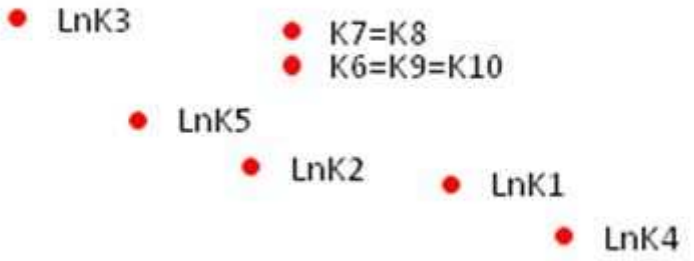

Figure 5-39. Inter-fibre Friction

Based on the groups obtained from the principle component, a second principle component analysis was performed. In this analysis, a certain fibre and yarn parameters were selected from the above groups in order

to refine and facilitate the interpretation of the PCA. The refined principle component is shown in the Figure 5-40.

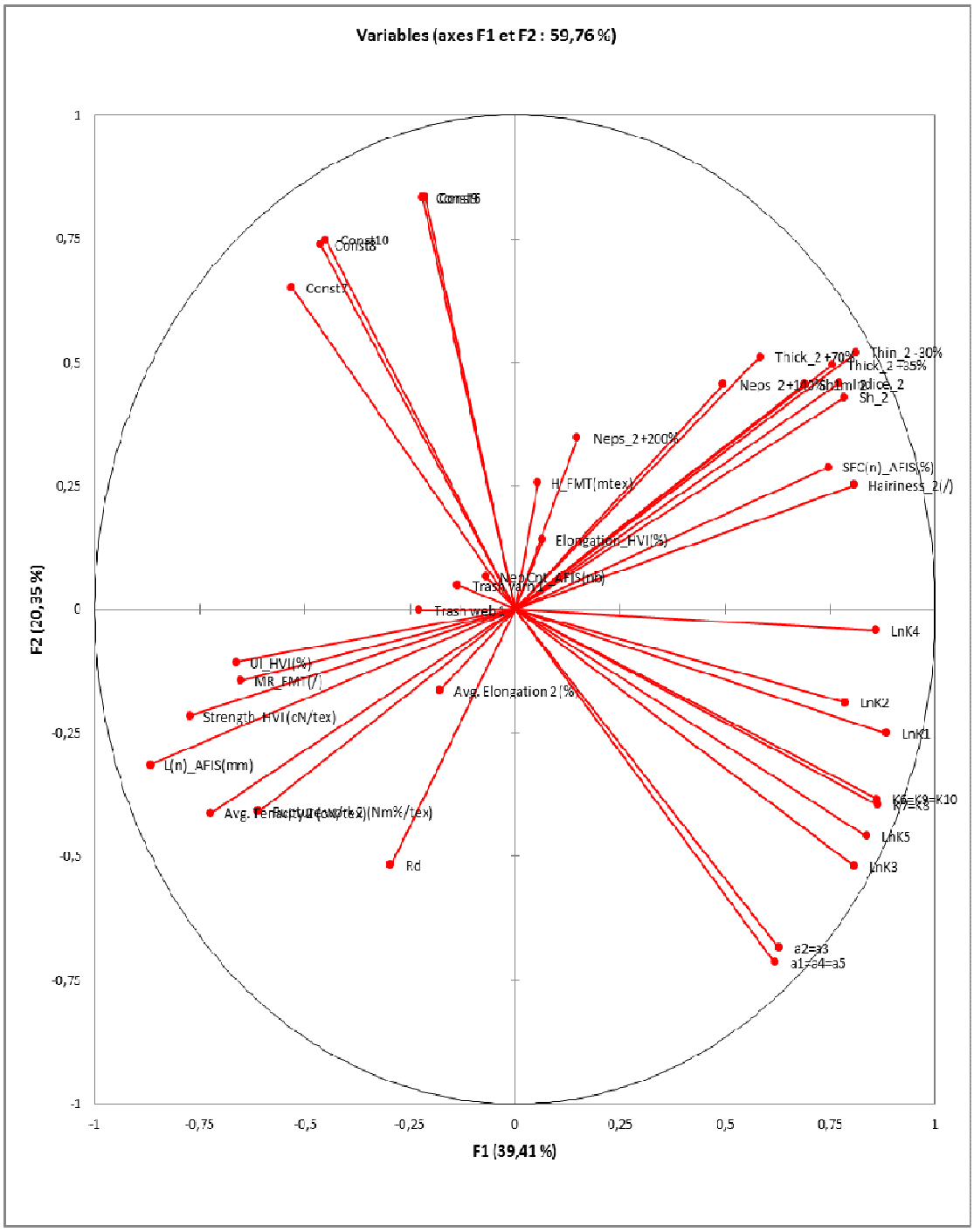

Figure 5-40. Refined Principle Component Analysis

5.5 Relationship between Fibre, Yarn and Fibre Frictional Properties

The Principle Component Analysis also gives correlation data. By using the correlation data, relationships were established between different fibre and yarn properties.

5.5.1 Correlation between Fibre and Yarn Tensile Properties

Fibre tenacity plays an important role in the yarn tenacity values. This is evident from the PCA Figure 5-36, that fibre length and uniformity also has a role in yarn tenacity. The correlation data is shown in the Table 5-30.

Variables	UHML_HVI (mm)	UI_HVI(%)	Strength HVI (cN/tex)	L(w)_AFIS (mm)	UQL(w)_AFIS (mm)	L(n)_AFIS (mm)	Avg. Tenacity 1 (cN/tex)	Avg. Tenacity 2 (cN/tex)	Avg. Tenacity 3 (cN/tex)
UHML_HVI (mm)	**1**								
UI_HVI(%)	**0.616**	**1**							
Strength HVI (cN/tex)	**0.652**	**0.535**	**1**						
L(w)_AFIS (mm)	**0.896**	**0.690**	**0.750**	**1**					
UQL(w)_AFIS (mm)	**0.948**	**0.634**	**0.696**	**0.968**	**1**				
L(n)_AFIS (mm)	**0.793**	**0.680**	**0.751**	**0.963**	**0.874**	**1**			
Avg. Tenacity 1 (cN/tex)	**0.624**	**0.554**	**0.741**	**0.744**	**0.677**	**0.751**	**1**		
Avg. Tenacity 2 (cN/tex)	**0.582**	**0.511**	**0.760**	**0.707**	**0.633**	**0.722**	**0.902**	**1**	
Avg. Tenacity 3 (cN/tex)	**0.517**	**0.475**	**0.707**	**0.648**	**0.566**	**0.671**	**0.884**	**0.866**	**1**

Bold values show significant difference from 0 correlation at α=0.05

Table 5-30. Correlation between Fibre and Yarn Tensile Properties

It is obvious from the correlation table that fibre length and uniformity index has a positive correlation with fibre strength as well as yarn strength. The fibre strength has a positive correlation and plays an important role in yarn strength. It can also be observed that the correlation between fibre length and yarn tenacity parameters decreases as the value of twist multiplier increases. Similarly fibre length by number and weight, uniformity index and also UQL by weight has positive correlation.

5.5.2 Correlation between Yarn Unevenness, Imperfections and Hairiness

These yarn parameters also form a group in the PCA (Figure 5-37 and 5-38). The correlation data for yarn unevenness, imperfections and hairiness is given in the Table 5-31.

Variables	CVm_2 (%)	Indice_2	Thin_2 -30%	Thin_2 -50%	Thick_2 +35%	Thick_2 +50%	Neps_2 +140%	Neps_2 +200%	Hairiness_2(/)	L(n)_AFIS (mm)
CVm_2(%)	**1**									
Indice_2	**0.839**	**1**								
Thin_2 -30%	**0.902**	**0.911**	**1**							
Thin_2 -50%	**0.887**	**0.864**	**0.915**	**1**						
Thick_2 +35%	**0.898**	**0.916**	**0.954**	**0.869**	**1**					
Thick_2 +50%	**0.880**	**0.918**	**0.916**	**0.861**	**0.979**	**1**				
Neps_2 +140%	**0.725**	**0.804**	**0.721**	**0.689**	**0.833**	**0.881**	**1**			
Neps_2 +200%	**0.401**	**0.512**	**0.370**	**0.320**	**0.555**	**0.639**	**0.876**	**1**		
Hairiness_2(/)	**0.598**	**0.665**	**0.734**	**0.620**	**0.646**	**0.580**	**0.358**	0.054	**1**	
L(n)_AFIS (mm)	**-0.729**	**-0.802**	**-0.844**	**-0.745**	**-0.770**	**-0.716**	**-0.534**	-0.198	**-0.847**	**1**

Bold values show significant difference from 0 correlation at α=0.05

Table 5-31. Correlation between Yarn unevenness, Imperfections and Hairiness

The data in above table indicates a strong positive correlation between all the above mentioned parameters. It is interesting to note that yarn index as a strong correlation with yarn imperfections. The correlation coefficient decreases as the imperfection size increases (see for example the difference between correlation coefficients for thin-30% and thin-50% with yarn index). As far as hairiness is concerned, maintaining all yarn processing parameters constant, the hairiness depends entirely on fibre length. Effectively, for the same fibre and yarn count, the number of protruding fibres is inversely proportional to fibre length. It can be seen from the above correlation table. On the other hand, the fibre length affects strongly yarn index and imperfection. So, the correlation coefficients between yarn hairiness and yarn unevenness and imperfections can be explained by the same cause which is fibre length. Yarn neps do not have strong correlation with fibre length, yarn imperfections and hairiness.

5.5.3 Correlation between Fibre Neps and Yarn Neps

The correlation between fibre and yarn neps are shown in Table 5-32 and related to the Figure 5-35.

Variables	Nep Cnt_ AFIS (nb)	Neps_1 +140%	Neps_1 +200%	Neps_1 +280%	Neps_2 +140%	Neps_2 +200%	Neps_2 +280%	Neps_3 +140%	Neps_3 +200%	Neps_3 +280%
Nep Cnt_ AFIS(nb)	**1**									
Neps_1 +140%	**0.603**	**1**								
Neps_1 +200%	**0.710**	**0.882**	**1**							
Neps_1 +280%	**0.664**	**0.772**	**0.956**	**1**						
Neps_2 +140%	**0.610**	**0.968**	**0.824**	**0.696**	**1**					
Neps_2 +200%	**0.747**	**0.875**	**0.944**	**0.885**	**0.876**	**1**				
Neps_2 +280%	**0.715**	**0.744**	**0.916**	**0.907**	**0.730**	**0.949**	**1**			
Neps_3 +140%	**0.595**	**0.960**	**0.794**	**0.661**	**0.971**	**0.833**	**0.679**	**1**		
Neps_3 +200%	**0.732**	**0.900**	**0.934**	**0.870**	**0.884**	**0.953**	**0.888**	**0.885**	**1**	
Neps_3 +280%	**0.680**	**0.794**	**0.914**	**0.888**	**0.767**	**0.916**	**0.903**	**0.757**	**0.953**	**1**

Bold values show significant difference from 0 correlation at α=0.05

Table 5-32. Correlation between Fibre Neps and Yarn Neps

There is positive correlation between fibre and yarn neps. So if cotton having large amount of neps is spun, there is strong possibility that it will have high value of yarn neps also. It seems evident that, the level of 200% yarn neps highlights the influence of the fibre neps on the yarn neps. The yarn twist does not affect this tendency. Also, the yarn twist does not affect strongly the influence of the fibre neps on the yarn neps.

5.5.4 Correlation between Fibre Parameters and Yarn Parameters

The fibre quality parameters such as fibre length, strength etc has a strong relation with yarn imperfections and yarn tensile properties. It is important to study this tendency and find the correlation between these parameters. The correlation data is shown in the Table 5-33 and related to Figures 5-36, 5-37 and 5-38.

Variables	UI_HVI(%)	Strength _HVI (cN/tex)	Elongation _HVI (%)	L(n)_AFIS (mm)	Avg. Elongation 2 (%)	Avg. Tenacity 2 (cN/tex)	Indice_2	Thin_2 -30%	Thick_2 +35%	Thick_2 +70%	Neps_2 +140%	Neps_2 +200%
UI_HVI(%)	**1**											
Strength_ HVI (cN/tex)	**0.535**	**1**										
Elongation_ HVI (%)	-0.182	**-0.209**	**1**									
L(n)_AFIS (mm)	**0.680**	**0.751**	-0.138	**1**								
Avg. Elongation 2 (%)	0.002	-0.041	**0.674**	0.150	**1**							
Avg. Tenacity 2 (cN/tex)	**0.511**	**0.760**	**-0.343**	**0.722**	0.034	**1**						
Indice_2	**-0.565**	**-0.609**	**0.217**	**-0.802**	-0.154	**-0.673**	**1**					
Thin_2 -30%	**-0.605**	**-0.712**	**0.210**	**-0.844**	**-0.191**	**-0.826**	**0.911**	**1**				
Thick_2 +35%	**-0.588**	**-0.627**	**0.268**	**-0.770**	-0.156	**-0.787**	**0.916**	**0.954**	**1**			
Thick_2 +70%	**-0.476**	**-0.434**	**0.252**	**-0.622**	-0.127	**-0.622**	**0.878**	**0.817**	**0.905**	**1**		
Neps_2 +140%	**-0.421**	**-0.363**	**0.320**	**-0.534**	-0.027	**-0.580**	**0.804**	**0.721**	**0.833**	**0.897**	**1**	
Neps_2 +200%	-0.167	-0.062	**0.278**	**-0.198**	0.037	**-0.287**	**0.512**	**0.370**	**0.555**	**0.728**	**0.876**	**1**

Bold values show significant difference from 0 correlation at α=0.05

Table 5-33. Correlation between Fibre and Yarn Quality Parameters

The yarn tenacity is strongly affected by the fibre tenacity, fibre length and fibre length uniformity in descending order. If all the fibres break during yarn tensile test, the yarn tenacity would be directly proportional to fibre strength. But the yarn breaks at a weak point. It can be observed by the correlation coefficients between yarn tenacity and thin places. The quantity of the weak points (thin places) is strongly related to the fibre length as discussed above. So fibre length affects yarn tenacity indirectly. The influence of fibre length on the yarn tenacity decreases with increase in yarn twist. The correlation values are 0.751, 0.722 and 0.671 for T_1, T_2 and T_3 respectively (see Annex F). The negative correlation values between yarn tenacity and short fibre content are -0.625, -0.621 and -0.599 for T_1, T_2 and T_3 respectively (see Annex F). This means that the weak places become less critical as the yarn twist increases and also the short fibres participate more toward yarn structure which eventually affect yarn tenacity. The fibre uniformity index is correlated with yarn imperfections and also affects yarn tenacity this way. So generally, the yarn imperfection has negative correlation with the yarn tenacity and fibre quality parameters. This means that shorter staple cotton will have more yarn imperfections. Similarly, the longer cotton fibres will have small number of thick places, small CV% and good yarn quality and yarn tenacity.

5.5.5 Correlation between Fibre, Yarn tensile properties and Frictional Coefficients

As one of the main objective of this research was to establish a relationship between fibre tensile properties, yarn tensile properties and the frictional coefficients. The correlation data for these parameters is given in the Table 5-34.

Variables	Strength_HVI (cN/tex)	L(n)_AFIS(mm)	SFC(n)_AFIS(%)	MR_FMT(/)	Avg. Elongation 2 (%)	Avg. Tenacity 2 (cN/tex)	Indice_2	LnK4	K7=K8
Strength_HVI (cN/tex)	**1**								
L(n)_AFIS(mm)	**0.751**	**1**							
SFC(n)_AFIS(%)	**-0.618**	**-0.860**	**1**						
MR_FMT(/)	**0.553**	**0.643**	**-0.730**	**1**					
Avg. Elongation 2 (%)	-0.041	0.150	-0.127	0.072	**1**				
Avg. Tenacity 2 (cN/tex)	**0.760**	**0.722**	**-0.621**	**0.403**	0.034	**1**			
Indice_2	**-0.609**	**-0.802**	**0.759**	**-0.603**	-0.154	**-0.673**	**1**		
LnK4	**-0.736**	**-0.706**	**0.570**	**-0.678**	-0.115	**-0.590**	**0.519**	**1**	
K7=K8	**-0.604**	**-0.600**	**0.527**	**-0.615**	-0.064	**-0.436**	**0.454**	**0.894**	**1**

Bold values show significant difference from 0 correlation at α=0.05

Table 5-34. Correlation between Fibre, Yarn tensile properties and Frictional Coefficients

We have chosen LnK4 and K7=K8 frictional coefficients (non-linear and linear model) to discuss as all the frictional coefficients are correlated as shown in the Table 5-26. The constant and the power *a* are not significant. From the previous research of Nowrouzieh [80], it was expected a strong correlation between yarn tensile properties, imperfections and the frictional coefficients. But this is not the case as shown by the correlation table. There is some correlation between the yarn tensile properties and frictional coefficients but this correlation is not highly significant. We have applied the models 7 and 8 to Shahram results. The average frictional coefficient value of all the 11 cottons is 0.710. For the 29 cottons studied in the present work, the mean value is 0.580. This difference seems to be very important. It may be due to either change in the cotton frictional properties (hypothesis 1) or the change of testing device (hypothesis 2). For this reason, we have tested the 29 cottons with only 4 repetitions by using the original testing device. The results were not statistically different with those presented here. The hypothesis 2 is discarded this way. There is another possibility; the 11 cottons chosen by Shahram were by chance

highly frictional. We think this last possibility has to be discarded as cottons were chosen randomly. The same choosing procedure was applied in the present study in CIRAD. There remains only the first hypothesis which means that the cotton frictional properties change with the time.
Effectively, the most recent cotton was of 2007 and the most ancient one was of 1996.
It is interesting to note that the effect of storage on cotton fibre behaviour during drawing process has been cited in the literature review [2].
Anyway, to explain the results in above table, we take the following hypothesis in consideration. As far as maturity is concerned, the inter-fibre friction depends upon the cotton maturity ratio. The lower maturity ratio yields lower frictional values. This effect may be due to geometrical shape of the fibre; there would be fewer points of contacts between the adjacent fibres. The negative correlation value between the yarn tenacity and the frictional coefficients may be due to positive correlation between the inter-fibre friction and yarn unevenness. This may be further explained by the fact that we measure the friction between bundles of fibres (thousands of fibres) and not between single fibres. As the cottons were in storage for a long time, this may result non-uniform change in overall behaviour of cotton wax. Therefore an increase in the global measured frictional coefficient may cause cluster slippage between fibre tufts which may yield to an increase in the yarn unevenness. Finally, as discussed previously, the yarn strength is also affected.

5.6 Conclusions

From the fibre statistical analysis it can be derived that a panel having wide range of fibre properties was selected. The fibre parameters are well distributed among the panel. The yarn tensile properties increase with an increase in twist multiplier as it is shown by yarn analysis. An effective procedure to treat force displacement curve and selection of force point was derived. This procedure is applied on all the SFT measurements. A wide range of frictional models were applied and the correlation between the models was also derived. There is no significant difference between the models. However, the linear frictional models are physically more acceptable, because the frictional coefficient, in this case, has physical

sense. An effective procedure to differentiate between cottons by using the frictional parameters was also devised. The principle component analysis was applied to all the fibre, yarn and frictional parameters. On the basis of this analysis different fibre and yarn properties groups were discussed. The correlation between different fibre yarn and frictional coefficients were also calculated.

Chapter 6-Conclusions and Perspective

The earlier version of SFT was discussed and some shortcoming in that version also discussed. Several preliminary trials were conducted to point out any problems in the earlier version. An improved Static Friction Tester was developed and the problems faced in the earlier version were solved. A simple and complete protocol to operate the modified SFT was also established. An effective procedure to treat force displacement curve and selection of force point was also derived.

A panel of 30 cottons was selected randomly from the available stock of CIRAD. The selected samples were opened thoroughly by the use of opening and blending machine. The random sampling was carried out after opening. The samples were tested to fully characterize the cottons in term of fibre properties. The panel covers wide range of available cottons. The cottons were then processed on the lab scale spinning machines to convert it into yarn. The yarn of 25 tex was spun by using three different twist multipliers. The resultant yarn was tested for Unevenness and tensile properties. The yarn tensile properties increase with an increase in twist multiplier as it is shown by yarn analysis.

The samples collected at drawing process were tested for inter-fibre friction on Static Friction Tester. A wide range of frictional models were applied and the correlation between the models was also derived. There was no significant difference between the models. However, the linear frictional models are physically more acceptable, because the frictional coefficient, in this case, has physical sense. An effective procedure to differentiate between cottons by using the frictional parameters was also devised.

The principle component analysis was applied to all the fibre, yarn and frictional parameters. On the basis of this analysis different fibre and yarn properties groups were discussed. The correlation between different fibre yarn and frictional coefficients were also calculated.

The fibre length and uniformity index has a positive correlation with fibre strength as well as yarn strength. The fibre strength has a positive correlation and plays an important role in yarn strength. It can also be observed that the correlation between fibre length and yarn tenacity parameters decreases as the value of twist multiplier increases. Similarly

fibre length by number and weight, uniformity index and also UQL by weight has positive correlation.

There are strong positive correlations between yarn unevenness, imperfections and hairiness. It is interesting to note that yarn index as a strong correlation with yarn imperfections. The correlation coefficient decreases as the imperfection size increases. As far as hairiness is concerned, maintaining all yarn processing parameters constant, the hairiness depends entirely on fibre length. Effectively, for the same fibre and yarn count, the number of protruding fibres is inversely proportional to fibre length. On the other hand, the fibre length affects strongly yarn index and imperfection. So, the correlation coefficients between yarn hairiness and yarn unevenness and imperfections can be explained by the same cause which is fibre length. Yarn neps do not have strong correlation with fibre length, yarn imperfections and hairiness.

There is positive correlation between fibre and yarn neps. So if cotton having large amount of neps is spun, there is strong possibility that it will have high value of yarn neps also. It seems evident that, the level of 200% yarn neps highlights the influence of the fibre neps on the yarn neps. The yarn twist does not affect this tendency. Also, the yarn twist does not affect strongly the influence of the fibre neps on the yarn neps.

The yarn tenacity is strongly affected by the fibre tenacity, fibre length and fibre length uniformity in descending order. If all the fibres break during yarn tensile test, the yarn tenacity would be directly proportional to fibre strength. But the yarn breaks at a weak point. This fact can be observed by the correlation coefficients between yarn tenacity and thin places. The quantity of the weak points is strongly related to the fibre length as discussed above. So fibre length affects yarn tenacity indirectly. The influence of fibre length on the yarn tenacity decreases with increase in yarn twist. The negative correlation values between yarn tenacity and short fibre content decrease in absolute value with the twist. This means that the weak places become less critical as the yarn twist increases and also the short fibres participate more toward yarn structure which eventually affect yarn tenacity. The fibre uniformity index is correlated with yarn imperfections and also affects yarn tenacity this way. So generally, the yarn imperfection has negative correlation with the yarn

tenacity and fibre quality parameters. This means that shorter staple cotton will have more yarn imperfections. Similarly, the longer cotton fibres will have small number of thick places, small CV% and good yarn quality and yarn tenacity.

As it has been mentioned above, all the frictional models discussed in the present work correlate with each other. On the other hand, the constant and the power *a* are not significant. Also, the results of this research work do not follow the previous research of Nowrouzieh where some strong correlations between yarn tensile properties, imperfections and the frictional coefficients were found. Our results show some correlation between the yarn tensile properties and frictional coefficients but this correlation is not highly significant. Our linear model applied to Nowrouzieh results gives an average frictional coefficient value of 0.710 for all the 11 cottons tested in his work. For the 29 cottons studied in the present work, the mean value is 0.580. This difference seems to be very important. Different hypothesis were discussed in the present work to explain this deviation from Nowrouzieh results. It seems that the more acceptable hypothesis would be the aging of cotton fibres. The time factor would affect the wax and/or fibre surface properties.

Never the less, the negative correlation value between the yarn tenacity and the frictional coefficients may be due to positive correlation between the inter-fibre friction and yarn unevenness. This may be further explained by the fact that we measure the friction between bundles of fibres (thousands of fibres) and not between single fibres. As the cottons were in storage for a long time, this may yield to a non-uniform change in overall behaviour of cotton wax. Therefore an increase in the global measured frictional coefficient may cause cluster slippage between fibre tufts which may yield to an increase in the yarn unevenness and a decrease in the yarn strength.

Some future work would be interesting to be carried out.

Firstly, at least one exact copy of SFT should be made and installed at CIRAD and/or another laboratory. Each new cotton arrived at CIRAD should be tested for frictional properties at both laboratories to point out eventual differences. The cottons should be retested periodically, the

frequency has to be discussed and decided following economic and technological aspects.

Secondly, for each cotton tested for friction, a thorough study for cotton wax content and its nature should also be carefully conducted.

The database so obtained this way can permit an effective way to interpret inter-fibre friction and also the effect of wax on fibre processability.

References

1. Ahmad, S., Sinoimeri, A. and Nowrouzieh, S. The Effect of the Sliver Fiber Configuration on the Cotton Inter-fiber Frictional Forces. Journal of Engineered Fabrics & Fibres (JEFF); 2012, Vol. 7 Issue 2, P87-93.
2. Anderson, S.L., Cox, D.R. and Hardy, L.D. Some rheological properties of twistless combed wool slivers, Journal of the Textile Institute, 1952, Vol: 43, P 362-379.
3. Audivert, R. and De Castellar, M.D. Practical aspects of drafting tenacity of cotton at the ring frame, Textile Research Journal, N9, 1971, Vol: 41, P 720-725.
4. Audivert, R., Villaronga, M. and Coscolla, R. Drafting force in the front zone of a double-apron drafting system, Textile Research Journal, N1, 1967, Vol:37, P 1-10.
5. Averous, M. and Karrer, V. Etude expérimentale des forces d'étirage sur machines de préparation, Publication de N. Schlumberger et Cie, Guebwiller, France.
6. Bardy, M. Contribution à l'étude de la cohésion des fibres dans les textiles linéaire, 1980, Thèse de docteur-ingénieur de l'Université de Haute Alsace, Mulhouse, France.
7. Barella, A. and Sust, A. Cohesion phenomena in cotton rovings and yarns, Influence of Fibres Characteristics on the Cohesion of Non-Twisted Slivers, Textile Research Journal, N4, 1964, Vol: 34, P 283-290.
8. Barella, A. and Sust, A. The relationship between minimum twist of cohesion and "Cutting Ratio" in cotton rovings, Textile Research Journal, N3, 1965, Vol: 35, P 285-288.
9. Barella, A. Phénomènes de cohésion dans les mèches de laine peignée, Rapport au comite technique de la F.L.I., PARIS Nov., Dec. 1959.
10. Barella, A. Un apport a l'étude de la cohésion des fils de laine peignée et autres fibres. Rapport au Comite Technique de la F.L.I., PARIS, Dec. 1957.

11. Baril, A., De Luca, L.B. and MAYER, M. Influence of temperature and humidity on forces for separating Fibres, Textile Manufacturer, July 1971, P 272-273.
12. Bartlett, G.W., Smith, T.M. and Thompson, H.A. Frictional properties of filament yarns and staple fibres as determined by stick-slip method, Textile Research Journal, 1953a, Vol: 23, P 647-657.
13. Bartlett, G.W., Smith, T.M. and Thompson, H.A. Mod. Text. Mag. 1953b 34, N4, P 51; N5, P 50, in Friction in textiles, part3: Test methods, London, Butterworth Scientific Publications, 1959.
14. Basu, S.C., Hamza, A.A. and Sikorski, J. The friction of cotton fibres, Journal of the Textile Institute, N 2/3, 1978, P 68-75.
15. Berberi, P.G. Effect of lubrication on spinning properties of dyed cotton fibres, Textile Research Journal, N6, 1991, Vol: 61, P 285-288.
16. Bowden, F.P. and Tabor, D. The friction and lubrication of solid, Oxford, London, 1950 and Part II 1964.
17. Brook, G. and Hannah, M. The measurement of forces in twisted wool roving, Journal of the Textile Institute, N1, 1955, Vol:46, P 23-40.
18. Brook, G. Physique Doc. Thesis, Leeds, UK, 1955.
19. Broughton, R.M., El Moghazy, Y. and Hall, D.M. Mechanism of yarn Failure, Textile research journal, 1992, Vol: 62, P 131-134.
20. Buckle, H. and Pollitt, J. An instrument for measuring the coefficient of friction of yarns against other material, Journal of the Textile Institute, 1948, Vol:39, P 199-210.
21. Burlet, J.E. Contribution a l'étude de la ténacité des rubans de fibres, Bulletin ITF, N15, 1975, Vol: IV, P 221-227.
22. Burte, H.M. Properties of apparel wool, Part III, Textile Research Journal, N7, 1953, Vol: 23, P 469-480.
23. Cavaney, B. and Foster, G.A.R. Some observations of the drafting forces of cotton and Rayon staple slivers, Journal of the Textile Institute, Vol: 45, 1954, PT 390-400.
24. CIRAD, Caractéristiques de fibre et techniques de mesure classiques, 2000, Centre de coopération internationale en

recherche agronomique pour le développement, Laboratoire de Technologie Cotonnière, Montpellier, France.

25. Cui, X.L., Price, J.B., Calamari, T.A. and Hemstreet, J.M. Cotton wax its relationship with fibre and yarn properties, Part I, Wax content and fibre properties, Textile Research Journal, N6, 2002, Vol:72, P 399-404.
26. Davis, L.W. Rayon Text. Mon., 1940, 21, 93, 155, 229, Friction in textiles, part3: Test methods, London, Butterworth's Scientific Publications, 1959.
27. Doraiswamy, P., Chellamani and Gnansekar, K. Effect of fiber properties on cohesive force of man made fibers, Synthetic Fibers, July-September, 1993, P 13-17.
28. EL Mogahzy, Y. and Broughton, R.M. A new approach for evaluating the frictional behavior of cotton fibers, Textile Research Journal, N8, 1993, Vol: 63, P 465-475.
29. EL Mogahzy, Y. and Broughton, R.M. Development of characterization methodologies of fiber surface characteristics: Surface/process analysis. National Textile Center. Research, Briefs, 1997, P 10-11.
30. EL Mogahzy, Y. and Broughton, R.M. Diagnostic Procedures for Multi collinearity Between HVI Cotton Fiber Properties, Textile Research Journal, N8, 1989, Vol: 59, P 440-447.
31. EL Mogahzy, Y. and Gupta, B.S. Friction in fibrous materials, part II: Experimental study of the effect of structural and morphological factors, Textile Research Journal, N63, N4, 1993, Vol: 63, P 219-230.
32. EL Mogahzy, Y., Broughton, R.M., Guo, H. and Taylor, R.A, Evaluation staple fiber processing propensity. Part1: Processing propensity of cotton fibers, Textile Research Journal, N11, 1998, Vol: 68, P 835-840.
33. Frydrych, R. and Drean, J.Y. A new methodology usable by researcher and spinners for short staple fibres micro spinning. Beltwide Cotton Conferences, January 4-8, 2000, San Antonio, TX, USA, P 1555-1556.

34. Frydrych, R. and Gourlot, J.P. Evaluation de la résistance du fil à partir des caractéristiques technologiques de la fibre obtenues sur HVI. *Coton et Fibres Tropicale*s, 48(3), 1993, P 201-204.
35. Frydrych, R., Héquet, E. and Brunissen, Ch. High speed stickiness detector: relation with the spinning process. Beltwide Cotton Conferences, January 4-7, 1995, San Antonio, TX, USA, P 1185-1189.
36. Frydrych, R., Tamime, O., Gourlot, J.P., GozE, E., Le Blan, T., Ahmed Salah, F. and Abdin, A.M. Sticky cotton effects on the carded spinning process. Beltwide Cotton Conferences, January 4-7, 2000, San Antonio, TX, USA, P 1517-1518.
37. Frydrych R., Gawrysiak G., 2007, Notes sur l'aptitude à la transformation des rubans d'étirage en micro-filature du CIRAD. Communication interne CIRAD, Montpellier, France.
38. Gamble, G.R. Implications of surface chemistry on cotton fiber processing, journal of cotton science, N8, 2004, P 198-204.
39. Gawrrysiak, G. Protocole de tests de TRASHCAM sur nappes de 20 g, 2005, Rapport interne CIRAD, France.
40. Ghosh, S., Rodgers, J.E. and Ortega, A.E. Rotor ring measurement of fiber cohesion and bulk properties of staple fibers, Textile Research Journal, N10, 1992, Vol:62, P 608-613.
41. Graham, J.S. and Bragg, C.K. Drafting force measurement as an aid to cotton spinning, Textile Research Journal, N3, 1972, Vol:42, P 175-181.
42. Graham, J.S. and Burley, S.T. Effects of drafting parameters on drafting force in cotton spinning, Textile Bulletin, N7, 1968, P 1-5.
43. Grimshaw, G. Hexag. Dig. No. 19, 1954, July, P 18, Friction in textiles, part3: Test methods, London, Butterworth's Scientific Publications, 1959.
44. Guo, H., EL Mogahzy, Y. and Broughton, R.M. The contribution of fiber friction to yarn quality, Beltwide Cotton Conferences, 1998, P 719-722.
45. Hannah, M. The theory of high drafting, Journal of the Textile Institute, 1950, PT 57-123.

46. Hatch, K.L. Textile Science 1993 West Publishing Company New York.
47. Henning, H.J. Melliand Textilberichte, 1937, 18, P 945, Friction in textiles, part3: Test methods, London, Butterworth's Scientific Publications, 1959.
48. Henshaw, D.E. The role of a lubricant and its viscosity in worsted carding, Journal of the Textile Institute, N12, 1961, Vol: 52, P 537- 553.
49. Hood, B.G. Investigation of the frictional properties of textile fibers under variable fiber stress, Textile Research Journal, 1953, Vol: 23, P 495-505.
50. Howell, H.G. and Mazure, J. Amontons's law and fiber friction, Journal of the Textile Institute, 1953, Vol: 44, PT 59-69.
51. Howell, H.G. Inter-fiber friction, Journal of the Textile Institute, 1951, Vol: 42, P 521-533.
52. Howell, H.G. The general case of friction of a string round a cylinder, Journal of the Textile Institute, 1953, Vol: 44, P 359-362.
53. Howell, H.G. The laws of static friction, Textile Research Journal, N8, 1953, Vol: 26, P 589-591.
54. Howell, H.G., Mieszkis, K.W. and Tabor, D. Friction in textiles, part3: Test methods, London, Butterworth's Scientific Publications, 1959.
55. Hsieh, Y.L. and Basra, A.S. Cotton Fibres, Development Biology, Quality Improvement and Textile Processing 1999. The Haworth Press Inc. New York.
56. Jacowski, T., Chylewska, B., Cyniak, D. and Czekalski, J. Tensile strength of untwisted fiber streams measured at dynamic condition, Fibres & Textiles in Eastern Europe, N2 (41), 2003, Vol: 11, P 18-21.
57. Kaidanovsky, N.L. and Haykin, S.E. J. Tech. Phys. U.S.S.R., 1933, 3, Friction in textiles, part3: Test methods, London, Butterworth's Scientific Publications, 1959.

58. Kamarov, V.G., Goldohmidt, V.G. and Simonov, V.B. Analysis of the dynamics of the drafting process, Tech. of Textile Industry, U.R.S.S., N4, 1969, P 57-61.
59. King, G. Some frictional properties of wool and Nylon fibers, Journal of the Textile Institute, 1950, Vol: 41, PT 135-144.
60. Kruger, P.J. Withdrawal forces in the processing of wool slivers, Part I, Journal of the Textile Institute, N10, 1967, Vol: 58, P 463-471.
61. Krumme, W. Z. Ver. Dtsch. Ing. 73, 303, 1929. Friction in textiles, part3: Test methods, London, Butterworths Scientific Publications, 1959.
62. Lake, J.J. and Bevoort, C. Enka Breda Rayon Rev., 1956, 10, N5, P 174, Friction in textiles, part3: Test methods, London, Butterworth's Scientific Publications, 1959.
63. Lawson, R., Worley, S. and Ramey, H.H. Relation of cotton fibres properties to sliver cohesion, Textile Research Journal, N11, 1977, Vol: 47, P 755-759.
64. Lindberg, J. and Gralen, N. Measurement of friction between single fibers, Part II: Frictional properties of wool fibers measured by the fiber-twist method, Textile Research Journal, 1948, Vol: 18, P 287-301.
65. Lindberg, J. and Gralen, N. Medd. Svenska Textile forskn Inst., 1948, N6, Friction in textiles, part3: Test methods, London, Butterworth's Scientific Publications, 1959.
66. Lindberg, J. and Gralen, N. Nature, Lond. 1948, 162, 112, Friction in textiles, part3: Test methods, London, Butterworth's Scientific Publications, 1959.
67. Lindberg, J. Relationship between various surface properties of wool fibers, Part II: Frictional properties, Textile Research Journal, 1953, Vol: 23, P 225-236.
68. Lord, E. and Heap, S.A. The origin and assessment of cotton fibre maturity, International Institute for Cotton, 1988, P 39.
69. Lord, E. Frictional forces between fringes of fibres, Journal of the Textile Institute, 1955, Vol: 46, P 41-58.

70. Lord, E. The characteristics of raw cotton. Manual of cotton spinning. Manchester: The Textile Institute and Butterworth's, 1961, P 333.
71. Lysenko, L.Y. and Kretsberg. TECHNO. TEXT. Of Industry, URSS, N6, 1961, P 63-68.
72. Makinson, K.R. A note on the theory of Lepidometre, Journal of the Textile Institute, 1949, Vol: 40, P 809-812.
73. Martindale, J.G. An instrument for the measurement of the forces operating between fibres during drafting, Journal of the Textile Institute, 1947, Vol: 38, P 151-166.
74. Mercer, E.H. and Makinson, K.R. The frictional properties of wool and other textile fibers, Journal of the Textile Institute. 1947, Vol: 38, P227-240.
75. Mercer, E.H. Austr.J.Sci., 1945, 7, 173, in Friction in textiles, part3: Test methods, London, Butterworth's Scientific Publications, 1959.
76. Mercer, E.H. J. Coun. Sci. Industr. Res. Austr., 1945, 18, 188, Friction in textiles, part3: Test methods, London, Butterworth's Scientific Publications, 1959.
77. Mercer, E.H. Nature, Lond. 1945, 155, 573, Friction in textiles, part3: Test methods, London, Butterworth's Scientific Publications, 1959.
78. Monfort, F. and Franck, M. Essais dynamométriques sur rubans et mèches non tordus laine peignée, Annales Scientifiques Belges, N0 2-6, 1959, P 19-40.
79. Morrow, J.A. The frictional properties of cotton materials, Journal of the Textile Institute, 1931, Vol: 22, P 425-440.
80. Nowrouzieh, S. Etude des phénomènes de cohésion et friction inter fibre : Cas du coton. 2007. Thèse de doctorant de l'Université de Haute Alsace, Mulhouse, France.
81. Olofsson, B. and Garlen, N. Measurement of friction between single fibre, Textile Research Journal, 1974, Vol: 17, 488-496.
82. Olofsson, B. and Garlen, N. Measurement of friction between single fibers, part V: Frictional properties of Viscose Rayon staple fiber, Textile Research Journal, 1950, Vol: 20, P 467-476.

83. Olofsson, B. A theoretical study of fiber friction, Textile Research Journal, 1950, Vol: 20, P 476-480.
84. Olsen, J.S. Measurement of sliver drafting forces, Textile Research Journal, N11, 1974, Vol: 44, P 852-855.
85. Pascoe, M.W. and Tabor, D. Research, Land. 1955, 8, S15, Friction in textiles, part3: Test methods, London, Butterworth's Scientific Publications, 1959.
86. Pierce and Lord, Shirley Institute Mem., N16, 1945, Vol:19, P 210-221, Friction in textiles, part3: Test methods, London, Butterworth's Scientific Publications, 1959
87. Plonsker, H.R. and Backer, S. The dynamics of roller drafting, Part I, Textile Research Journal, N8, 1967, Vol: 37, P 673-687.
88. Plonsker, H.R. and Backer, S. The dynamics of roller drafting, Part II, Textile Research Journal, N9, 1969, Vol: 39, P 823-830.
89. Postle, L.J., Ingham, J. and Cox, D.R. The measurement of inter fibre friction in sliver, Journal of the Textile Institute, 1952, P 77-90.
90. Rajiba, N. Fibre de coton : microstructure et propriétés de surface, 2007, Thèse de doctorant de l'Université de Haute Alsace, Mulhouse, France.
91. Roder, H.L. Measurements of the influence of finishing agents on the friction of fibers, Journal of the Textile Institute, 1953, Vol: 44, PT 247-265.
92. Roder, H.L. The relation between fiber friction and the behavior of fibers and yarns during processing, Journal of the Textile Institute, 1955, Vol: 46, P 84-100.
93. Roehrich, O. Appréciation de la maturité du coton au moyen d'appareils air-flow, ITF Bulletin. 61(93), 1961, P 44-49.
94. Saxl, E.J. J. Franklin Inst., 1936, 221, 789, Friction in textiles, part3: Test methods, London, Butterworth's Scientific Publications, 1959.
95. Saxl, E.J. Textile Research Journal, 1939, 9, P 444-50, Friction in textiles, part3: Test methods, London, Butterworth's Scientific Publications, 1959.

96. Scardino, F.L. and Lyons, W.J. Fibre surface properties in relation to linear assemblies during processing, part I, Textile Research Journal, N10, 1967, Vol: 37, P 874-880.
97. Scardino, F.L. and Lyons, W.J. Fibre surface properties in relation to linear assemblies during processing, part II, Textile Research Journal, N11, 1967, Vol: 37, P 982-988.
98. Scardino, F.L. and Lyons, W.J. Fibre surface properties in relation to linear assemblies during processing, part III, Textile Research Journal, N12, 1967, Vol: 37, P 1005-1008.
99. Scheier, S.C. and Lyons, W.J. Studies of the surface geometry of fibres, part II, Improved instrumentation and representative results on camel hair and Dacron, Textile Research Journal, N6, 1964, Vol:34, P 410-416.
100. Sellers, W.B. Textile World, 1934, 84, 2408, Friction in textiles, part3: Test methods, London, Butterworth's Scientific Publications, 1959.

101. Simpson, J. and De Luca, L.B. Effects of sliver weight entering drawing on Fibre hook removal. Textile Research Journal, N7, 1965, Vol: 35, P 675-676.
102. Simpson, J. and De Luca, L.B. The effect of testing condition Fibre Drag, Part I, Textile Research Journal, N1, 1963, Vol: 33, P 62-68.
103. Singh, M., Singh, P.V., Patil, N.B. and Petkar, B.M. Improvement of yield and fibre strength in medium and superior-medium staple upland cotton (*Gossypium Hirsutum*). *Indian J. Agri. Sci*. 61(1), 1991, P 11-15.
104. Sinoimeri, A. Friction in textile fibres and its role in fibre processing, Wear Vol.267 Issue 9/10 2009. P 1619-1624.
105. Speakman, J. and Stott, E. A contribution to the theory of milling, Part I, A method for measuring the scaliness of wool fibers, Journal of the Textile Institute, 1931, Vol: 22, P 339-344.
106. Speakman, J., Chamberlain, N.H. and Menkart, J. The Lepidometer- An instrument for measuring the scaliness of animal fibers, Journal of the Textile Institute, 1945, Vol: 36, T91.

107. Tabor, D. Friction, Adhesion and Boundary lubrification of polymers in advance in polymer friction and wear, Plenum Press NY, Vol 5A, 1974, P 5.
108. Tarrin, J.C. and Gouault, J. Le cohésiometre en filature, Industrie Textile, 1973 : N1019, P 52-56 ; N1023, P 269-275.
109. Taylor, D.S. Some observation on the movement of fibres during drafting, Journal of the Textile Institute, 1954, Vol: 45, PT 310-322.
110. Taylor, D.S. The measurement of fiber friction and its application to drafting force and fiber control calculation, Journal of the Textile Institute, 1955, Vol: 46, P 59-83.
111. Taylor, D.S. The velocity of floating fibres during drafting of worsted sliver, Journal of the Textile Institute, 1959, Vol: 47, P 233-237.
112. Van der Vegt, A.K. and Schuringa, G.J. The relation between wool felting and single-fiber properties, Textile Research Journal, 1956, Vol: 26, P 9-16.
113. Vernekar, S., Vishwanath, B.A. and Ghosh, B. Fiber friction, The Indian textile journal, September 1999, 16-21.
114. Viswanathan, A. Frictional force in cotton and regenerated cellulosic fibers, Journal of the Textile Institute, 1966, Vol: 57, PT30-40.
115. Viswanathan, A. Some Experiments on the friction of cotton fibers, Journal of the Textile Institute, 1973, Vol: 64, P 553-557.
116. Vittie, J.M. and Barr, A.E.D. Fiber motion in roller and apron drafting, Journal of the Textile Institute, 1960, Vol: 52, P 147-156.
117. Vroomen, F. Théorie de l'étirage par grappes en préparation de filature, Annales textiles belges 4-12, 1968, P 43-66.
118. Wagget, G. The tensile properties of card and draw frame slivers, Journal of the Textile Institute, 1952, Vol: 43, P 380-395.
119. Wegener, W. and Bechlenberg, H. Les mesures des forces de tension Rayonne fibranne et fibres synthétiques, 1955 : N4, P 323-333, N5, P 409-417, N7, P 670-686.

120. Wegener, W., Contortosa, L. and Hess, V. Influence des conditions de marche des intersections de préparation sur la force d'étirage, sur la régularité et sur la longueur des fibres du ruban, Melliand Textilberichte, N55, 1974, P 11-16.
121. Wood, C. Dynamic friction of viscose fibers and relative humidity, Journal of the Textile Institute, 1954, Vol: 45, P 794-802.
122. Wood, C. Dynamic friction of Viscose fibers, Journal of the Textile Institute, 1952, Vol:43, P 338-349.
123. Zellweger-Uster. 1984. Uster mesure la régularité, Uster, Suisse.
124. Zellweger-Uster. 1985. Uster Tensorapid, essais de résistance sur fils et retors, Uster, Suisse.

Annexes